Final Report 1999-09

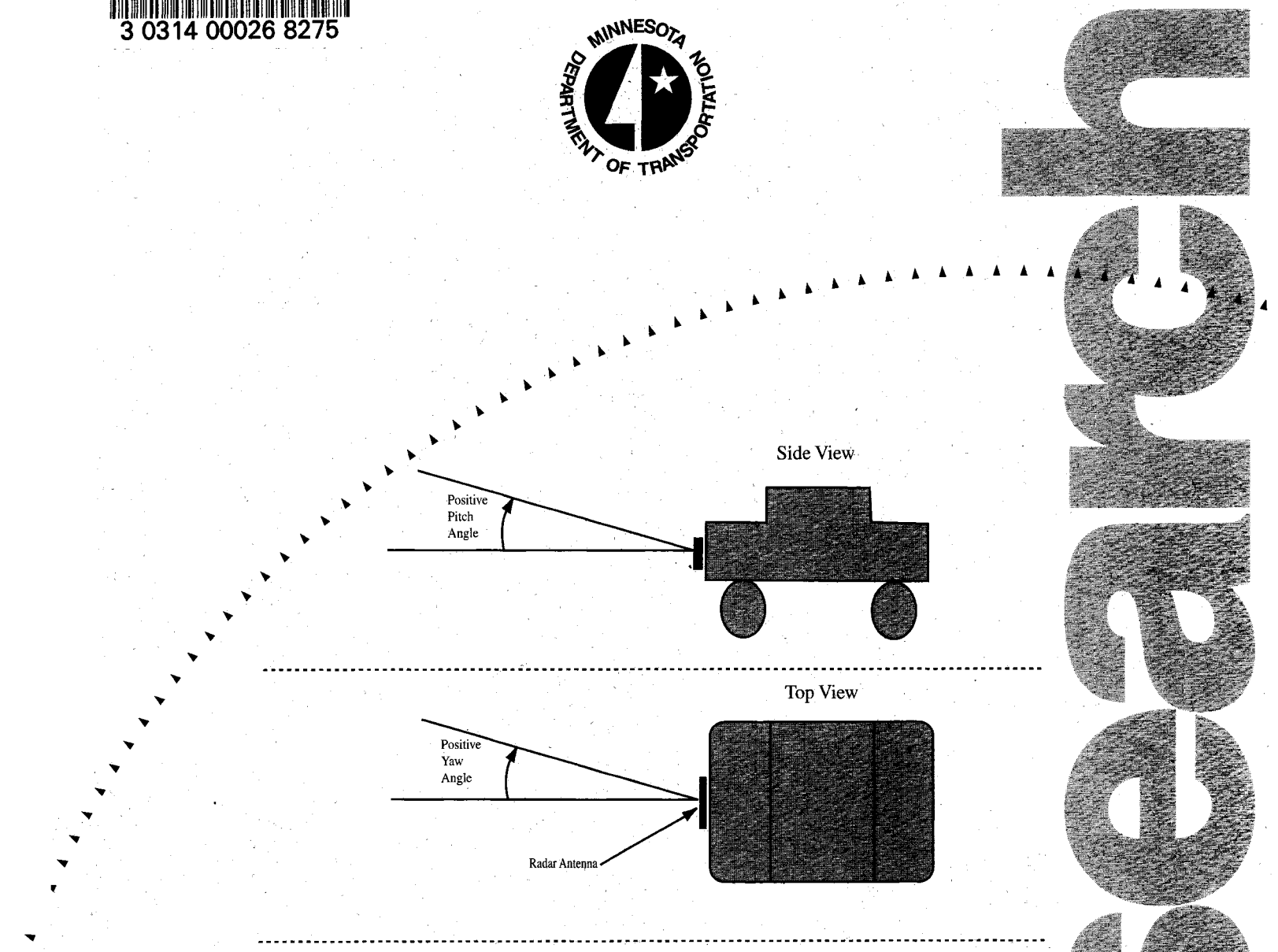

Evaluation of Radar for Snowplows: Initial Results

41981495

Technical Report Documentation Page

1. Report No.	2.	3. Recipient's Accession No.
MN/RC - 1999-09		

4. Title and Subtitle	5. Report Date
EVALUATION OF RADAR FOR SNOWPLOWS: INITIAL RESULTS	April 1998
	6.

7. Author(s)	8. Performing Organization Report No.
Alec Gorjestani, Thanh Pham, Sundeep Bajikar, Max Donath	

9. Performing Organization Name and Address	10. Project/Task/Work Unit No.
University of Minnesota Department of Mechanical Engineering 111 Church Street, S. E. Minneapolis, Minnesota 55455	11. Contract (C) or Grant (G) No. (C) 74708 TOC # 29

12. Sponsoring Organization Name and Address	13. Type of Report and Period Covered
Minnesota Department of Transportation Office of Research Services 395 John Ireland Boulevard, Mail Stop 330 St. Paul, Minnesota 55155	Final Report 1997 - 1998
	14. Sponsoring Agency Code

15. Supplementary Notes

16. Abstract (Limit: 200 words)

Heavy or blowing snow often causes poor visibility for snowplows. This report presents the results of a one-year preliminary study to evaluate the performance of an off-the-shelf radar unit for improved detection of objects under snow and blizzard conditions.

Researchers developed a geometrical computer model of radar range and closure rate measurement to provide a baseline for comparison with experimental results. They varied parameters such as radar orientation, location, and differential vehicle speed to determine their effect on radar performance.

The radar's accuracy improves as the speed differential between vehicles increases, according to the research findings. Furthermore, slight deviations in orientation and location do not seem to greatly influence the radar's ability to detect other vehicles.

The radar also was tested under falling snow conditions. The radar effectively detected target vehicles under 'light' and 'moderate' snow conditions with visibility down to less than one half mile. However, the very small number of snow events in the winter of 1997-98 limits the ability to make conclusions about the radar's performance under such conditions.

Since the study began, commercially available radar technology has improved significantly, and researchers recommend testing the improved radar units in the future.

17. Document Analysis/Descriptors		18. Availability Statement
automotive radar 24 GHz FMCW radar evaluation of radar in snow	collision avoidance snowplow applications	No restrictions. Document available from: National Technical Information Services, Springfield, Virginia 22161

19. Security Class (this report)	20. Security Class (this page)	21. No. of Pages	22. Price
Unclassified	Unclassified	110	

Evaluation of Radar for Snowplows: Initial Results

Final Report

Prepared by

Alec Gorjestani, Sundeep Bajikar, Thanh Pham, Max Donath
Department of Mechanical Engineering
University of Minnesota
111 Church St. S.E.
Minneapolis, MN 55455

April 1998

Published by

Minnesota Department of Transportation
Office of Research Administration
First Floor
395 John Ireland Boulevard, Mail Stop 330
St Paul, MN 55155

Acknowledgments

We would like to thank Jack Herndon and others at Mn/ROAD for their flexibility and assistance with the experiments. John Scharffbillig also deserves our thanks for acquiring vehicles for radar testing, and for chairing the advisory panel. Thanks are also extended to Ed Fleege for providing information on weather sensors, and Kevin Wixom (formerly of) and Mike Lesher of Eaton VORAD for their technical support. We would also like to thank Bob Milton of the Department of Aeronautics of Mn/DOT and the people at the Anoka and Cambridge airports for their cooperation with the precipitation sensor experiments.

We would like to thank Sameer Pardhy for help with preparing the radar display images for this report.

This project was partially supported by Mn/DOT and the Center for Transportation Studies at the University of Minnesota.

Table of Contents

List of Figures

List of Tables

Executive Summary

Poor visibility conditions contribute to a large percentage of accidents each year. Lack of visibility (which leads to the inability to detect the presence of obstacles and other vehicles on the road) is of particular concern in areas that experience bad weather conditions for a good part of the year. Since there have been a number of fatalities suffered as a result of fast moving vehicles hitting slow moving snowplows, as well as damage due to snowplows hitting abandoned vehicles and other objects buried in the snow, technologies that detect such objects need to be investigated.

The primary objective of this project was to provide Minnesota Department of Transportation (Mn/DOT) with information that would be useful for planning and designing future safety systems for snowplows. This project's goal was to evaluate the performance of off-the-shelf commercially available radar units in snowfall.

An EVT-200 radar, part of the Eaton VORAD collision warning system, was acquired. The radar was mounted to a Navistar tractor (the host vehicle) and a series of experiments were conducted using a moving host and a stationary car of known location as a target. We simultaneously collected range and closure rate data from the radar and from the other sensors (including a high accuracy Differential Global Positioning System (DGPS) receiver) resident in the tractor (host vehicle). The experiments were repeated using various mounting configurations and under different weather conditions.

The EVT-200 was able to consistently detect a target vehicle under a variety of circumstances. In particular, the radar is relatively insensitive to small orientation deviations that are caused by uncertainty in mounting. Furthermore, the ability to detect vehicles in the far edges of its field of view makes this sensor very robust. We did, however, discover that the sensor was sensitive to vibration, which caused it to detect vehicles with no relative velocity to the host vehicle and to sometimes sense a phantom vehicle instead of the desired target vehicle. Eaton VORAD indicated that it has fixed this problem with its newer radar units.

Results from a computer based geometric simulation driven by the GPS data collected during the experiments were compared to the actual experimental data. This comparison revealed that the sensor is more accurate at higher relative speeds (between host and target vehicle). Furthermore, the range data became more accurate as the host approaches the target. Fortunately, the areas where the sensor performs best correspond to the higher risk driving situations (high relative speed, low range).

The EVT-200 performed well without major signal degradation under light and moderate snow conditions. Due to the unusually warm winter in 1998, we were unable to test it under severe blizzard conditions. However, in light and moderately blowing snow (visibility down to less than 0.5 mile) the radar was able to detect the target vehicle through the snow. There seems to also be a temperature effect that needs further analysis. Given the limited sets of test performed during a season with relatively few snow events, further tests are warranted.

A prototype Driver Assistive Display (DAD) was developed which demonstrated that the target vehicle's location (obtained from radar) can be effectively displayed to the snow plow driver in multiple views. The target was displayed as a red circle which grew in area as it approached the host vehicle. The target information can be displayed on either a flat panel display or a heads up display projected onto the windshield. A preliminary rear view 'virtual mirror' prototype was also developed for lab demonstration purposes. Additional work will be needed before an accurate implementation on a snowplow is possible.

We recommend that before mounting radar units to a snow plow, a geometric analysis be conducted using the information learned thus far to determine the optimal mounting location and orientation to provide the best coverage for the determined region of interest. This is important due to the small effective field of view of presently available radar and the position of the plow in front of the truck. Also, it would be desirable to purchase newer radar technology which now exhibits a wider field of view and provides an azimuth angle to the target (not available for the EVT-200). Given a known heading angle to the target, it would then be possible to filter out reflections from road side clutter.

Chapter 1

1. Introduction

This chapter introduces the rationale behind the evaluation of radar for snowplow applications. It also provides a brief literature review of different target sensor technologies with a particular focus on different types of radar. Then, it describes typical applications and research studies where radar is the main sensing technology. Finally, the objective and goals of the project are discussed.

1.1 Background

Poor visibility conditions contribute to a large percentage of accidents each year. Lack of visibility (which leads to the inability to detect the presence of obstacles and other vehicles on the road) is of particular concern in areas that experience bad weather conditions for much of the year. Drivers of snowplows in particular suffer because most of their driving occurs during snowfall and blowing snow, with the road and other vehicles around them often covered with snow. Not only are the driving lanes hard to discern, but the snowplow operation itself contributes to severe visibility limitations due to the plume of snow produced by the front blades.

Since there have been a number of fatalities suffered as a result of fast moving vehicles hitting slow moving snowplows as well as considerable damage due to snowplows hitting abandoned vehicles and other objects which are buried in the snow, a technology to detect these vehicles and objects needs to be investigated.

1.2 Available Vehicle Detection Sensors

The sensing of objects and vehicles can be accomplished with different technologies, but most involve emitting a waveform and measuring return echoes. The following list of sensor technologies accomplish range detection in different ways and, therefore, have different advantages and disadvantages.

1.2.1 Ultrasonic

Ultrasonic distance sensors measure the time-of-flight of a short burst of sound energy to calculate a range to the target. Typically, a high frequency (40k - 80kHz) signal is sent by a transmitter and a microphone detects the reflected sound. Measurement of the time interval between transmitting the pulse and receiving a reflection, along with knowledge of the speed of sound, can be used to calculate the range to the reflector. Ultrasonic sensors are relatively inexpensive and are small in size. The major disadvantages are the poor reflectivity of various targets, the considerable variation with temperature of the sound wave propagation speed in air and the low maximum sensing range (10 m maximum) [1]. Results are often affected by local variations in humidity and wind conditions. In particular, the low maximum range makes this technology inappropriate for higher speed vehicular applications.

1.2.2 Passive Infrared

Passive infrared (PIR) sensors measure the thermal energy emitted by objects in the vicinity of the sensors. PIR sensors are not very precise, thus, have limited applications. One vehicle-based application is the detection of a person in the path of a backing vehicle. Again, low maximum sensing range renders this technology inappropriate for higher speed vehicular applications.

1.2.3 Vision Systems

Vision systems for distance measurement use an electronic imaging camera to view an object as it moves. Image processing techniques are used to select and measure the distance to targets. Distance measurement can be derived from detailed prior knowledge of the geometry of the object to be tracked. Other methods use structured light sources, e.g. a plane of light generated by a laser, and process the image which consists of the laser beam distorted by the object. Vision systems provide long range measurements (100 m +) and good directionality. They suffer under poor weather conditions and the effects of ambient light and are often slowed by significant computer processing. The degradation of the performance of this sensor in poor visibility conditions makes the use of vision systems difficult in snow plow applications.

1.2.4 Laser Radar

Laser based radar sensors emit a frequency modulated beam and measure the time-of-flight or phase delays for the reflection off the target that returns to the receiver. These sensors have long range (maximum around 100 m), narrow beams which provide good directionality, and fast response times [2]. Narrow beams have a small coverage area therefore requiring mechanical scanning or beam splitting. The performance of laser radar can be degraded due to dirt on lenses, heavy rain/snow or thick fog and car exhaust emissions. Laser radar has been used in automotive applications and may be a candidate for use on snowplows. More research needs to be conducted on their performance in heavy snow conditions to determine if their performance degradation is severe enough to rule them out for snow plow applications.

1.2.5 Radar

Radar based sensors emit high frequency electromagnetic waves and measure the reflected (from a target) signal. Frequency and phase shifts in the returned signal can be used to determine the range and range rate to the target [3]. Radar comes in primarily three forms: Frequency Modulated Continuous Wave (FMCW), Impulse, and Spread Spectrum (SS). This technology provides good resistance to harsh weather conditions, reasonably long range coverage, and the ability to communicate with vehicles that are under detection [4]. Some disadvantages include the considerable cost of such units and the inability of some units to indicate the azimuth location of an obstacle within their wide beam angle. Modern radar units, however, are coming down in price and providing a more accurate target location (azimuth to target). Radar's unhindered performance in poor weather conditions and continually decreasing cost make it a good candidate for snow plow applications. A more detailed investigation into the current state of radar technology follows.

1.3 State of Radar Technology

Radar technology has a long history and was first introduced for military applications during World War II. More recently, the transition from a cold war economy has forced military suppliers to look towards the private sector for applications of technology developed for the

military. Recent advances in Millimeter Monolithic Integrated Circuit (MIMIC) technology have provided further incentive for companies to develop an automotive radar for use in Collision Warning/Avoidance systems (Section 1.4). MIMIC technology integrates much of the radar transmitter, receiver, and signal processing hardware onto a one or two piece chip set. As with any electronic device, massive integration leads to lower manufacturing costs, and therefore lower product costs. Moreover, this integration reduces the size of hardware, and facilitates the integration of the radar components in the vehicle without adversely affecting the vehicle design. As radar systems become smaller and less expensive, the demand for these systems will continue to grow [5].

Three primary methods are used to emit and detect radar signals; FMCW, Pulsed and SS. FMCW is the most common technique for deriving range and range rate to target because it is the least complicated and therefore the least expensive to manufacture. Pulsed Doppler method involves a simple configuration, but the speed measurement is more difficult and a wide frequency band is required [6]. The spread spectrum method is more robust against interference and can provide inter-vehicle communication as well as ranging in the same unit. It is, however, more complicated and more expensive [7].

Until recently, radar provided measurement along only one degree of freedom. There was no way of knowing the lateral position of the reflecting target with a resolution less than the radar beam width. New developments in radar technology have produced a new generation of automotive radar that measure an azimuth angle to the target, as well as its range and range rate. The extra degree of freedom allows much more effective filtering of the road scene for collision warning/avoidance systems.

1.3.1 Radar Manufacturers

To put the current state of the art into perspective, automotive radar systems from Europe, Japan, and the United States will be discussed.

Europe - A number of European companies have been involved in automotive radar and vehicle control. We only list the ones who publish in this area in U.S. technical journals. Phillips [8] has focused on 94 GHz FMCW radar for automotive applications. Military millimeter wave radar typically operates at 94 GHz, and therefore equipment which operates at this frequency is readily available and has been thoroughly studied. Phillips has developed and demonstrated a FMCW radar unit with an antenna aperture size of 100 mm x 150 mm for automotive applications. This unit has a cone angle of 1.5 °, and provides a usable range of 128 m.

CelsiusTech Electronics AB of Sweden have developed a FMCW radar which operates at 77 GHz. Their sensor uses mechanical scanning to produce an azimuth scan of ±8.5 degrees with a maximum range of 200 m and an accuracy of 0.3 m. Relative velocities between -100 and +100 m/s can be detected with a data acquisition rate of 10 Hz [9].

Volkswagen (in conjunction with the Technical University of Braunschweig) have developed a forward looking 77 GHz FMCW radar with a maximum range of 128 m with an accuracy of 30 cm. The relative velocity of targets can be detected from -80 km/h up to 240 km/h with a resolution of 2.5 km/h [10]. This unit supports an impressive data acquisition rate of 100 Hz.

Japan - Few technical papers regarding automotive radar systems have come from Japan. This may be for two reasons. First, they may not wish to "show their hand" on what could be a very important (and potentially high volume) option for automobiles. Second, since W.W.II, the Japanese defense industry has been essentially nonexistent. Most of the 70-100 GHz radar technology today has been developed for military applications under secret or classified programs. Nevertheless, we were able to find a few citations to companies developing automotive radar.

The Furukawa Electric CO. has designed a 76 GHz spread spectrum radar sensor with a 3-beam switched antenna for measurement of an azimuth angle to target. This sensor has a maximum range of 100 m, detects relative velocities between -200 km/h to 200 km/h, and has a data up-date rate of 20 Hz [11].

Toyota Motor Corporation has developed a 60 GHz FMCW radar for rear-end collision avoidance. It provides a maximum range of 100 m [12]. Azimuth is provided by mechanical scan of the 2° x 2° beam. No resolution or accuracy data was provided.

Other radar units have been described by various companies at ITS exhibitions but little to no technical information is publicly available. These technologies are important to Intelligent (or Adaptive) Cruise Control and it is obvious that radar technologies are part of the systems which have begun to appear on the market this year (Toyota, Mitsubishi, etc.).

United States - Raytheon Electronic Systems have developed a FMCW radar that tracks the range, range rate, and angular location of obstacles in the field of view. This unit operates in the 76-77 GHz frequency range and has a maximum range of 100 m. Range accuracy is quoted at less than 0.5 m [13]. Relative speed can be tracked between -160 Km/h and +160 km/hr with an accuracy of less than 1.5 Km/h. The Raytheon unit has an azimuth field of view of 9 degrees and has a stated azimuth angle accuracy of 0.2 degrees. Data is provided at 20 Hz.

The Northrop Grumman Corporation has developed a 24 GHz FMCW radar with a maximum range of 100 m with one meter accuracy. Relative speed specifications are 100 mph receding and 200 mph approaching with an accuracy of one mph [14]. This sensor has a 5 degree azimuth beam width, but provides no azimuth to target data.

HE Microwave Corp. has designed a side zone automotive radar. The requirements of a side zone radar system differ from a forward looking radar in that the beam azimuth must be much larger to provide greater coverage of the adjacent lane while the maximum range should be small to avoid detecting objects on the side of the road. Accordingly, the side zone radar designed by HE Microwave Corp. has an azimuth coverage of 100 degrees, a maximum range of 5.2 m and a range rate coverage of ±26.7 m/s [15].

Eaton VORAD Technologies manufactures an off-the-shelf collision warning system (EVT-200) that comes with a 24 GHz FMCW radar. The antenna aperture size is 14 cm by 19.5 cm with a

depth of only 3.8 cm. A maximum range of 110 m and a maximum closing rate of 160 km/hr are specified [16]. Range and range rate data is acquired at 10 Hz (no azimuth data). The azimuth beam angle is four degrees.

Eaton VORAD has also designed a prototype monopulse Doppler radar which has a 12 degree azimuth field of view and provides azimuth angle to target at a 0.1 degree accuracy. This unit has two antennas and two receivers but is smaller than its predecessor because it operates at 77 GHz (aperture area decreases with increasing frequency). Differences in the returning signal power between the two receivers are used to measure the angle to target. Eaton VORAD plans to sell the new radar unit (EVT-300) in the spring of 1998.

1.3.2 Laser Radar Manufacturers

Leica [17] has used an infrared (IR) laser radar to develop an Inteligent Cruise Control system. The transmitter/receiver package is 9.9 cm x 8.4 cm x 11.0 cm, has a range of 150 m and has a specified accuracy of ±0.2 m and ±1.6 km/hr. The beam angle is 3°, and the system provides distance and relative velocity to the target at a rate of 10 Hz. UMTRI is evaluating a fleet of vehicles outfitted with the Leica ODIN sensor as part of an evaluation of adaptive cruise control [18].

Laser Atlanta Optics have developed a multi-beam laser radar that provides range data on target vehicles from 3 to 250 feet and closing velocity data from 0 to 120 mph. A custom beam splitter provides an instantaneous field of view of 0.17 degrees [19]. The total field of view is 11 degrees azimuth.

For their collision avoidance system, Mazda Motor Corp. developed a scanning laser radar with a wide (23°) field of view. The scanning time is 32 ms (31.25 Hz) with an azimuth resolution of 0.17 degrees. The maximum range for this sensor is 120 m.

1.4 Application of Vehicular Radar

Vehicular radar systems can be broken down into five major categories. The first four employ forward looking radar and are listed in increasing system complexity. The fifth category explains an application of radar for use in a lateral vehicular control system.

1.4.1 Driver Warning Systems

Driver warning systems indicate a safe following distance to the vehicle ahead and warn the driver of inadequate following distance or excessive closing rates to the vehicle ahead. Eaton VORAD produces a system which provides a warning for unsafe vehicle following; a side looking "blind spot" monitor is also available [20]. This system was originally installed on 2400 Greyhound buses, and uses a system of green, yellow, and red lights combined with audible signals to provide the driver additional time to make decisions regarding braking, throttle, and steering actions. A newer version was developed based on the experience gained from this system deployment. This latter version has been installed on many truck fleets around the U.S. and Canada.

1.4.2 Intelligent Cruise Control

Intelligent Cruise Control (ICC) uses forward looking radar, infrared, or laser sensors to automatically maintain the proper vehicle spacing instead of just regulating vehicle speed as is done with traditional cruise control. ICC looks ahead to determine distance and closing rates, and adjusts throttle position to maintain safe headway. If changes in throttle position fail to provide adequate deceleration, ICC can force the automatic transmission to shift to lower gears, invoking engine braking.

Eaton VORAD has developed an ICC for heavy trucks called SmartCruise™ [21]. The system employs the same radar used in the VORAD T200 collision warning system along with a tractor equipped with an electronically controlled diesel engine.

1.4.3 Forward Collision Avoidance

Forward Collision Avoidance systems detect obstacles in the forward path of a vehicle and provides information regarding heading and closing rates for those obstacles. This category includes driver assistance schemes where the suggested collision avoidance countermeasures are

provided to the driver via a Head Up Display (HUD) and automatic systems where the vehicle controller processes sensor information to compute and execute the best collision avoidance countermeasure.

1.4.4 Autonomous Collision Avoidance

Autonomous Collision Avoidance incorporates a radar array placed on the periphery of the vehicle to provide real time maps of the local environment. With adequate real local maps, the vehicle control computer can execute collision avoidance maneuvers without external input from the driver. Such a system can automatically compute and execute merging, braking, and safe lane change maneuvers in cases where inadequate time is available for a driver response.

1.4.5 Lateral Vehicular Control

The ElectroScience Laboratory at Ohio state University has developed a forward-looking chirp monopulse radar that provides both road-vehicle guidance and collision avoidance. A frequency selective surface stripe laid in the middle of the highway lane reflects the forward-looking radar energy, which is forward scattered from normal roadway surfaces. The backscattered energy is sensed by the radar and used for automated guidance, while standard obstacle detection technology can be performed in conjunction with the highway stripe sensing [22].

1.5 Objective of Project

The primary objective of the evaluation of radar for snowplows project is to provide Minnesota Department of Transportation (Mn/DOT) with information that would be useful for planning and designing the Maintenance Concept Vehicle, a joint effort sponsored by Mn/DOT, Iowa DOT and Michigan DOT. This project will investigate how well off-the-shelf radar units function in snowfall.

After a careful evaluation of radar, the project aims to investigate ways of displaying the information provided by the radar to snow plow drivers.

1.5.1 Eaton VORAD EVT-200 Radar

An EVT-200 radar was purchased as part of the Eaton VORAD collision warning system which is available off-the-shelf. We chose this model of radar because it is commercially available and Eaton VORAD was willing to make the adjustments necessary to provide us with raw range and range rate data. They were also willing to provide technical support and meet our schedule.

The EVT-200 is a one dimensional sensor that provides range to target as well as the rate of change of the range to target. It is sold with their collision warning package for trucks, but Eaton VORAD modified their hardware/software to allow access to the range and range rate data at 10 Hz. The maximum range specification is 110 m and the maximum closing rate is 160 km/h [16]. The beam has a narrow azimuth angle of four degrees and the antenna is about the size of a thick license place (16.4 cm x 20.6 cm x 3.8 cm).

The EVT-200 measures the speed of moving objects by Doppler shift methods, wherein the magnitude and frequency shift of an energy wave reflected off a mobile target is proportional to its relative velocity. Ranging is accomplished by Continuous Wave Frequency Modulation (CWFM) methods. The phase shift of the returning signal is used to measure the range to the target.

1.5.2 Optech Sentinel 100

To determine how well a laser based sensor functions in snowfall, we purchased the Optech Sentinel 100. This sensor is primarily designed as a level monitor and object positioner. Optech claims that the radar can perform under adverse conditions; specifically, dust and fog. They sell the units for mining applications where dust is a major issue. We are interested in determining whether the sensor performs well under snow conditions.

The Optech is specified to have a maximum range of 250 m for most materials (longer ranges for very light reflective materials), but does not provide the range rate to target. An accuracy of ±5 cm, a resolution of one mm and a repeatability of ±5 cm are specified. The laser based sensor emits a point source of light and has an extremely small beam divergence (5 mrad).

The Optech Sentinel 100 measures the distance to the target by the Time Of Flight (TOF) principle, referring to the time it takes for a pulse of energy to travel from the transmitter to an observed object then back to the receiver. A high accuracy clock measures the round trip time between a light pulse emission and the return of the echo resulting from reflectance off an object. Multiplication of the measured round trip time and the speed of light (1 foot/nanosecond) produces the range to target. The Optech 100 averages a number of theses measurements (the number of samples can be set by the user) to improve the accuracy of the range measurement.

Chapter 2

2. Experimental Design

In this chapter we discuss the design of the radar experiments. We explain the philosophy behind the design in the context of determining the characteristics of the sensor. Then, we explain the design of a computer simulation that uses Differential Global Positioning System (DGPS) location data to simulate radar for comparison with the experimental results.

2.1 Overview

The purpose of this project is to determine how well the EVT-200 detects objects (other vehicles) under both fair and snowfall conditions so that the information can be presented to snow plow drivers. To that end we designed the experiment to emulate real driving scenarios. The information gathered in this project can then be used to help determine where to mount radar on a real snow plow.

The radar was mounted to a Navistar tractor (the same vehicle used in the SAFETRUCK research project) in various configurations and driven towards a stationary car. Henceforth, we will refer to the Navistar tractor as the host vehicle and the stationary car as the target vehicle. We simultaneously collected data from the radar and from the other sensors already resident in the host vehicle. The experiments were then repeated with various configurations and weather conditions.

2.1.1 Vehicle and Sensor Configurations

The target vehicle was parked in the right lane of the two lane Minnesota Road Research Facility (Mn/ROAD) low volume test facility near Albertville, Minnesota. Experiments were performed with the host vehicle in the same lane as the target vehicle to explore how well the sensor detects a vehicle in its lane (directly in its field of view). Then, the host vehicle was moved to the adjacent (left) lane and the experiment repeated to determine whether the radar detects vehicles not directly in its field of view (see Figure 2.1).

The radar was mounted in various positions around the truck to better understand its sensitivity to lateral displacement with respect to target vehicles. The mounting provides six different locations around the truck (see Figure 2.2) where the radar can be located. It can be positioned in the front or rear of the host as well as the left, center or right. We only used the front right (FR), front center (FC), back center (RC) and back right (RR) positions because the results on the left side can be deduced by lateral symmetry. A picture of the radar mounted on the front in the center position is shown in Figure 2.3.

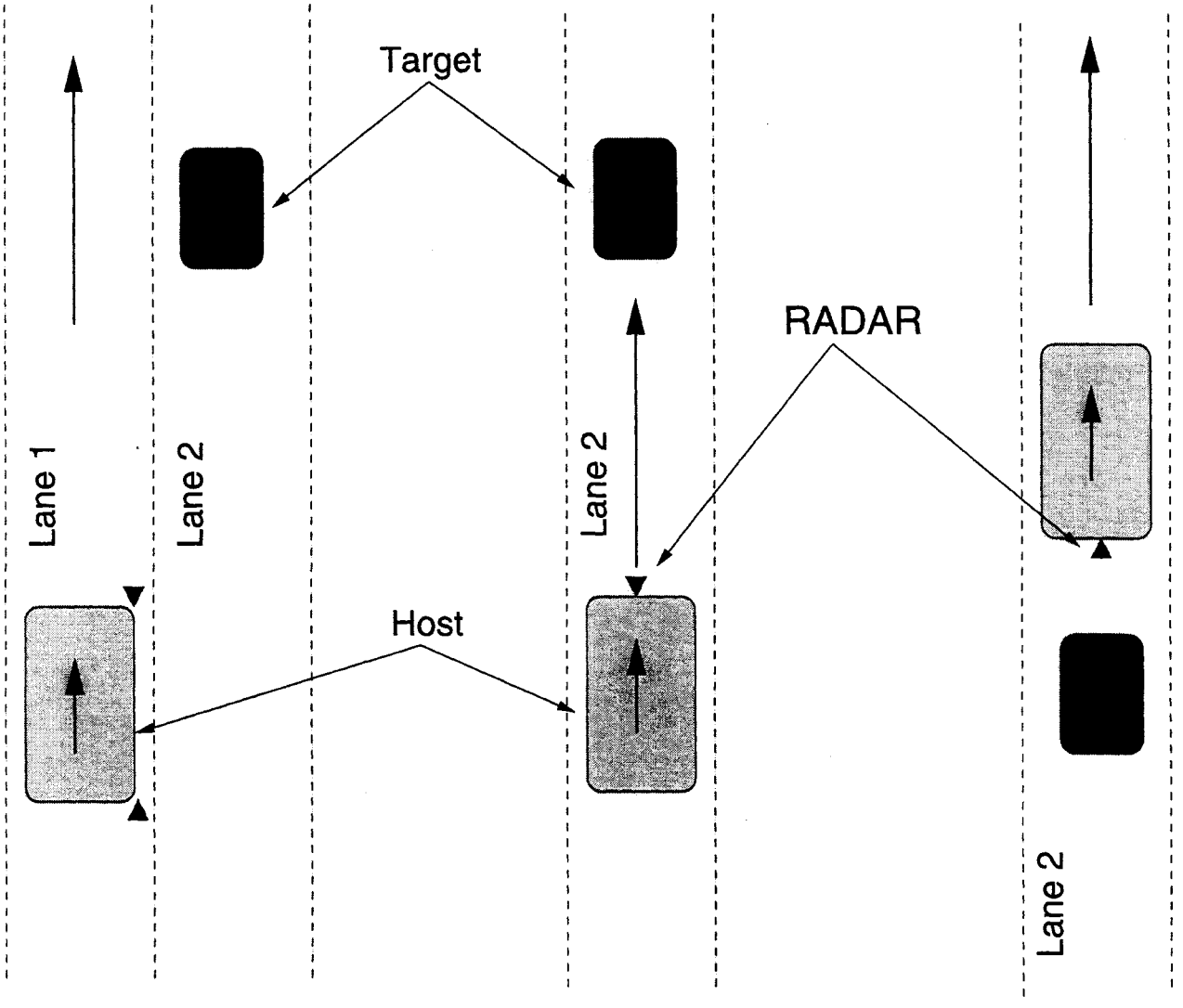

Figure 2.1: Various host - target configurations

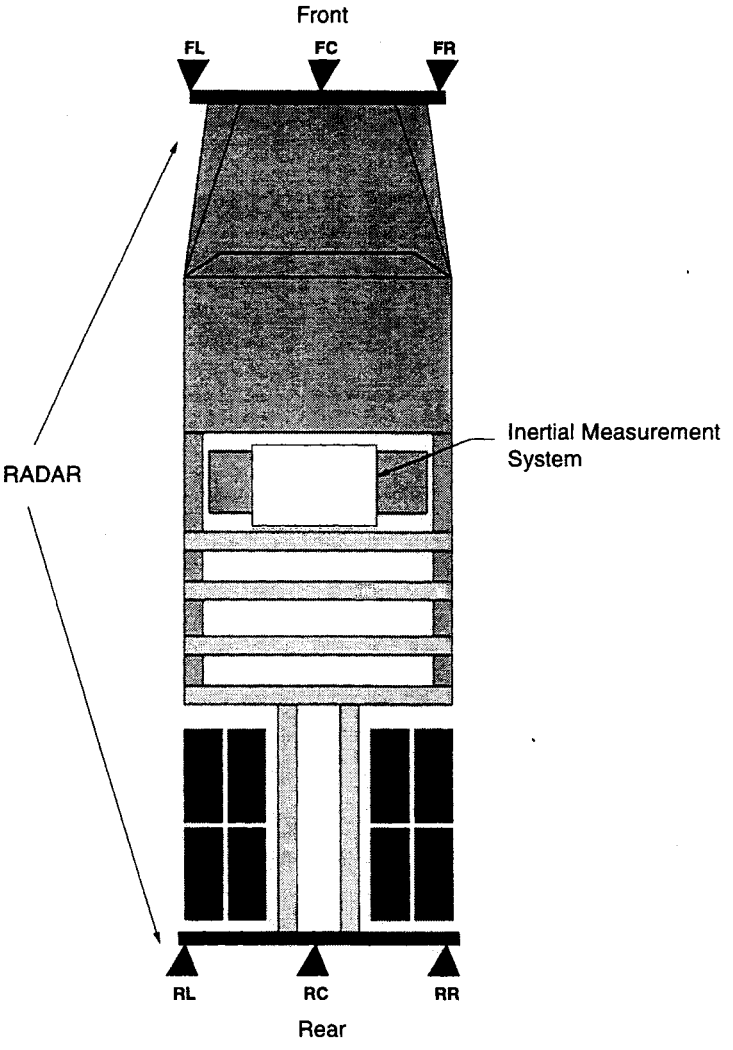

Figure 2.2: Possible mounting locations

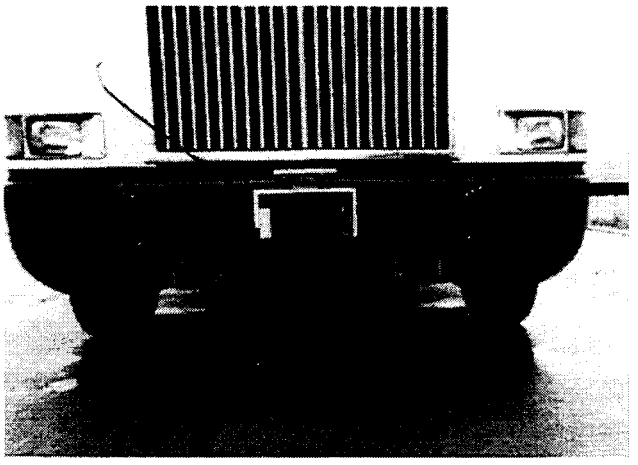

Figure 2.3: Radar mounted in the front center (FC) position

2.1.2 Parameters

To test the radar's ability to detect other vehicles in a variety of scenarios, we designed the experiment so that certain parameters can be modified individually. With the flexibility to change the configuration of the experiment, we were able to test the effect of several key parameters: speed, yaw, pitch, lane position, and radar location. These parameters were varied one at a time, while the rest were held at their 'default' values.

The most logical parameter to alter was the speed of the host vehicle. Since Doppler radar depends on a differential motion between host and target, it made good sense to test if performance degrades at lower differential speed. We varied the speed of the host vehicle from 30 mph to 5 mph. A snowplow travels at roughly 30 mph when its blade(s) is down. The lowest speed of 5 mph was to test the ability of the radar to pick up a target vehicle that is 'creeping' towards the host.

Our goal was also to determine how sensitive the radar is to mounting orientation. In a practical installation, it is very difficult to mount the radar to a known and small tolerance. We also sought to find an optimal orientation as well as the effects due to misalignment during installation. To that end, the mounting was designed to allow precise adjustment and measurement of the radar's

orientation. The orientation was separately varied by two degrees of freedom; yaw and pitch. Yaw is rotation about a vector pointing in the positive Z direction (upward from the road's surface). It can best be pictured from a bird's eye view as the angle in which the radar is pointing as measured from the vehicle's longitudinal axis (see Figure 2.4). The pitch is the up and down angle in the vertical plane. It can best be pictured from looking at a side view. It is the angle in which the radar points upward or downward (measured from the horizontal plane).

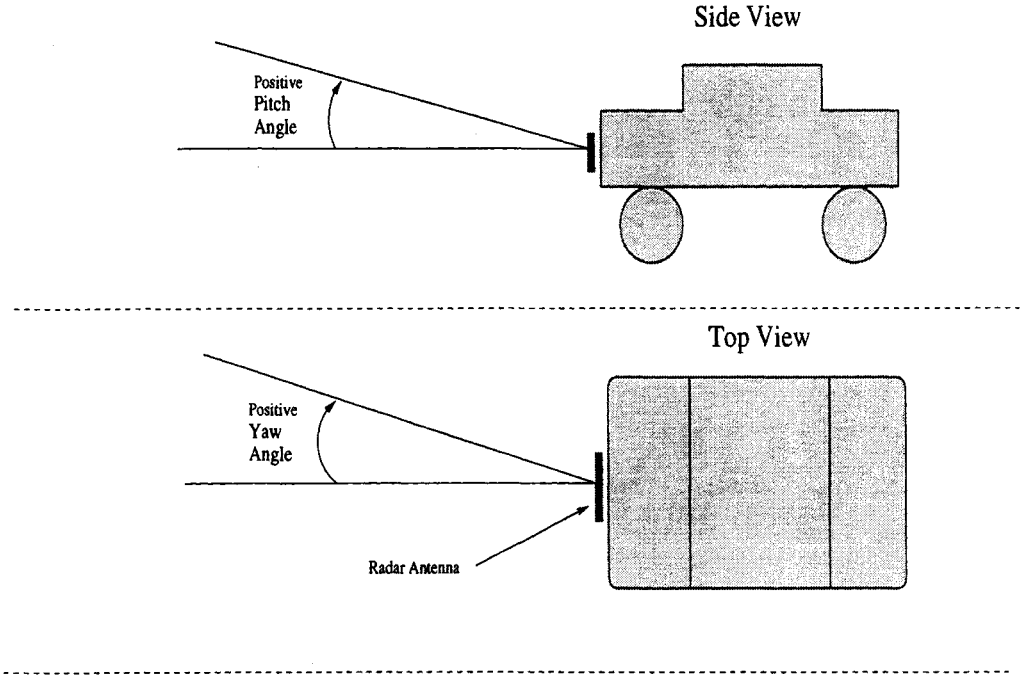

Figure 2.4: Definition of positive yaw and pitch angles

Finally, the radar's position on the truck and the truck's lane position were varied as described in the previous section. Mounting the radar at different locations on the truck can provide insight as to where is the best location for detecting desired targets (an abandoned vehicle for example). It is also important to know if the radar unit, pointing straight in the direction of travel, detects vehicles in adjacent lanes. This situation would create problems for accident warning/avoidance systems because an object in the adjacent lane would be detected, and its lane position would therefore be ambiguous resulting in a false alarm or inappropriate response.

2.2 Hardware and Software

The mounting was designed to provide the maximum flexibility in radar position and orientation. At the same time it also had to be rugged and removable. As mentioned above, we decided it was important to be able to position the radar at different locations on the host. This was accomplished using an eight foot square tube which had holes drilled to provide mounting locations in the center and at the two corners of the tractor. The bar was used for experiments in both the front and rear, providing six possible radar locations (see Figure 2.2).

We provided two separate orientation degrees of freedom using two turntables with vernier dials. The dials provide a resolution of less than one degree. The yaw provided by one of the turntables is the angle about a vertical axis. Positive yaw is defined as counter clockwise when viewed from above (see Figure 2.4). Zero is along the forward longitudinal axis of the vehicle. The pitch is provided by the second turntable and is defined as counter clockwise, as seen from the side view, and is measured from the horizontal plane (parallel to the road). Positive yaw is defined upward. A schematic and photograph of the turntables and axis of rotation is shown in Figure 2.5 and Figure 2.6.

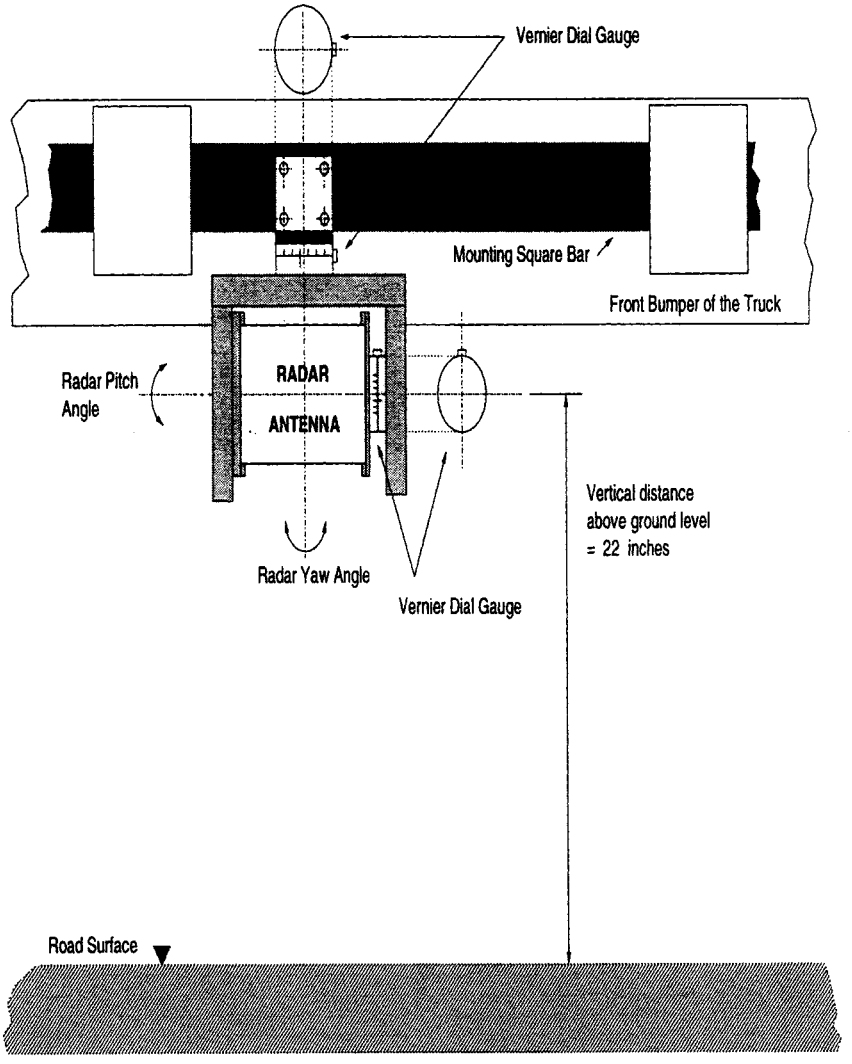

Figure 2.5: Schematic of mounting apparatus

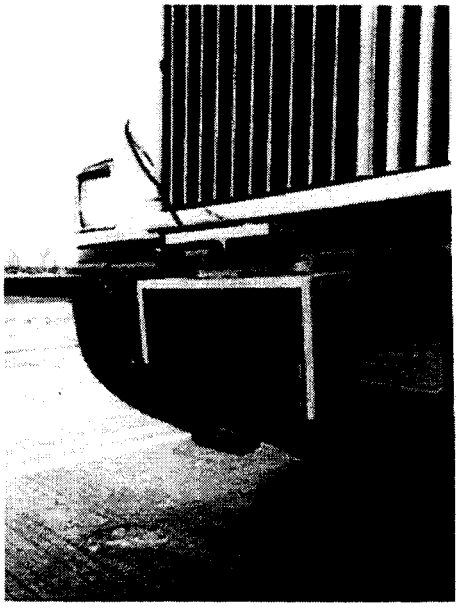

Figure 2.6: Photograph of mounting system

Software was written to collect data coming from the radar unit's CPU as well as the data from the other sensors on the Navistar truck (DGPS, gyro and accelerometer). Eaton VORAD modified their CPU unit so that we could directly receive the range and range rate values. Accordingly, we wrote software to collect this data using the VxWorks operating system running on a target Motorola MVME147 processor board connected to a VME bus. The other sensor data collected includes location from DGPS measurements, and acceleration and yaw rate. The radar provides range and range rate reading at 10 Hz, while the GPS produces location data at five Hz. Since we are using DGPS to compare the radar readings (through simulation, see discussion later), we chose to synchronize data collection around DGPS; in other words, at five Hz. The data for each experiment was collected in real time and stored for analysis.

2.3 Computer Simulation

In order to compare the radar results with an analytical or predicted result, DGPS was chosen as the ground truth. The Novatel DGPS unit aboard the tractor has a longitudinal accuracy of less than 5 cm with a standard deviation of 35 cm [23]. One can enter the position of the moving host vehicle (measured by GPS dynamically) and of the target vehicle (measured statically by

positioning the vehicle next to survey nails) into a geometric solid modeling software package. This type of software allows us to model the shape and specifications of the vehicles and of radar units as 'solid' entities. The surface facets between intersecting 'solids' can be computed and then used to calculate the range and range rate between the host and target assuming ideal behavior. To compare the actual radar readings to the predicted values based on the DGPS readings, a three dimensional graphical computer simulation was developed using the World Tool Kit (WTK) C solid modeling library. The simulation used a model of the Navistar tractor and a mid-size sedan on a straight two lane road. The movements of the host in this virtual world were controlled directly by the readings from DGPS recorded during the experiment.

A geometric model of radar was developed which calculates the range and range rate of the target vehicle by determining where the virtual radar beam intersects the vehicle's virtual space. The simulated radar can be placed at different locations around the truck (in the same way as they are located in the experiments), but can be oriented in only one degree of freedom (yaw). Pitch adjustment was not modeled due to the added complexity of adding a third dimension variable to the radar beam calculations. The two dimensional radar beam forms a triangular plane and the range is calculated from the shortest point of intersection between the target and the virtual radar beam.

The target vehicle was precisely located by using surveyed nails resident at the Mn/ROAD low volume test track. These survey nails, which line the road at 100 ft intervals, provide accurate locations in state plane coordinates. The car was placed at a measured offset from a survey nail for every experiment (see Figure 2.7). The DGPS data collected in real time during the experiment along with the location of the target vehicle previously recorded provided the simulation with the information it needed to place the host and target vehicle in the virtual world.

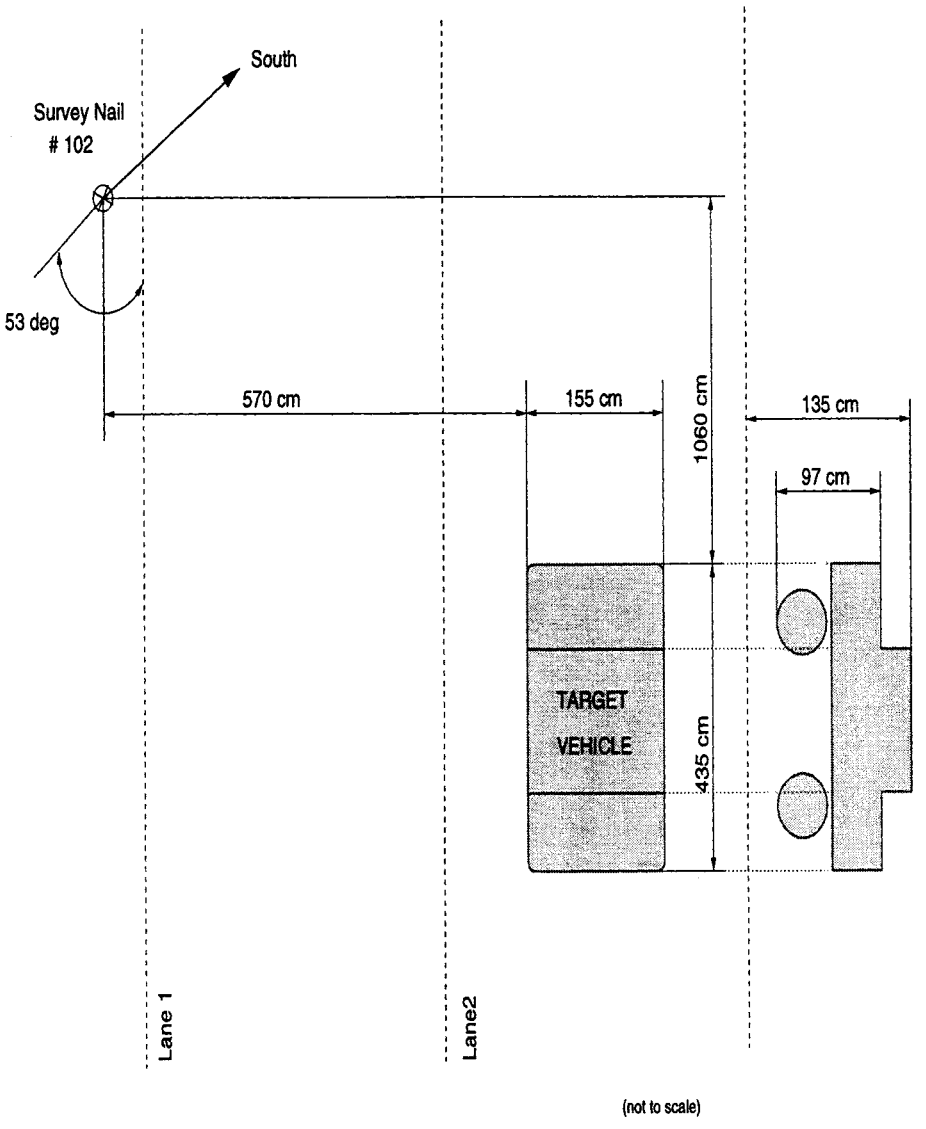

Figure 2.7: Location of the target vehicle by survey nail

This simulation was created in order to determine what the radar readings would be in a 'noiseless' idealized world. The actual radar unit receives reflections from the road, signs and other roadside objects, e.g., the Mn/ROAD test track has utility cabinets on the side of the road which may cause reflections. The computer simulation has no roadside objects, thus providing us with the expected radar readings for the target only. This information can be used to determine what parts of the signal are unwanted 'noise' and require filtering.

Chapter 3

3. Results

In this chapter we discuss the results of the radar experiments. First, we present the results of the fair weather experiments and the effects of the parameters characterized in the previous chapter. Then, the experimental data will be compared with the simulation data. Finally, we will present the results of the experiments run during snowfall conditions.

3.1 Results Obtained During Fair Weather

It was important to first learn about the performance of the EVT-200 in good weather conditions in order to have a baseline for evaluating its performance in snow. Furthermore, we wanted to determine how sensitive the radar is to parameters such as differential speed, yaw, pitch, etc. This is important so that we can determine potential mounting positions and orientations on a variety of vehicles given each vehicle's design constraints.

For brevity in figure captions, we shortened the notation for the experimental parameters that were adjusted during the experiments. The parameters, their abbreviations, and values are listed in Table 3.1. Many different configurations were used and the numerous abbreviations on the figures that follow may be difficult to keep track of. It may be helpful for the reader to bookmark Table 3.1 for future reference.

Experimental Parameters Varied in Radar Experiments	
Abbreviation	Parameter Description and Value
Pos FC	Radar Located in Front Center of Truck
Pos FR	Radar Located in Front Right of Truck
Pos RC	Radar Located in Rear Center of Truck
Pos RR	Radar Located in Rear Right of Truck
Yaw 0	Radar Oriented with zero degree yaw angle
Yaw 2R	Radar Oriented with a yaw angle of two degrees to the right
Yaw 2L	Radar Oriented with a yaw angle of two degrees to the left
Pitch 0	Radar Oriented with a pitch angle of zero degrees
Pitch 1D	Radar Oriented with a pitch angle of one degree downward
Pitch 2D	Radar Oriented with a pitch angle of two degrees downward
Pitch 2U	Radar Oriented with a pitch angle of two degrees upward
Pitch 4D	Radar Oriented with a pitch angle of four degrees downward
Pitch 4U	Radar Oriented with a pitch angle of four degrees upward
Pitch 6D	Radar Oriented with a pitch angle of six degrees downward
Pitch 6U	Radar Oriented with a pitch angle of six degrees upward
Speed 5	Host vehicle traveling at five mph
Speed 10	Host vehicle traveling at 10 mph
Speed 20	Host vehicle traveling at 20 mph
Speed 30	Host vehicle traveling at 30 mph
Same	Host and vehicle are in the same lane (right)
Adjacent	Host is in the adjacent (left) lane, target in the right lane

Table 3.1: Parameter Abbreviations

3.1.1 The Effect of Relative Speed

The target vehicle was stationary and positioned in the right lane of the two lane Mn/ROAD low volume test track (Figure 3.1). Therefore, the relative speed between the host and target vehicles is simply the speed of the host. We varied the speed of the tractor from 5 mph to 30 mph (roughly the speed at which snowplows operate with their blades down during a snow storm).

It should be noted that we started to collect data when the host achieved the desired testing velocity. This was the case for all experiments in which the host was in motion. We did not trigger data collection by a measured predetermined distance from the host, but at a distance that was greater than the sensor's maximum range. Even though we show the experiment time on the horizontal axis of the upcoming figures, there is no relationship between each experiment and absolute time (measured from data collection start time). For this reason, we shifted some of the data sets by a constant time interval whenever better clarity was achievable (i.e. prevent

overlapping data). The relative time between data points is accurate because we synchronized our data collection based upon the GPS data acquisition rate of five Hz.

Figure 3.1: Mn/ROAD low volume test track

To isolate the effect of relative speed, the yaw and pitch angles of the radar were held constant for each run. The results of the experiment with the radar mounted in the front center position and traveling in the same lane of the target are shown in Figure 3.2 and Figure 3.3.

First, notice that the radar produces a zero range and range rate when no target is detected. This is evident at the beginning of the 30 mph experiment (experiment time zero to seven seconds). The range is also zero when the host comes to a full stop because radar isn't designed to detect objects with no relative velocity to itself (both host and target vehicle stationary).

The range data collected when the host was traveling at 30 mph is much 'cleaner' than the data at five mph. This trend held true for all speeds in between 5 and 30 mph (not shown to prevent cluttering the figure). This result is expected due to the fact that the sensor uses the Doppler effect to detect targets. Electro-magnetic waves reflected off of moving objects (relative to source) will return with a shift in frequency and phase. The EVT- 200 uses this fact to obtain the

range and range rate readings, respectively. Small Doppler shifts (relative velocity) provide lower accuracy due to the precision limits of the circuitry.

The range results for the five mph experiment are more inconsistent at greater ranges than at close ranges. Targets at large ranges return weak signals due to attenuation of electromagnetic waves in the atmosphere, specular scattering and scintillation. This compounds the problem by not only providing a narrow Doppler shift due to the low relative speed, but also a weak signal which is difficult to discern among signal noise.

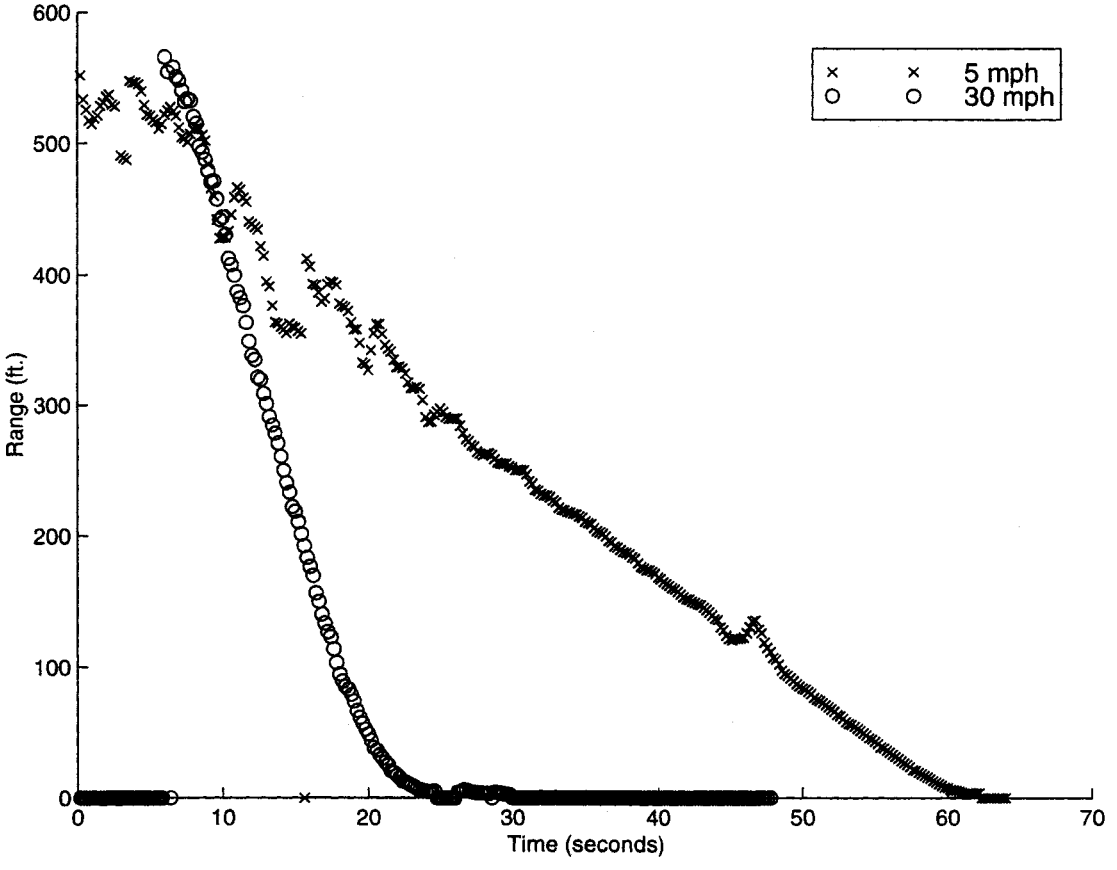

Figure 3.2: Effect of relative speed on range with Pos FC, Yaw 0, Pitch 0, Same Lane

Figure 3.3 shows the range rate reading from the same experiment. Notice that range rate signal is fairly clean in both experimental runs. This observation holds for all the experiments performed on the EVT-200. The sensor measures range rate more accurately than range.

The area of the figure where the range rate is constant shows when the host was traveling at a constant speed towards the target. The area of the figure where the range rate decreases (absolutely) shows when the host was decelerating in order to avoid a collision with the target vehicle (acceleration is the derivative of velocity and since the target vehicle is stationary, the range rate equals velocity).

The range rate readings get noisier as they approach zero ft/s. This effect is clearly related to the low relative speed between the host and target which produces small frequency shifts. Fortunately, this effect is easy to filter out by determining a cut off range rate reading where the sensor is no longer effective.

Since the range rate data has less noise and is generally more robust than the range data, we will henceforth show only the range plots unless there is a specific effect we want to discuss. This will also cut down on the number of plots in this report, but not limit the amount of information we wish to present.

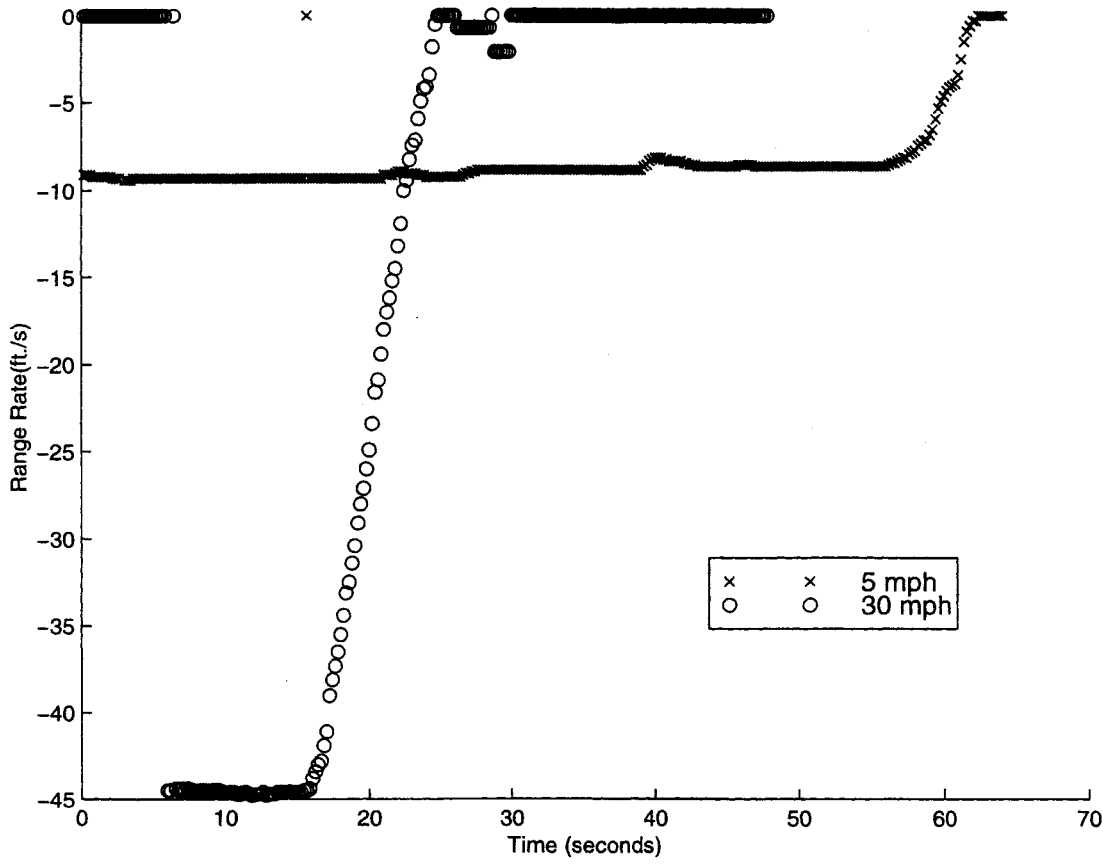

Figure 3.3: Effect of relative speed on range rate with Pos FC, Yaw 0, Pitch 0, Same Lane.

We performed the same experiment, but with the radar on the front right position on the host, the host in the adjacent (left) lane and the radar pointed two degrees to the right (Yaw 2R). The results are shown in Figure 3.4. Again, the range readings for higher speeds are better than the smaller relative speed experiment. At longer ranges, the radar had difficulty consistently detecting the target vehicle when the speed differential between the two vehicles was low. Furthermore, for the 10 mph experiment, the radar lost lock on the target vehicle between 200 and 300 ft. This result is difficult to explain because we are not privy to the internal target detection algorithms used in the EVT-200. We did observe, however, that this behavior only occurred when the relative speed between the host and target was low and when the radar was not pointed directly at the target. Both these situations consistently proved most challenging for this radar unit.

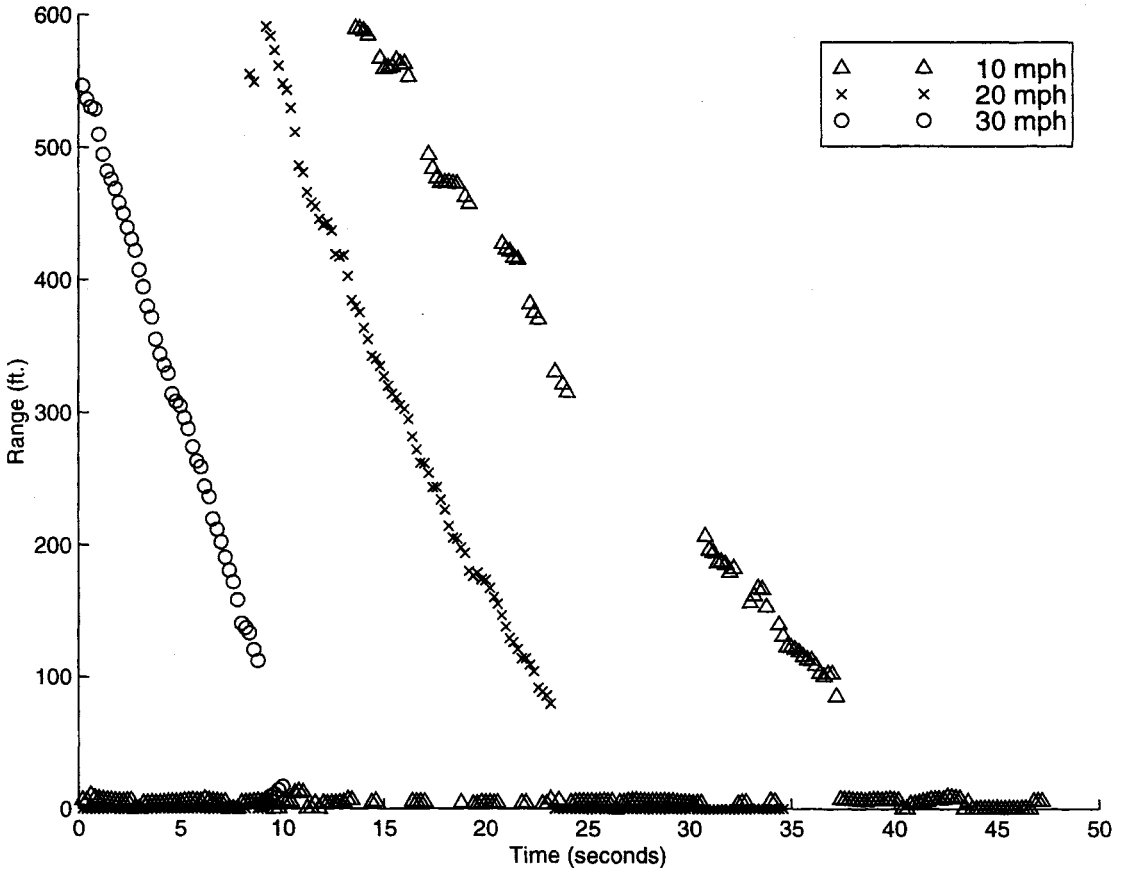

Figure 3.4: Effect of relative speed on range with pos RC, Yaw 2R, Pitch 0, Adjacent Lane

3.1.2 The Effect of Yaw Angle

The radar mount that we used allows the yaw angle of the radar to be independently adjusted and measured. This was used to see how sensitive the radar is to yaw orientation deviation. This experiment was conducted to evaluate the effect of inaccurate mounting of the radar in the yaw direction. Figure 3.5 shows the results when the radar was located in the front center position and the host vehicle was driven toward the target in the same lane. The yaw was then changed to two degrees to the right and two degrees to the left. We chose two degrees because the azimuth cone angle of the radar is specified to be four degrees. Degradation of the signal would logically start to happen at that orientation because only the far edge of the main lobe would be reflected by the vehicle.

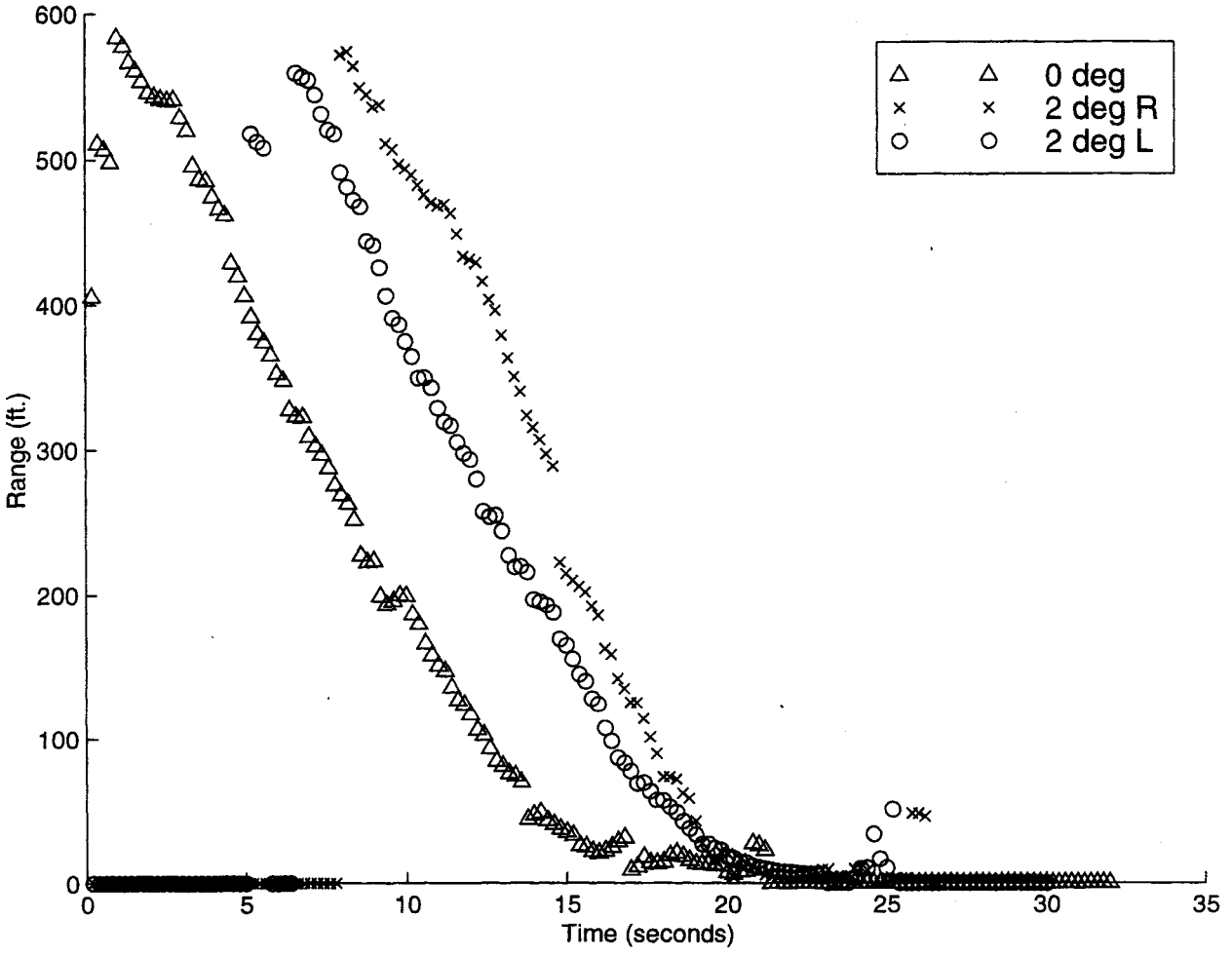

Figure 3.5: Effect of Yaw on range with Pos FC, Pitch 0, Speed 30, Same Lane

The results show that there is no significant difference in the resulting range data. This result is somewhat surprising. One would expect that the signal at the outer edge of the main lobe would be slightly attenuated, causing reflections at long ranges difficult to detect. A possible explanation of the radar's tolerance to yaw deviations of two degrees is that the beam diverges at a greater than four degree azimuth angle. We decided not to pursue experiments at a larger yaw angle because mounting misalignments at two degrees was clearly noticeable to the eye. Maintaining a mounting tolerance under two degrees should be readily achievable.

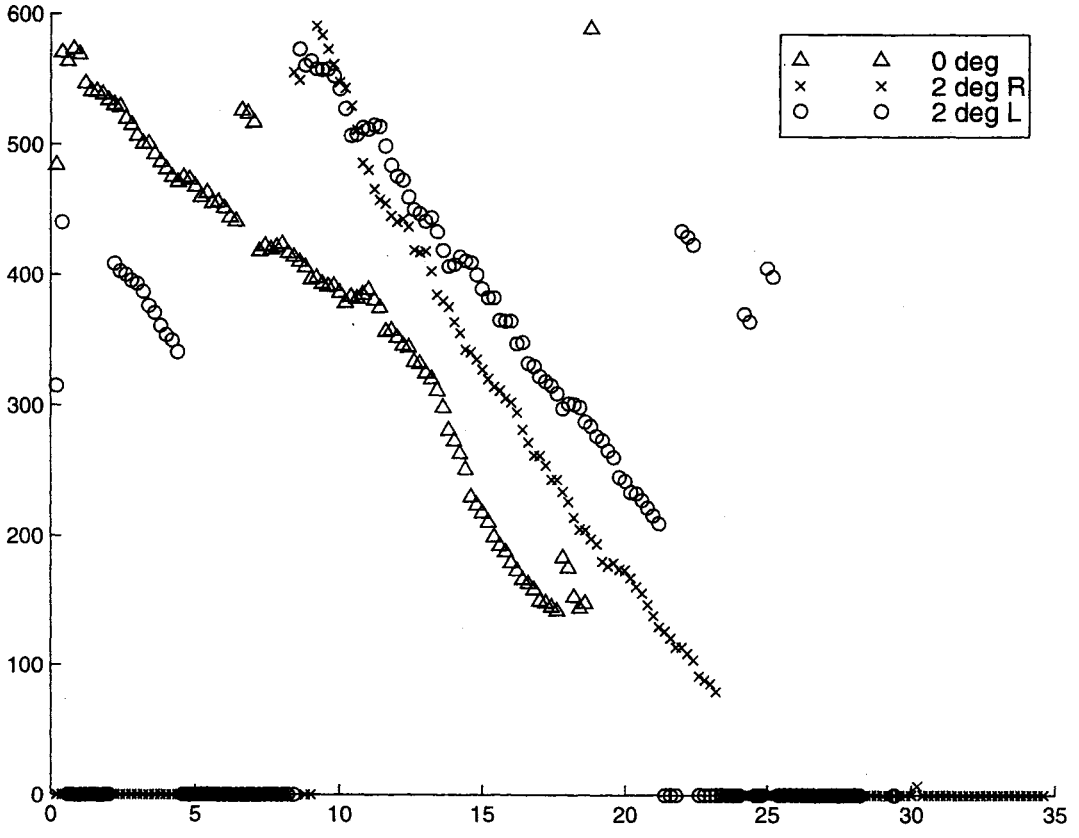

Figure 3.6: Effect of Yaw on range with Pos FR, Pitch 0, Speed 20, Adjacent Lane

The experiment was repeated with the radar located on the front right of the vehicle while the host traveled in the adjacent (left) lane (see Figure 3.6). We wanted to determine if the radar would detect a target in an adjacent lane and if yaw deviations affected this detection capability. When the radar was pointed to the right (Yaw 2R), it detected the target at a longer range and continuously tracked it down to a range of about 80 ft. When the radar was pointed straight ahead (Yaw 0), it tracked the target down to around 140 ft. The worst case is when the radar was oriented with a yaw of two degrees to the left (Yaw 2L). With that orientation, it lost track of the target vehicle at over 200 ft. Furthermore, it detected objects other than the target vehicle. This behavior is predictable given the geometry of the radar beam and the orientation of the radar antenna. It is interesting that the radar could even detect the target vehicle with a yaw of two

degrees to the left, because the radar beam cone is specified as diverging at four degrees in azimuth. This provides more evidence that the cone angle may be larger than four degrees.

3.1.3 The Effect of Pitch

The mount that we used for the radar also provided the ability to adjust and measure the pitch angle. A vernier dial was used to measure the pitch angle which was varied from zero to six degrees in the upward an downward direction.

The results of an upward pitch angle are shown in Figure 3.7. As expected, an upward pitch aims the radar such that it does not detect the target vehicle at large ranges. At a zero degree pitch angle, the target was first detected at a range of just under 600 ft. At four degrees pitch, the radar first detected the target at around 500 ft. Finally, at six degree downward pitch, the radar didn't detect the target vehicle until it was slightly over 200 ft. from the host.

It should be pointed out that there are no overhead obstructions (e.g. overpasses, road signs and the like) at the Mn/ROAD test track. On real highways, reflections off of these highway features may cause false target detection readings. For that reason, it is desirable to orient the radar with a zero or slightly negative pitch. In fact, the installation guide to the Eaton VORAD collision warning system recommends that the antenna be aligned one degree downward from horizontal [24].

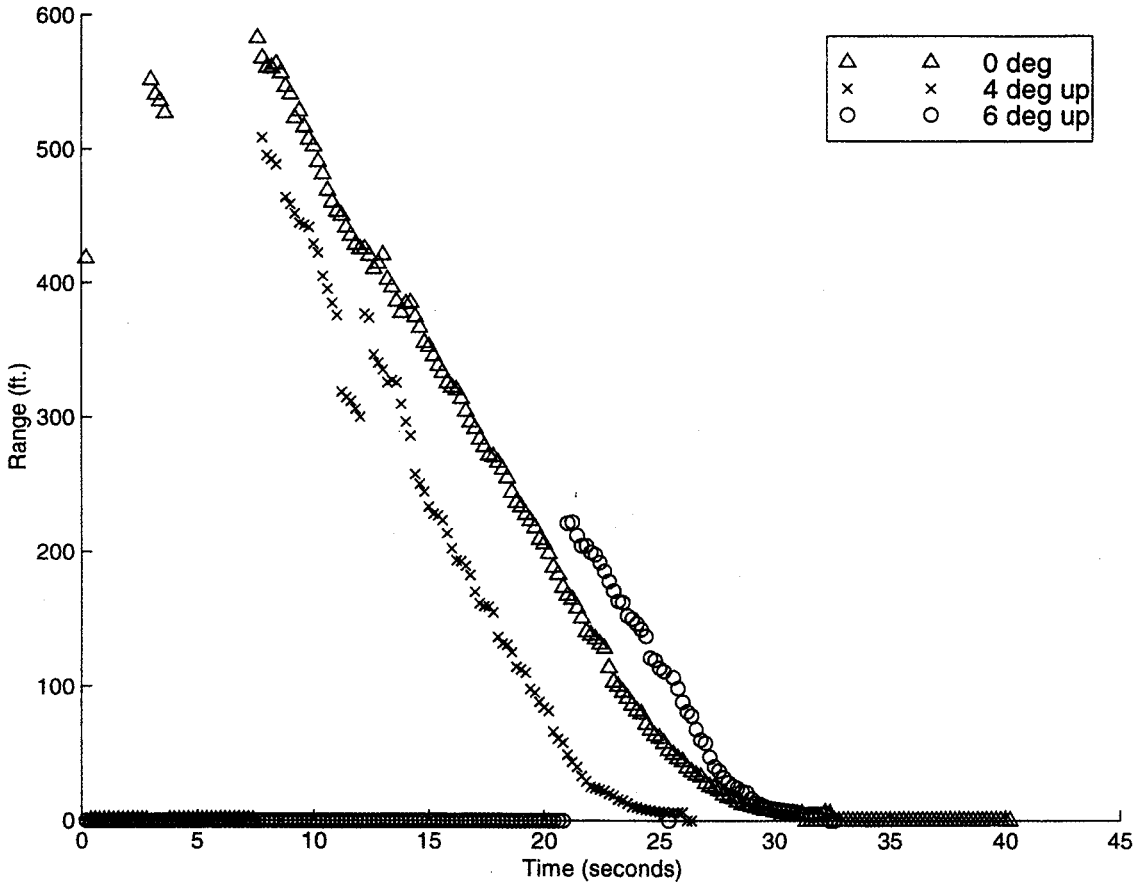

Figure 3.7: Effect of Upward Pitch with Pos FC, Yaw 0, Speed 20, Same Lane

The pitch was also adjusted to point downward and the experiments were repeated with a negative pitch up to six degrees downward. The results are similar to the upward pitch. As the pitch angle decreases (greater negative value), the maximum range at which the radar could detect the target vehicle decreases. This is most likely due to the radar signal reflecting off the pavement (forward scattering). Another effect observed during these sets of experiments was that the range was measured to be around 6000 ft for a few data points with a downward pitch of six degrees (this was not shown in Figure 3.8 because the large scale caused by the 6000 ft readings makes the rest of the data points indiscernible). We inquired Eaton VORAD about this unexpected result and they claim to have corrected this in their newer units. It is also very simple to filter out these very large range readings, so no further investigation was warranted.

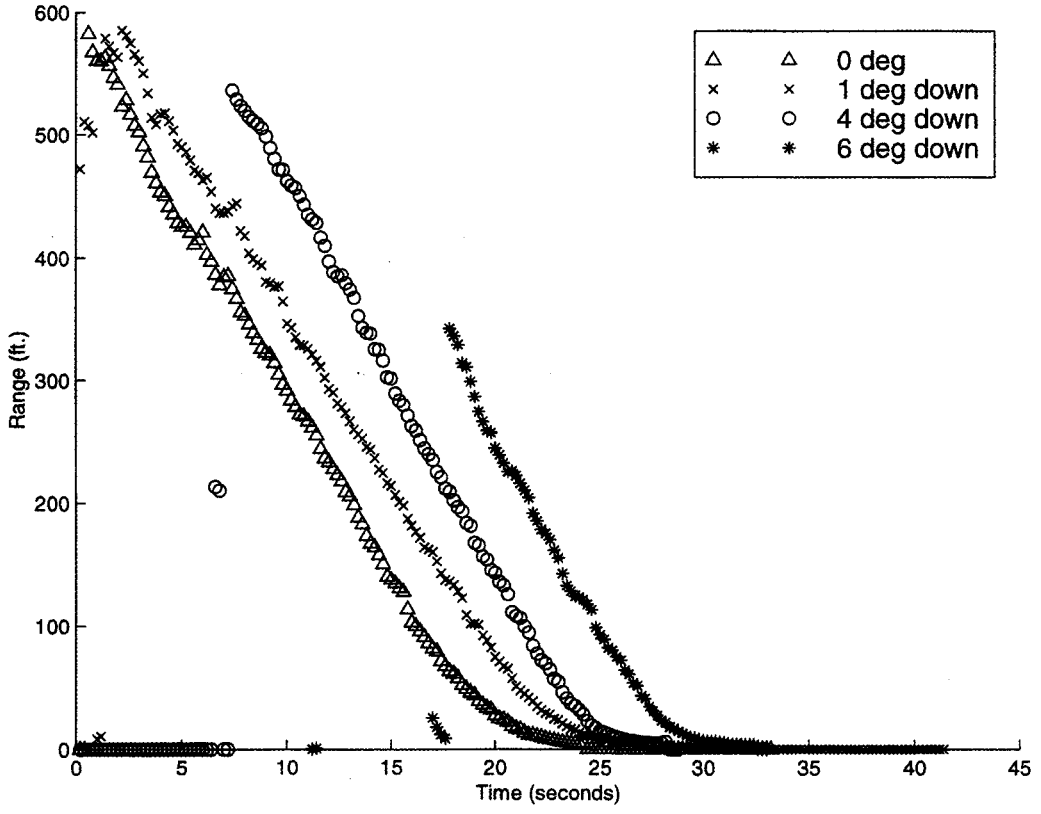

Figure 3.8: Effect of downward pitch with Pos FC, Yaw 0, Speed 20, Same Lane

3.1.4 The Effect of Radar Location

The mounting was designed to allow the radar to be placed in six different locations on the truck (see **Figure 2.2**). Four of these locations were used during the radar experiments because the other two (front left and rear left) can be inferred by symmetry.

It may not be possible to mount the radar in the direct center (laterally speaking) of a snow plow due to the large blade mounted on the front. The experimental results of Figure 3.9 show this effect when the radar is placed at the extreme front right corner of the host and is driven toward a target in the same lane (worst case). Notice that the radar was able to detect the target vehicles in both mounting locations. The range reading did show more variation with the radar mounted on the far right of the host than in the direct center. The center is clearly the best location to mount

the radar for detecting vehicles directly in front of the host, however, the radar still detects vehicles not directly in its line of sight if lateral mounting offsets are unavoidable.

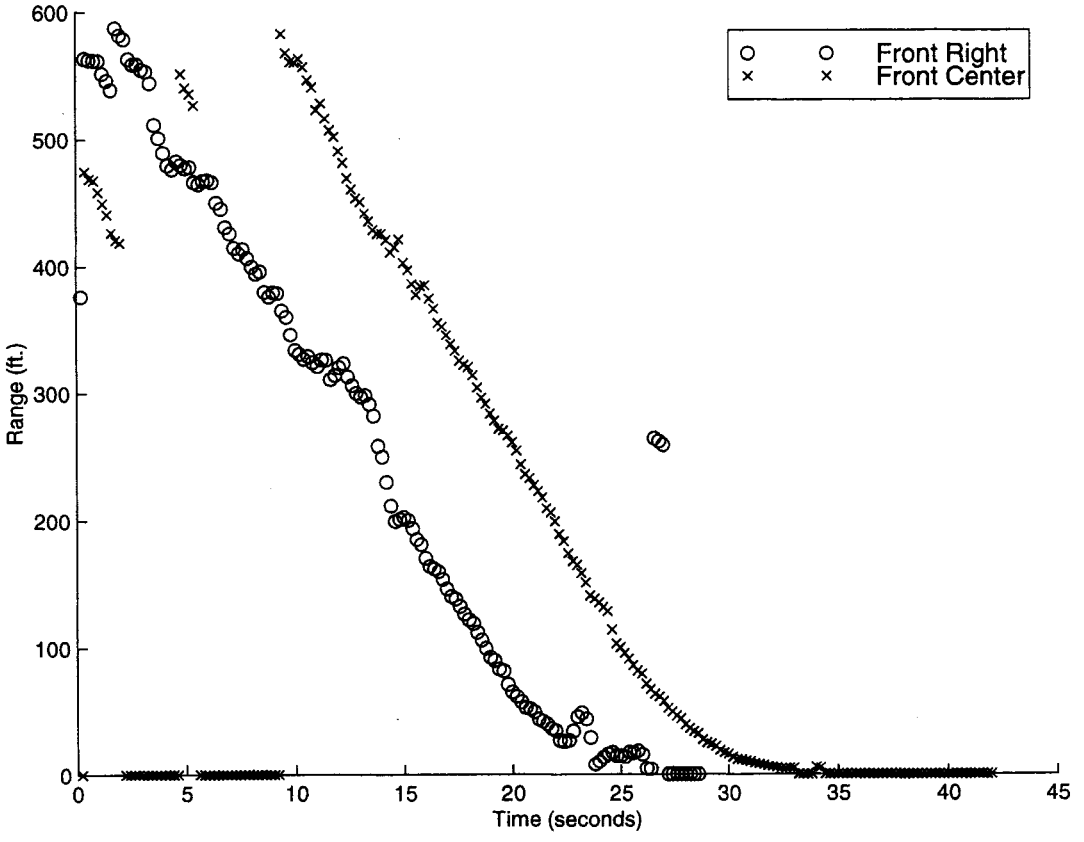

Figure 3.9: Effect of radar location on range for Yaw 0, Pitch 0, Speed 20, Same lane

The data collected with the radar mounted in all four test positions on the host is shown in Figure 3.10. The radar unit can detect vehicles that are moving away from it equally well as vehicles that are approaching it. Of course, vehicles with positive relative speeds (moving further apart from each other) pose less of a threat than ones with a negative relative speed (approaching each other). For this reason, a majority of time was spent analyzing the situation where the two vehicles have a negative relative speed. Furthermore, we performed a majority of the experiments with the radar on the front of the host because we were able to more easily control the host's speed and we had better visibility of the target vehicle which made the experiment safer. If we

would have mounted the radar on the back of the host to perform negative relative velocity experiments we would have had to drive the host in reverse. The gear ratio when the transmission was in the reverse limited the speed at which we could perform such an experiment. Also, it is more difficult to see the target vehicle and radar when it is mounted on back.

It may be desirable to have a radar mounted on the back of a snow plow to measure the velocity of fast approaching vehicles from behind. As far as the radar is concerned, this situation is the same as the one we tested extensively, namely, driving a front mounted radar toward a stationary vehicle. The radar does not know the host's velocity or where it is mounted but just measures relative velocities from reflecting targets. The results from the front mounting position should be valid for rear mounting experiments.

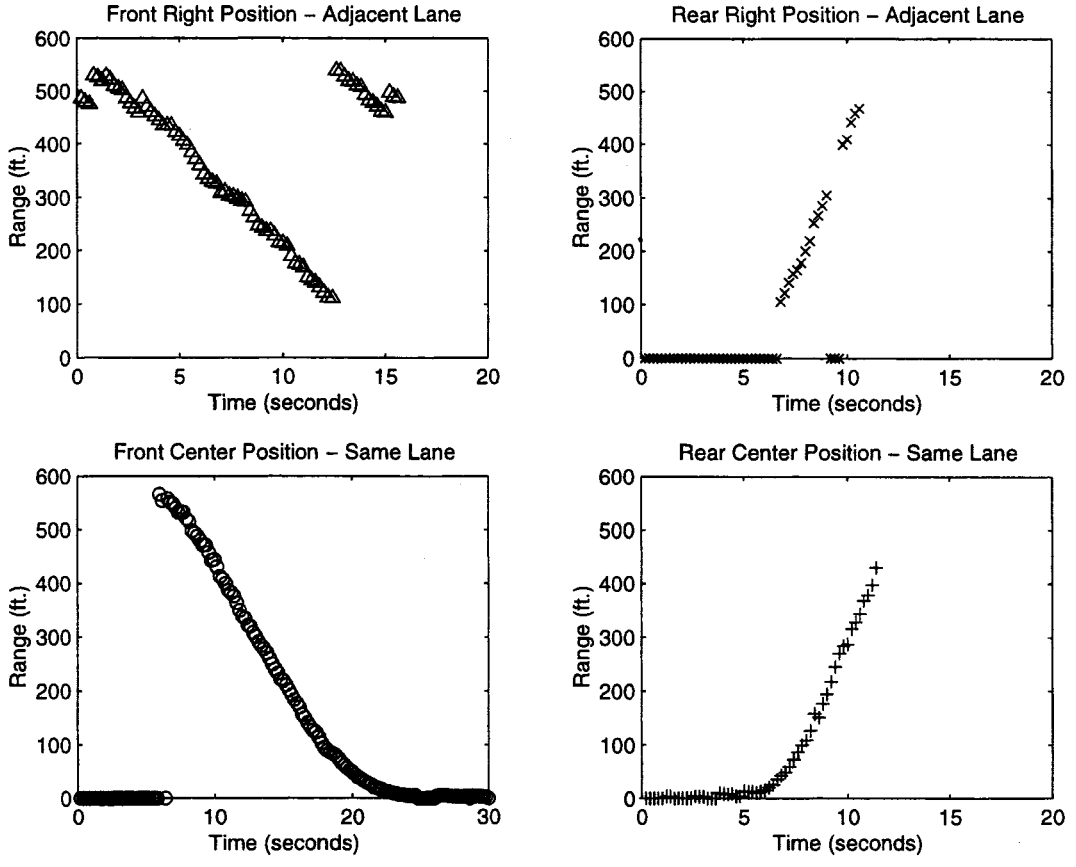

Figure 3.10: Range plots from all four radar locations, Yaw 0, Pitch 0, Speed 30

3.1.5 The Effect of Vibration

Since the principal physical phenomenon behind the EVT-200 is the Doppler effect, vibrations caused by the host vehicle itself may effect the normal operation of the sensor since vibrations are, in effect, small displacements (velocity). For example, assume the host is stationary but the engine is running. Do the vibrations from the engine produce enough relative motion compared with the wavelength of the electromagnetic wave for the radar to detect another stationary vehicle? Could the vibration cause the radar to register a target which is not there? To answer these important questions, an experiment was performed in which the host vehicle was stationary and the target was moved. The host vehicle's engine was turned off to eliminate vibrations to the radar antenna.

Up to now, every experiment was performed with the host in motion and the target stationary. In these set of experiments, the host was stationary in the right lane and the target vehicle was driven toward it at different speeds. First, a static experiment was performed in which the target vehicle was parked at about 35 ft in front of the host. Data was collected when the truck engine was turned on and idling and when the truck engine was turned off (no vibration). The results are shown in Figure 3.11.

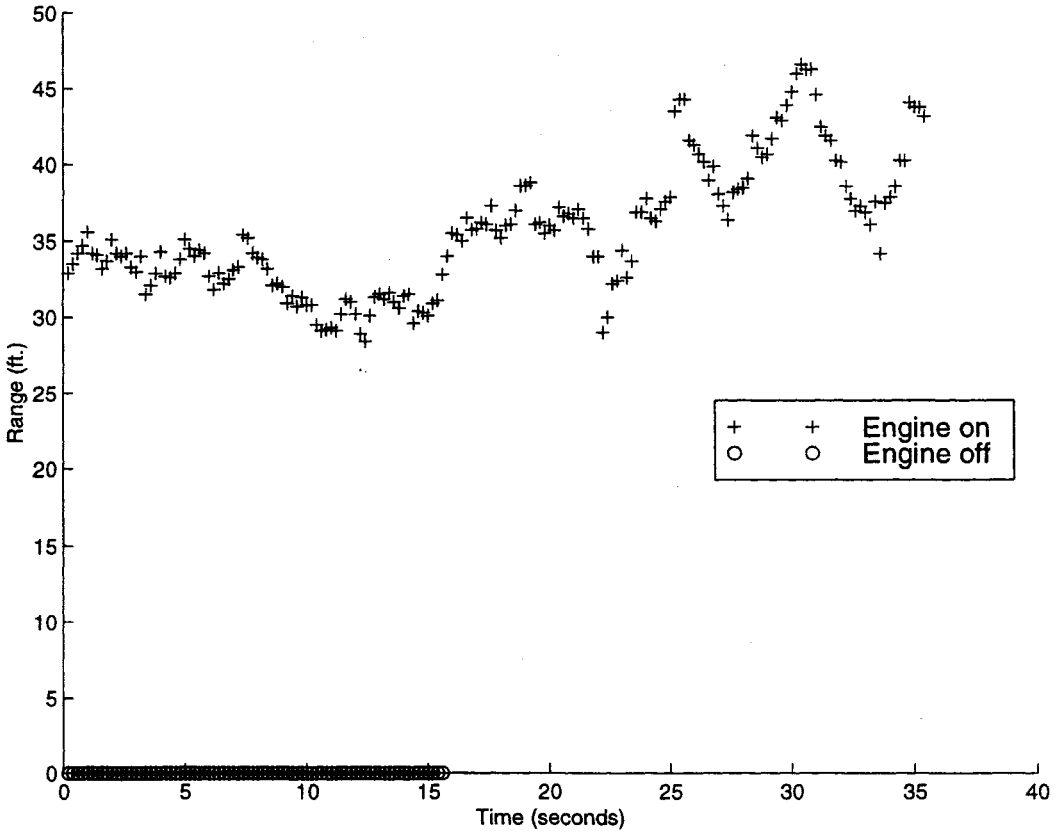

Figure 3.11: The effect of vibration on range - static experiment

It is clear that the radar detected the target vehicle when the truck's engine was on, even though there was no relative velocity between the vehicles. Conversely, the radar did not detect any objects when the truck engine was off. The only modified parameter was the vibration and it is clear that the vibration of the engine was enough to cause the radar to detect the target vehicle even though the relative velocity between the two vehicles was zero. Another interesting result of this experiment is in the range rate data, shown in Figure 3.12. The range rate held mostly constant and at -0.6 ft/s when the radar was subjected to vibration. It is zero when there is no vibration.

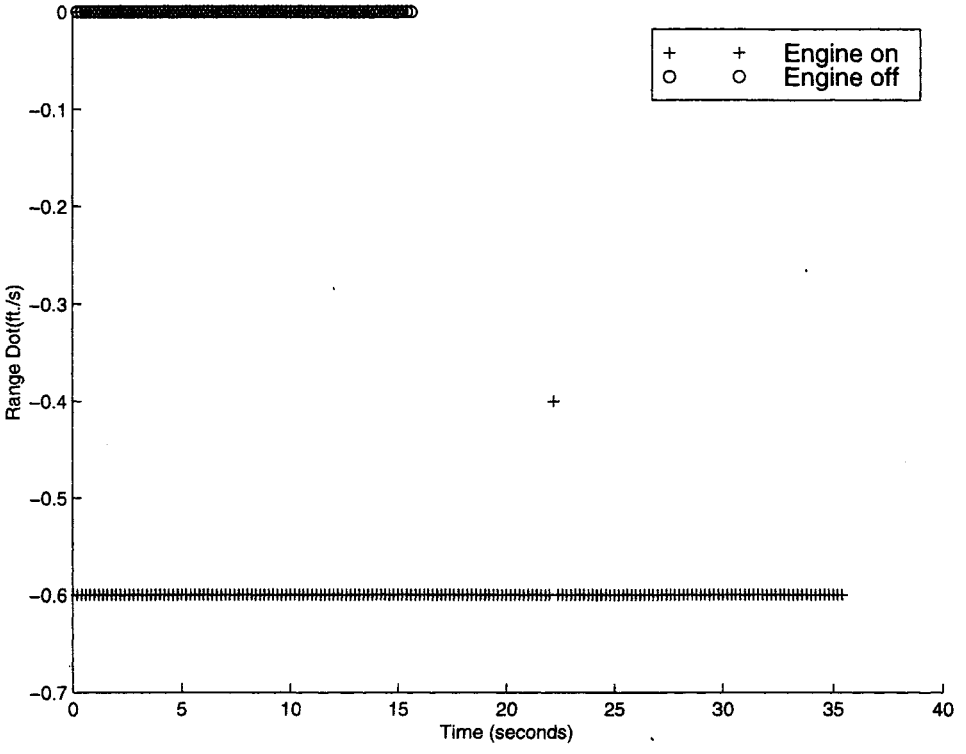

Figure 3.12: The effect of vibration on range rate - static experiment

The same experiment was repeated with the target vehicle moving towards the host vehicle at 10, 20 and 30 mph. The result when the target vehicle was driving toward the host at 20 mph is shown in Figure 3.13. When the host vehicle's engine was turned off (no vibration), the radar detected the target at around 600 ft and tracked it all the way until it stopped in front of the host. When the truck engine was on (vibration), the radar 'wandered' at a range of around 100 ft until the target was within 100 ft. Only then did the radar switch to tracking the target.

Further evidence of this is shown in the range rate plot in Figure 3.14. With the truck engine off, the radar detects the target vehicle accelerating towards it at a large range (positive relative acceleration is indicated by increasing range rate). Once the target reached its desired speed it maintained that speed for around ten seconds and then decelerated to a stop to avoid colliding with the host (this is shown by the decreasing range rate). For the vibration (engine on) experiment, the range rate value was constant at around 1 ft/s until the target vehicle approached

within about 100 ft. The radar then switched to tracking the target vehicle as evidenced by the range rate value jumping to match the target vehicle's speed.

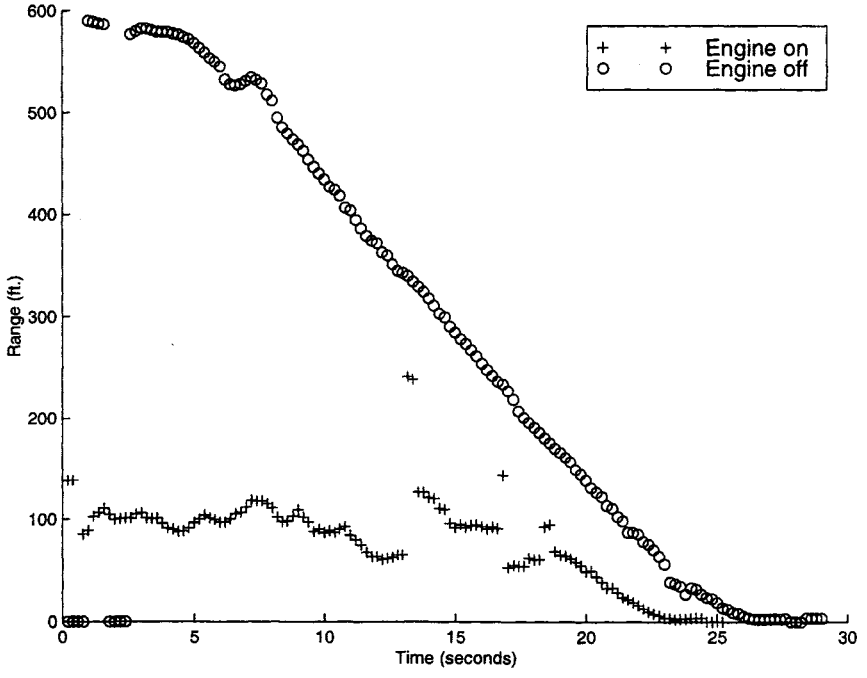

Figure 3.13: The effect of vibration on range with target moving at 20 mph

The EVT-200 incorporates a filtering algorithm and a target detection algorithm. We are not privy to the details of the algorithms, therefore, we contacted Eaton VORAD for an explanation. They stated that a capacitor which was sensitive to vibration was the culprit. They also said they have fixed this problem and that newer EVT-200 radar units are not sensitive to engine vibrations.

On a snowplow, the blade scrapping along the pavement produces an even harsher vibratory environment. Future tests on newer units should be conducted to confirm that the vibration sensitivity issue with the EVT-200 has been resolved.

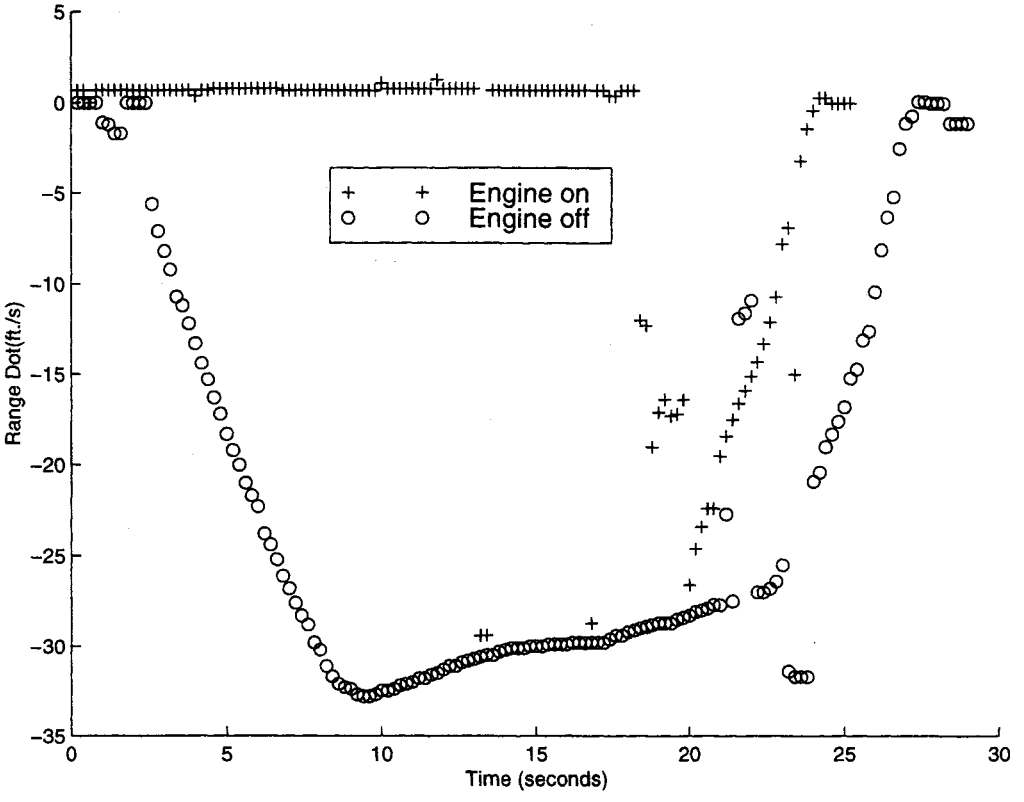

Figure 3.14: The effect of vibration on range rate with target moving at 20 mph

3.1.6 Repeatability

It is important for a sensor to produce the same results under the same set of conditions. We tested the repeatability of the EVT-200 by repeating the same experiment several times. The results of this experiment are shown in Figure 3.15. The data points in this figure are the average range of three experiments with the same parameters (speed, yaw, pitch). Note that only ranges less than 350 ft are considered because the Eaton VORAD specifications only guarantee this value as the maximum range of the sensor [24]. The vertical lines are the standard deviation of each averaged data point. Clearly the standard deviation decreases as the range decreases. Table 3.2 quantifies this observation by averaging the standard deviations for a 50 ft range of range values. The standard deviation is smallest at the 0 - 50 ft range and grows with increasing range.

This observation indicates that the sensor could have more difficulty calculating the range to a target accurately at longer ranges. We will further investigate this behavior in the next section when we compare the experimental data to the expected data obtained by a computer model.

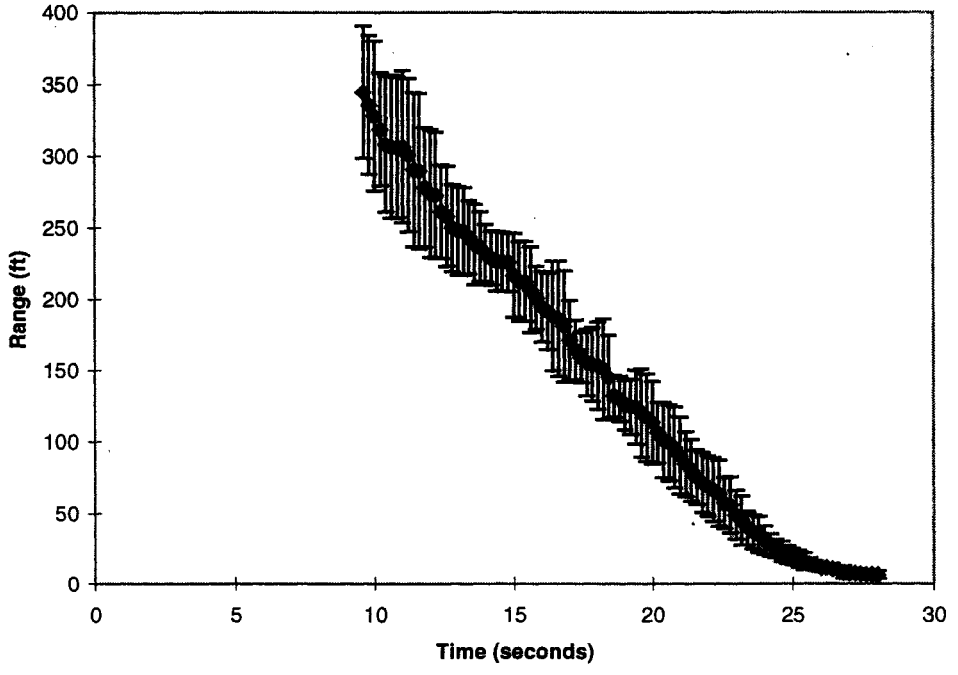

Figure 3.15: Repeatability of range for Pos FC, Yaw 0, Pitch 0, Speed 10, Same Lane. The bar at each point represents ±1 std. deviation.

Average Standard Deviation	
Range(ft)	Average σ (ft)
0 - 50	6.4
51 - 100	22.4
101 - 150	23.6
151 - 200	25.2
201 - 250	25.7
251 - 300	44.9
301 - 350	48.0

Table 3.2: Average standard deviation of range for three identical experiments

3.2 Comparison Against Predicted Values Based on Simulation

To compare the radar's measurements with ground truth, Differential Global Positioning System (DGPS) data collected during the experiments was used to drive a computer simulation that produces expected range data using a geometric radar model. Knowledge of where the target is located, host and target geometry, and collected DGPS data are used to arrive at an expected range for the radar sensor.

A graphical C languaged-based solid geometric modeling library called World Tool Kit (WTK) was used to create a virtual three dimensional geometrical simulation of the experiment. Actual DGPS data collected during the experiments was used to drive the simulation. Every DGPS location in the experiment tells the simulation where to locate the virtual host vehicle. The target vehicle was located by measuring its offset distance from a known surveyed location (see **Figure 2.7**).

It should be noted that while the virtual world in the simulation is three dimensional, the radar beam was modeled in two dimensions. In this solid modeling environment, the radar beam can be modeled as a 'solid' entity. The range is then calculated by determining which facets of which objects are 'intersected' by the radar's transmitted beam 'volume'. However, instead of a three dimensional cone representing the radar beam, a two dimensional triangular plane (parallel to the ground) was used to detect the target vehicle. Furthermore, to simplify the geometry and programming associated with the contours of the target vehicle, an invisible box was placed surrounding the target vehicle. Intersections between the radar beam and the imaginary box are used to calculate the range readings of the virtual radar. This compromise is justified by the fact that we do not know where on the target vehicle the actual reflections of the radar that we were using occur. The most common reflection locations of radar on vehicles are the bumper, license plates, transmission housing and tires [25]. Since these lie at different longitudinal distances from the host we cannot predict for certain what the exact range should be, even though the DGPS has a longitudinal accuracy of less than five cm [23]. It is reasonable to assume, however, that a majority of the reflections occur at the bumper and back end of the car because it has a larger cross sectional area than the tires or transmission housing and it lies roughly normal to the radar's

line of sight. The computer simulation assumes that the reflections occur at the location of the bumper. The possible uncertainly caused by this assumption is less than the length of the target vehicle and should be taken into consideration when reviewing the following results.

The simulation results for an experiment with the radar oriented straight ahead and the host traveling at 10 mph and in the same lane as the target is shown in Figure 3.16. As in the previous section, we have only displayed data for range values less than 350 ft, which is the maximum range specified by the manufacturer. The lower subplot is the error between the measured radar range and the predicted range calculated from DGPS during simulation. The average error for this experiment was -8.0 ft and the standard deviation of the error was -10.2 ft. The plot shows that the experimental range data becomes increasingly divergent from the simulated data as the range increases. Any error in measuring the target vehicle location or radar mount location would result in a constant offset and would not explain this growing difference. A weak return signal caused by attenuation in the atmosphere and a small phase shift (used to calculate range) caused by the small relative speed between the host and target would seem to be the reasons for these experimental results.

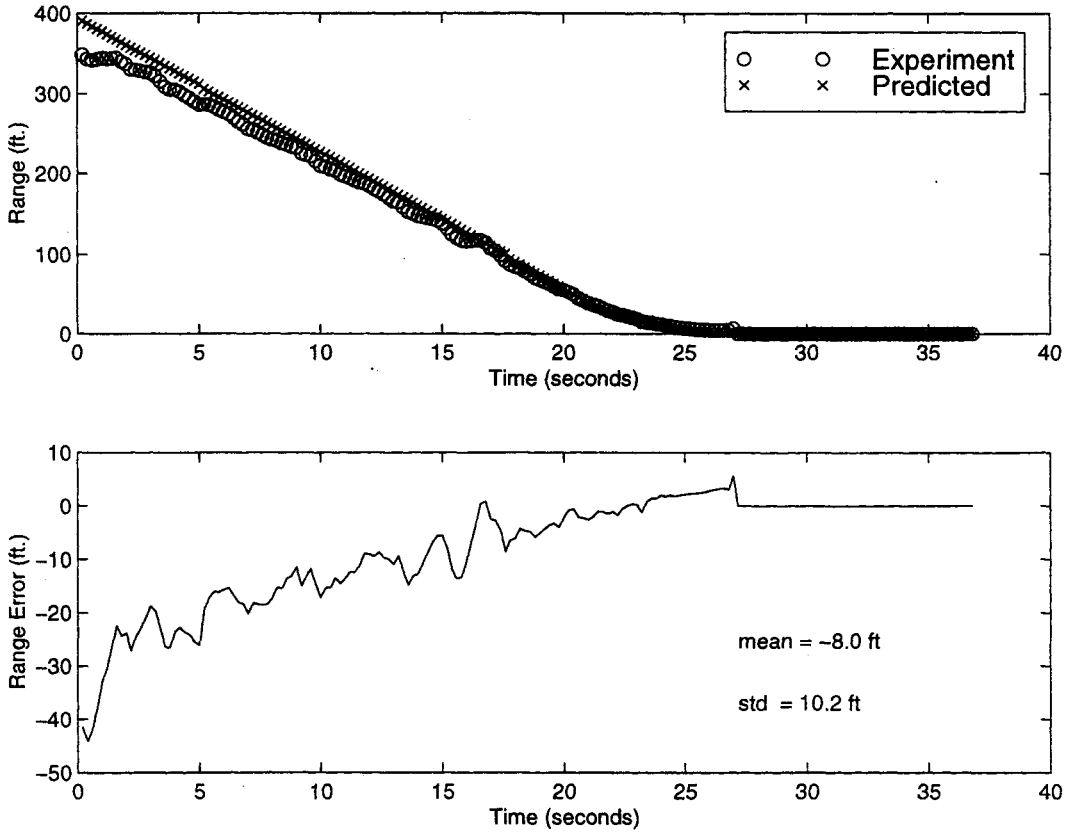

Figure 3.16: Experimental vs. simulated range for Pos FC, Yaw 0, Pitch 0, Speed 10, Same Lane

The simulation was run for the same configuration for the host traveling at 30 mph. The result is shown in Figure 3.17. Notice that the mean error decreased from -8.0 ft to -3.5 ft and the standard deviation decreased from 10.2 ft to 7.6 ft compared to the 10 mph experiment. The trend of an increasing difference between experimental and simulated range data at larger ranges is still apparent, but less prominent. The greater phase shift of the reflected signal due to the larger speed differential was most likely responsible for the improved results. Nevertheless, the weak reflection due to atmospheric attenuation and specular scattering offset the wider phase shift at large ranges.

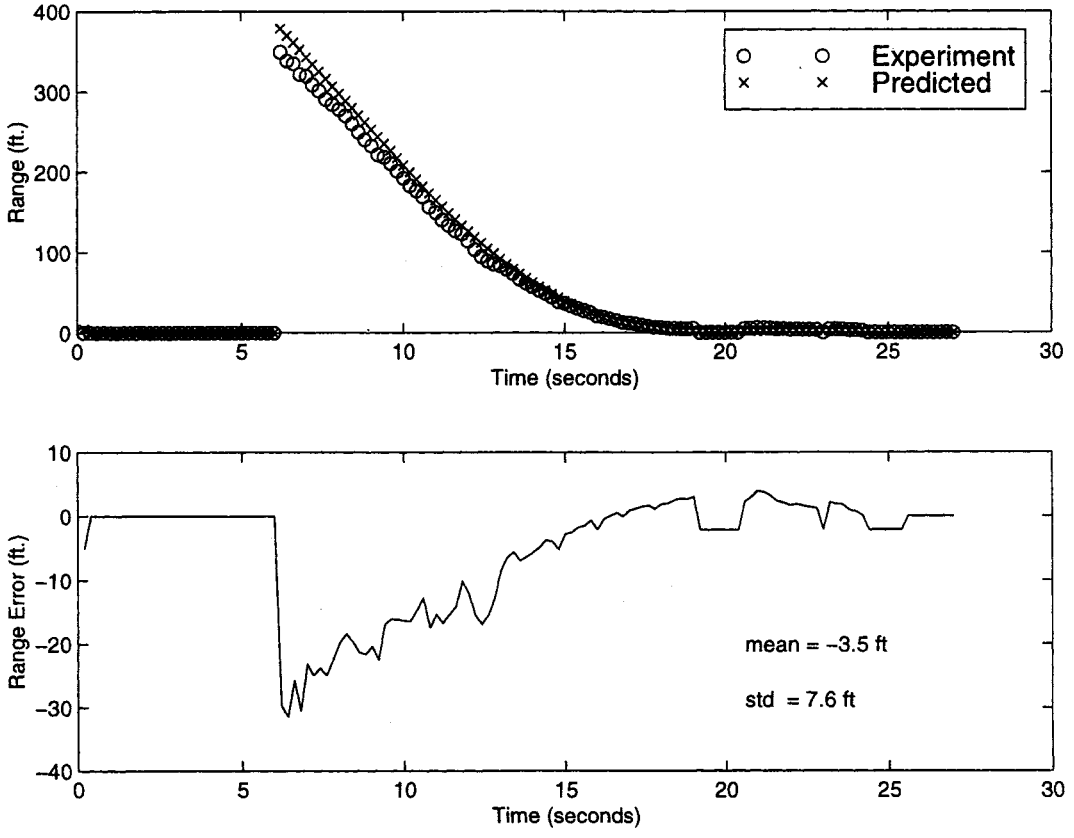

Figure 3.17: Experimental vs. simulated range for Pos FC, Yaw 0, Pitch 0, Speed 30, Same Lane

The results for the radar mounted on the front right and the host traveling at 20 mph in the adjacent lane are shown in Figure 3.18. The mean error was 3.2 ft and the standard deviation was 8.4 ft. It is interesting that the error was roughly the same at longer range and closer range. The error did increase at ranges greater than 350 ft (not shown because the maximum specified range of this sensor is 350 ft). The geometry of the radar beam (four degrees azimuth divergence) and the orientation of the radar (2R) in this experiment are such that the radar was not able to detect the target vehicle down to very low range as evidenced by both the experimental and the simulated range data. Thus, it is not possible to predict if the range error would have decreased further as the range decreased below 100 ft.

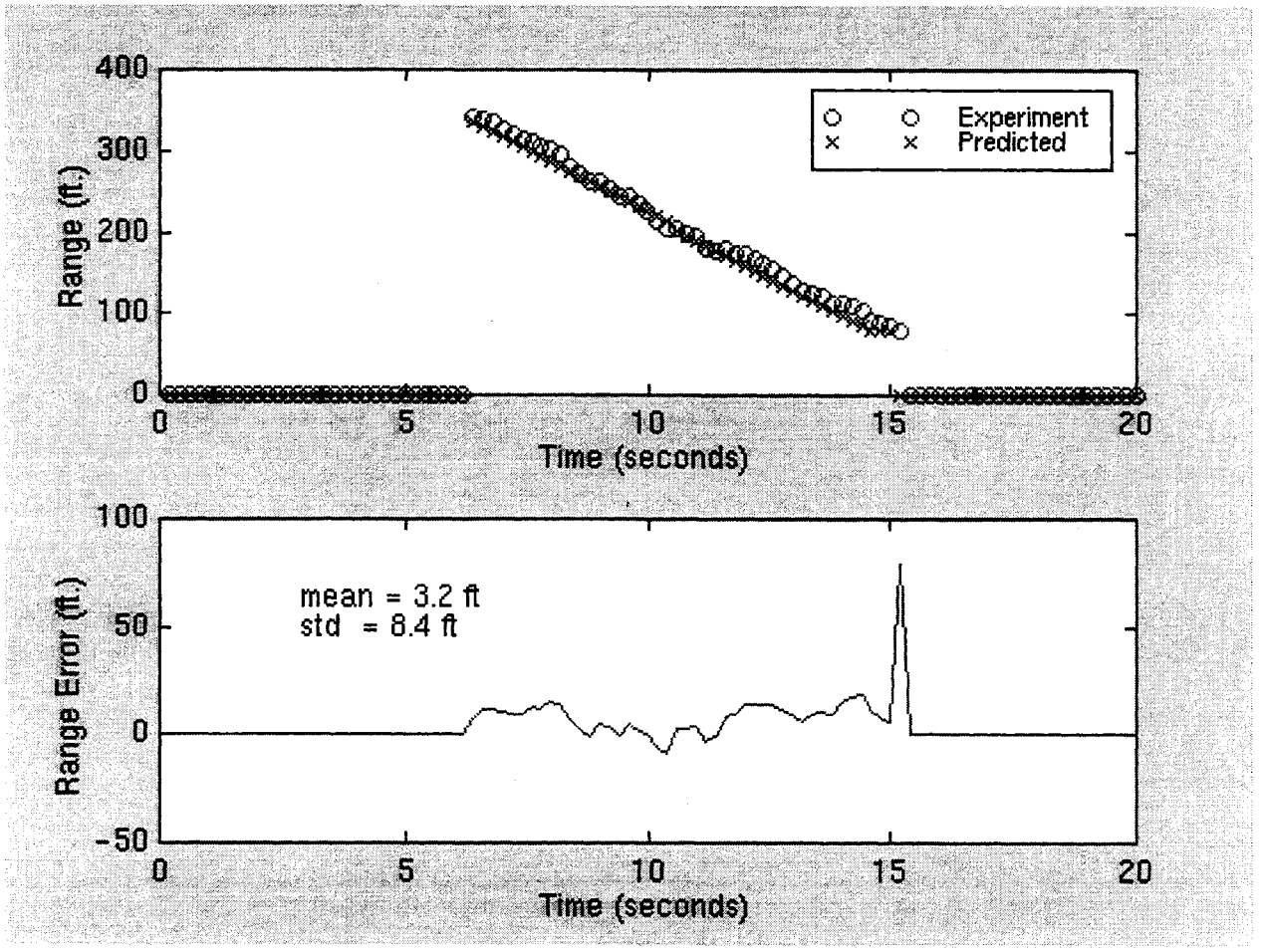

Figure 3.18: Experimental vs. simulated range for Pos FR, Yaw 2R, Pitch 0, Speed 20, Adj. Lane

Figure 3.19 shows the same experimental configuration except the host was traveling at 30 mph. Consistent with previous results, the mean error and standard deviation decreased due to the increased differential velocity between host and target.

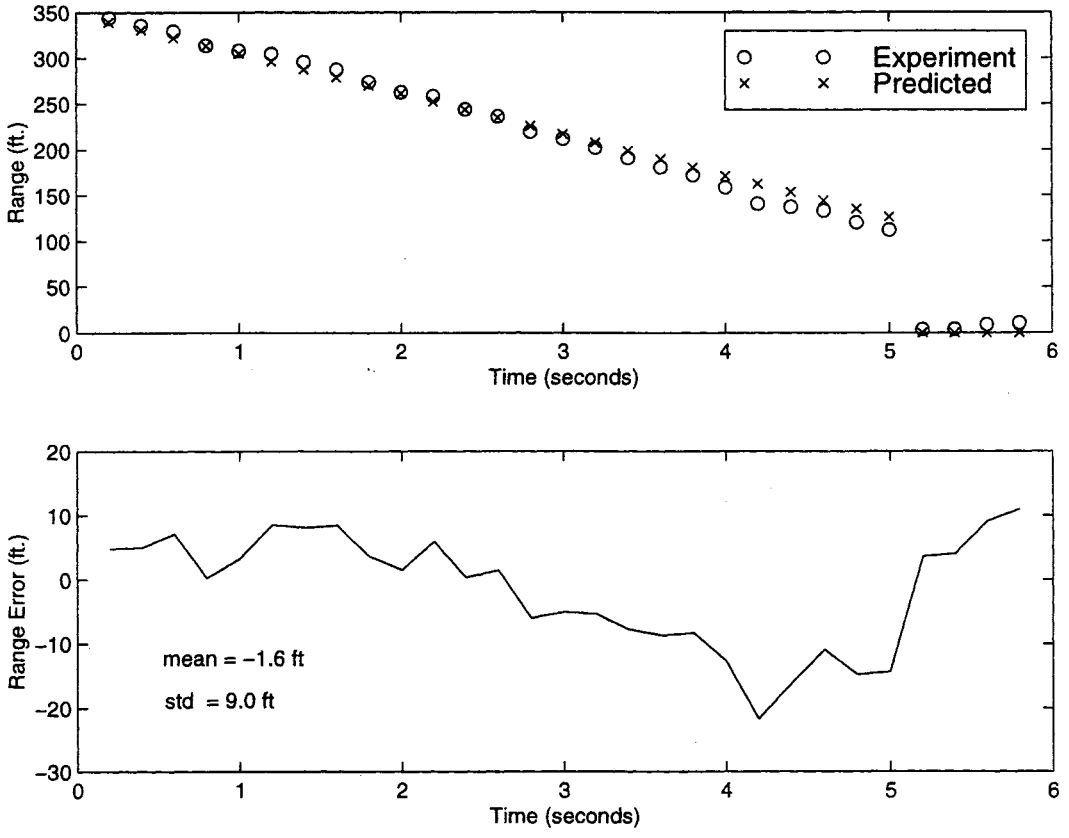

Figure 3.19: Experimental vs. simulated range for Pos FR, Yaw 2R, Pitch 0, Speed 30, Adj. Lane

The final results shown in Figure 3.20 demonstrate the sensitivity to the orientation of the radar. This plot shows the results when the radar is pointed at two degrees to the left while the host is in the adjacent lane with respect to the target. Since the azimuth angle of the radar beam is specified to be four degrees, the radar should not have been able to pick up the target vehicle. In the idealized simulation world, all angles are exact and, indeed, the simulated radar did not detect the target. In the experimental data, the radar did detect the target. This may be because the actual cone azimuth is greater than four degrees. Also, any slight miscalibration during the experiment may have caused this result.

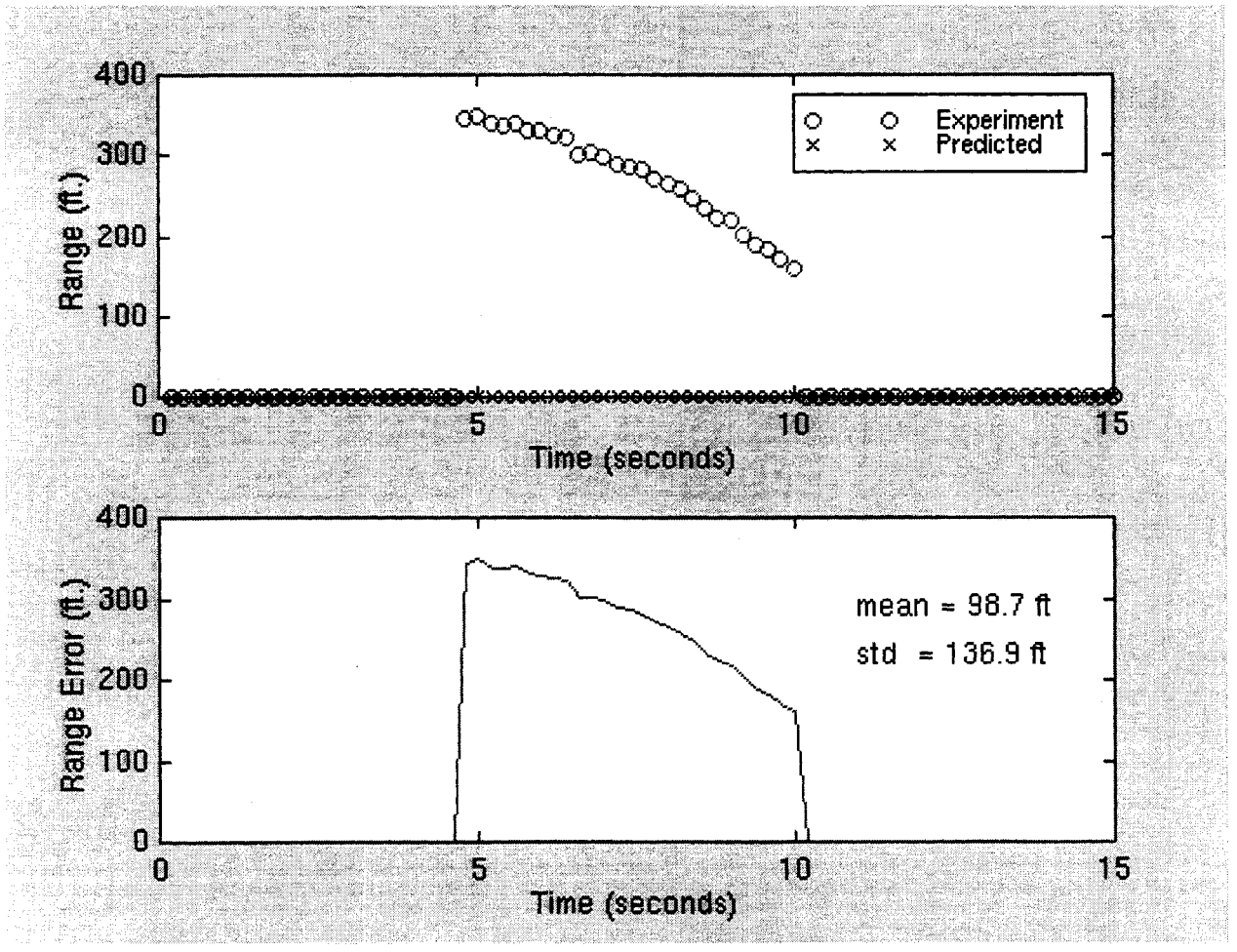

Figure 3.20: Experimental vs. simulated range for Pos FR, Yaw 2L, Pitch 0, Speed 30, Adj. Lane

3.3 Optech Sentinel 100 Results

The Optech Sentinel 100 laser range finder was placed inside a weather proof enclosure and mounted directly on top of the radar. The mounting was designed so that the pitch of the laser can be adjusted independently of the radar. This sensor does not provide range rate to target, only range.

The host was driven toward the target in the same lane with the laser mounted in the front center position. The results are shown in Figure 3.21. The laser range finder was able to detect the target vehicle at around 170 ft and smoothly track it all the until the host vehicle stopped. Notice that this sensor had no problem detecting the target vehicle at the end of the experimental run,

when the host vehicle came to a halt. This due to the fact that this is a time of flight sensor and does not rely on the Doppler effect. The fact that the laser didn't detect the target vehicle at long ranges was probably due to the mounting. The laser unit was mounted above the radar by about one ft (see Figure 3.22). At zero pitch, the laser was pointing toward the windshield of the target vehicle which may reflect the laser beam upward due to its contour. The Optech comes with a visible light pointer which can be used to aim the laser beam to the desired target. The weatherproof enclosure, however, blocked the path of this auxiliary light beam which made aiming the laser beam difficult. This may seem like a poor enclosure design, but the enclosure was designed for a newer product. We purchased it because it was sized correctly to fit the Sentinel 100 and we were under time constraints due to the impending snow fall. A customized enclosure would have taken too long to design and build at the time.

We were unable to fully test the laser sensor and weren't able to test it during snowfall because the unit malfunctioned right before the winter experiments. We sent the unit back to Optech for repair. They returned it to us in a week and fixed the problem, but when we assembled the laser inside the weatherproof enclosure, the enclosure developed a power problem. By this time, we missed the small time window during which snow fell in the unusually warm Minnesota winter of 1997-98.

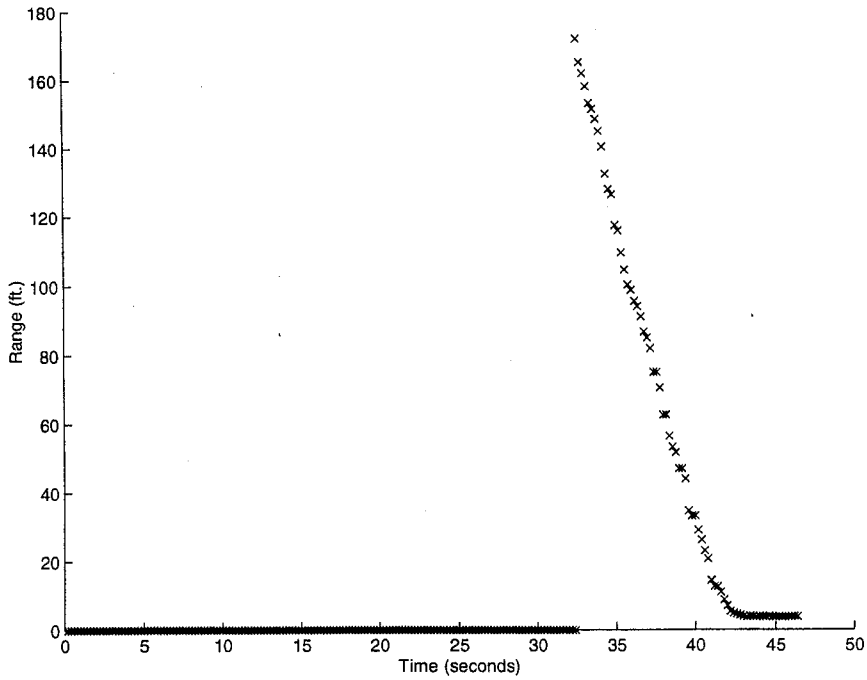

Figure 3.21: Optech range readings for Pos FC, Yaw 0, Pitch 0, Speed 10, Same Lane

Figure 3.22: Optech enclosure mounted above the radar

The reasons we could not start testing this sensor earlier in the winter were that we could not obtain the weatherproof enclosure until late January and we were evaluating the present weather sensor in the early part of winter (see the Appendix for weather sensor evaluation). We did not receive any appreciable snow fall events in February which pushed back the experiments to March.

3.4 Results Obtained During Snowfall

Snow plow drivers must be out during the worst weather conditions. Additionally, the plume of snow generated by the front blades creates a difficult visibility problem for snow plow drivers. Abandoned vehicles buried in snow pose yet another threat to the driver. Our goal was to test the radar under heavy snow conditions to determine whether it can detect a vehicle covered in snow. To quantify the weather conditions at the time of the experiments, we acquired a Vaisala present weather detector. Appendix A describes our evaluation of this sensor. We should point out that our main objective was not the evaluation of the precipitation/visibility sensor but the evaluation of the radar. Given time and other constraints, we performed a very limited comparison of the PWD11 using only sensors available to us locally.

3.4.1 Experimental Results During Snowfall

A target vehicle was parked at the Mn/ROAD test track so that it would naturally be covered with snow during the snowfall season.. A van equipped with the Vaisala PWD-11 (Figure 3.23) weather sensor was located up the track at approximately 700 ft from the target vehicle. It would have been preferable to have the weather sensor located closer to the experiment, but the van might have been picked up by the radar due to its large cross sectional area. The distance was not deemed to be a problem since the weather is not significantly different over such short distances.

The snowfall experiments were performed in the exact same way as the fair weather experiments. The host vehicle was driven towards the target vehicle at different speeds. We did not vary the orientation of the radar for these experiments because our goal was to isolate the effect of snow

on the ability of the radar to detect the target vehicle. Therefore, yaw and pitch were held constant (zero) for the duration of these experiments.

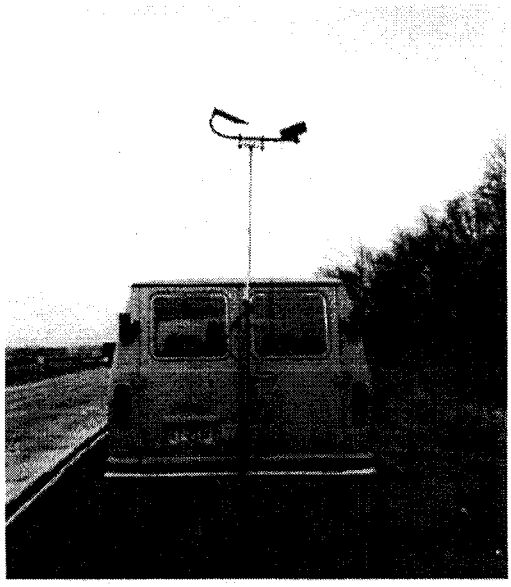

Figure 3.23: Vaisala weather sensor mounted on van

The data from the Vaisala weather sensor provided instantaneous weather information captured in the instant weather code, visibility and water intensity fields. Two weather codes are output by the sensor; National Weather Service (NWS) and WMO SYNOP codes. Table 3.3 lists the supported weather codes that are pertinent to this experiment. The instantaneous Meteorological Optical Range (MOR) is also provided by the PWD-11. The maximum visibility of this sensor is 2000 m. Last but not least, the unit measures the precipitation intensity as mm of water per hour (mm/hr). This measurement indicates how much water mass is in the snow (wet snow vs. powdery snow).

Vaisala Output - Weather Codes			
NWS Code	Weather Type	WMO Code	Weather Type
		70	Snow
S-	Light Snow	71	Snow, light
S	Moderate Snow	72	Snow, moderate
S+	Heavy Snow	73	Snow, Heavy

Table 3.3: Vaisala supported weather codes

Through the aforementioned indicators, the instantaneous weather conditions at the time of each experimental run can be quantified. Henceforth, when we refer to 'light snow' or any other description of the weather conditions, we are quoting the data provided by the PWD-11 weather sensor, as indicated by the weather codes. In the following plots, the instant water intensity and the visibility are provided in the legend to indicate the instantaneous weather conditions at the time of the experiment.

The first set of experiments was performed on March 15, 1998. According to the PWD-11, the snow was light. Figure 3.24 shows the results of an experiment performed in light snow conditions with a visibility of 1101 m (0.68 miles) and a water precipitation rate of 1.14 mm/hr. The first thing we noticed is that the 'no snow' data collected during the winter of 1998 was not as good as the data collected in the fall and summer of 1997 (fair weather). This lead us to believe there may be an undesirable temperature effect because all other experimental parameters were the same for both the winter and summer/fall experiments. Our theory was further corroborated when we collected data in the summer of 1998. The range and range rate data was very similar to the fair weather data collected the previous summer/fall. This certainly rules out a malfunction of the radar unit. Given the time critical nature of our experiments, we decided to proceed and compare the snowfall data with the 'no snow' data collected in the winter, to eliminate any temperature effect from the experiment. The comparison of data, both collected in cold weather, can still be used to determine whether snow affects the performance of the EVT-200.

The radar was able to detect the target vehicle through the snow at low ranges. However, at long ranges, the radar had more difficulty picking up the target. The water precipitation rate of 1.14

mm/hr was the largest measured by the PWD-11 during the snowfall experiments. The snow was correspondingly wet.

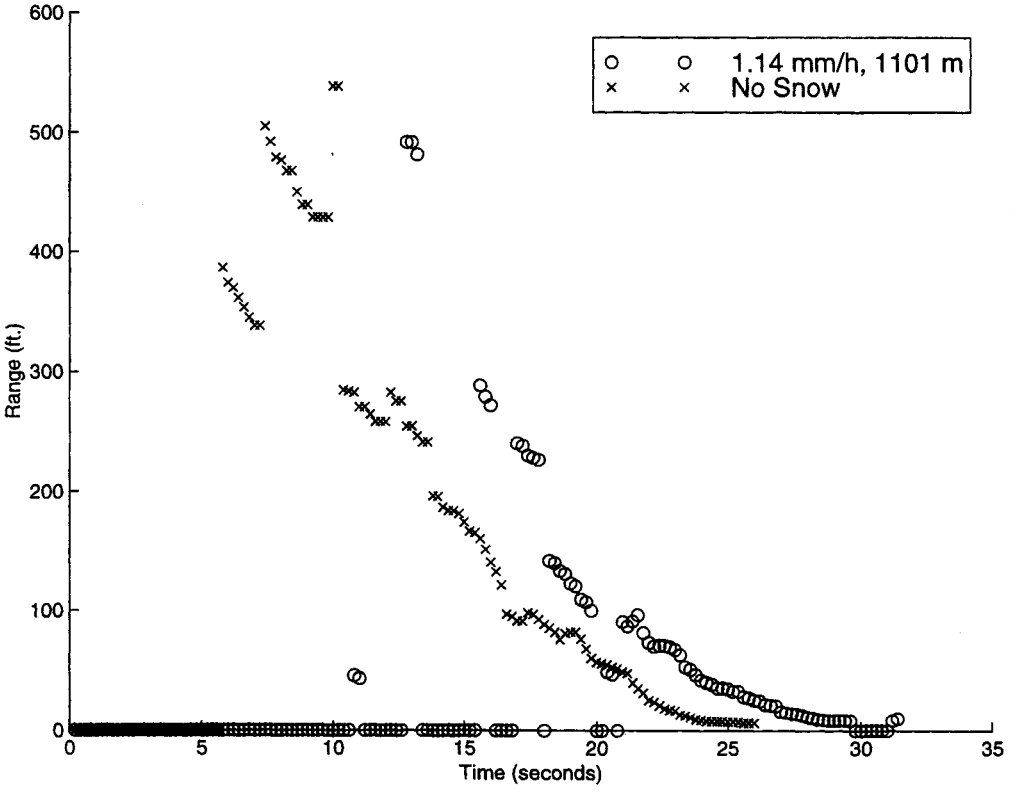

Figure 3.24: The effect of light (but wet) snow on range, Pos FC, Speed 30, Same Lane

On March 31, 1998 we were able to perform an experiment in moderate snow. Figure 3.25 shows the result when the visibility was 738 m (0.46 miles) and the water intensity was 0.39 mm/hr. Again, the radar was able to detect the target vehicle, although it locked onto the target at a closer range. The visibility of 738 m was the lowest visibility obtained during the snow experiments. The low visibility along with the low water intensity indicate that the snow was dry (powdery) but was coming down heavily enough to lead to a visibility of under ½ mile.

The snow may cause a slightly increased attenuation of the radar signal. In addition, the target vehicle had accumulated snow on it during the duration of the storm which may have caused more

scattering of the radar waves. However, the radar was able to detect the target vehicle in light and moderate snow conditions.

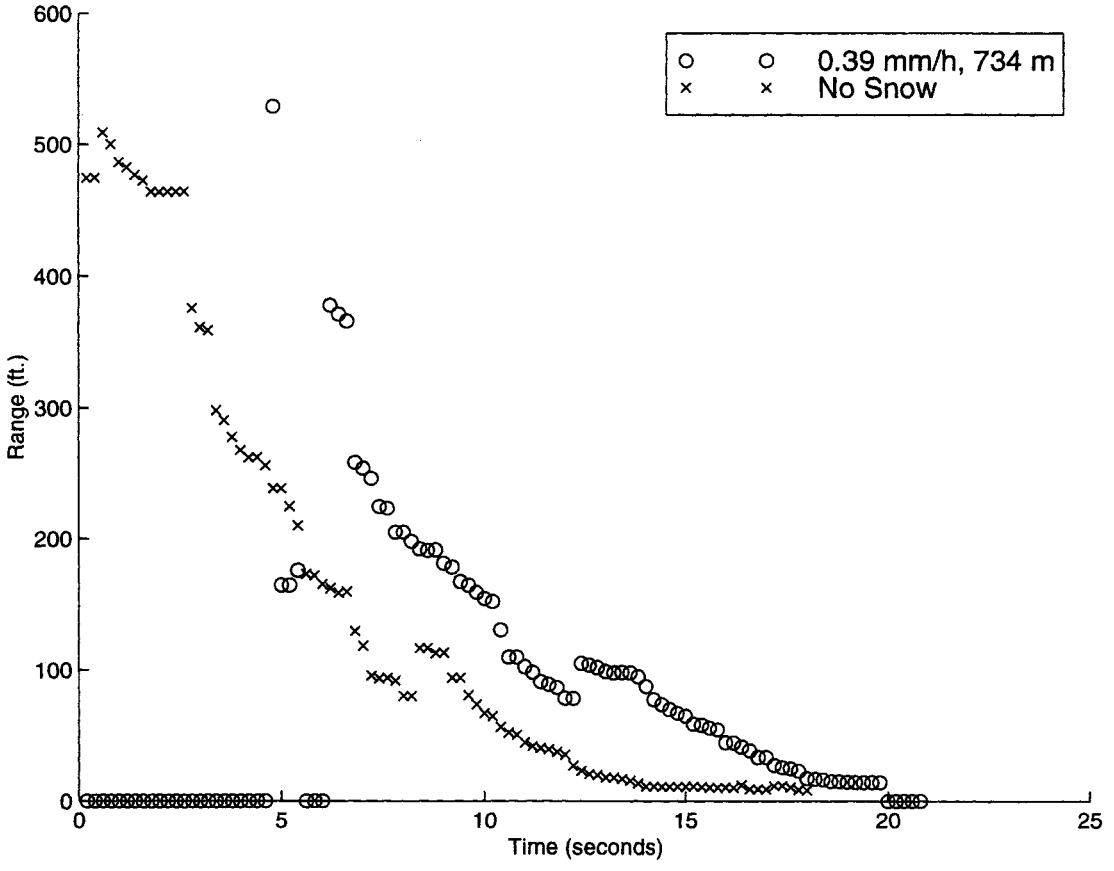

Figure 3.25: The effect of moderate snow on range, Pos FC, Speed 30, Same Lane

The winter of 1998 in Minnesota was unusually warm. We were unfortunately unable to perform an experiment in heavy snow or blizzard conditions because we did not experience these weather conditions for a long enough duration in order to perform an experiment. Clearly data from only one experiment each for light and moderate snowfall is not enough to be conclusive. However, the results from light and moderate snow indicate that the radar has the ability to detect the target vehicle through the snow, although its capability to detect the target at long ranges may be slightly reduced.

Chapter 4

4. The Driver Assistive Display (DAD)

4.1 Background

During the last few years, the University of Minnesota and the Minnesota Department of Transportation have been working together to improve the safety of heavy vehicles on highways. The overall goal has been to investigate how reductions in accidents can be achieved by integrating emerging sensing and control technologies. The emphasis in this chapter is on the effective integration of sensory information and its representation in the form of a graphical display, to assist driver perception and control under varying road and weather conditions.

The design of a Driver Assistive Display System (DAD) requires that one know what information the device should display, how fast this information should be available, and finally, what aspects of human driving it will enhance. We have been exploring different approaches for understanding and improving the driver-vehicle interface.

We have begun to develop a common architecture in which information displays will assist drivers in performing driving tasks when normal visual cues are not present (due to e.g. low visibility), and have demonstrated automated guidance systems that replace human steering in the event that human reaction times are too slow. Such systems should work in tandem within a driver centered organization, in which sensing and control is focused on the human driver. As more serious constraints are applied on the driver's ability to "see" and to "react", successive layers of assistive subsystems would come into play. The following section summarizes the functions of a display based on radar detected obstacles integrated with GPS-based vehicle position, which is the primary focus of this chapter.

Obstacles detected by radar must be correctly positioned on the display of the roadway as viewed from the driver's perspective. Thus, it is first necessary to provide the driver with a high fidelity view of the approaching road.

Based on analyzing the various driver-steering models, we believe that the following information must be provided to the driver (directly or implicitly) to enable one to track a given roadway using the displayed visual field of the road.

1. *Preview (Anticipatory information)*

   The preview requirements vary depending on a variety of driving conditions including speed, size of the vehicle, the driver's emotional condition, weather conditions, etc. The literature is not necessarily consistent but it would seem that a minimum of 1.1 to 1.2 seconds of preview information is necessary for the driver to securely steer the vehicle and stay within the lane.
2. *Lateral Position Error*

   This is the principal variable on which a lateral steering feedback control loop (from a driver-steering perspective) is closed.
3. *Yaw Angle Error*

   The yaw (angle about a vertical axis) information helps to reduce the oscillations that may be introduced by a pure lateral position controller.

The parameters listed above are also incorporated in some fashion into almost all of the successful automated vehicle guidance systems which attempt to mimic human based steering systems. By designing systems which make this information available, one can provide the needed sensory perception to the driver when normal sources of data are occluded (i.e. under poor visibility conditions). Furthermore, automated systems can be designed around these data sources in the event that human reaction characteristics are the limiting factor (e.g. steering in very narrow lanes, in tunnels or bridges, steering control to avoid collision).

Given our human centered approach to driving, it is important to integrate the needed sensory information and provide it to the driver in the most natural way possible. We feel that the best

way to present the necessary roadway information (while operating under adverse weather conditions) is by simulating the visual road pattern that would normally exist under favorable conditions and projecting it on to the windshield. The obstacles detected by the radar are integrated into this display. In the following sections of this report, we describe a software architecture based on the requirements for the DAD mentioned in this section.

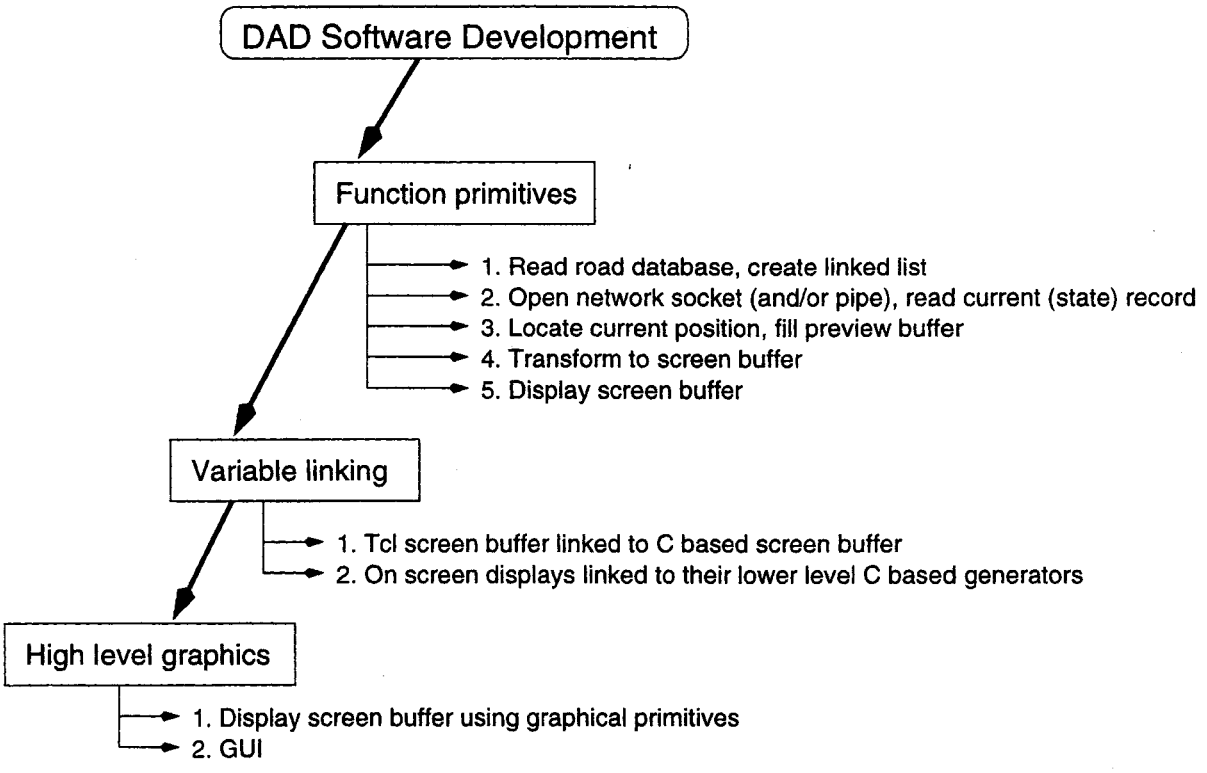

Figure 4.1: Software organization

4.2 The DAD Software Architecture

Please refer to Figure 4.1, which illustrates the fundamental elements of the DAD software architecture.

The DAD program has been implemented as a combination of 'C' language code at the lowest level, superimposed with high level scripts written in Tcl/Tk (Tool Command Language / Toolkit). Tcl/Tk are a set of public domain 'C' libraries that are available in a compiled form on

any standard UNIX-like system. It is available for many other systems as well. The current design can be run on Tcl version 7.5 or later, supported with Tk version 4.1 or later. The DAD program described here is basically a Tcl/Tk application. It was created by starting with the basic Tcl/Tk application called 'wish' (Windowing Shell), and adding to it the necessary modules/commands for DAD functionality. New commands based on the functional primitives illustrated in Figure 4.1, were declared to the Tcl interpreter so that top level code can be written very succinctly using these commands in conjunction with pre-existing Tcl/Tk commands [26].

4.3 Description of Operation

Please refer to Figure 4.1 for a schematic on the organization of the DAD software.

The DAD computes three separate views to assist with navigation. For demonstration purposes, these have been combined on one screen (see Figure 4.4), but in the final implementation each should be located appropriately with respect to the driver. The forward view is the primary view that basically contains all the information (road boundaries, obstacles) in the correct perspective and calibrated based on the available sensing capabilities. The rear view (bottom of DAD screen) provides the "rear view mirror" view, also contains the road boundaries, and obstacles in the correct perspectives, as they should appear in a real rear-view mirror. The plan view (to the right of the DAD screen) shows the vehicle's position on the road from a bird's eye point of view. The relative positions of the obstacles corresponding to their appearance in the forward view are also shown in this view. Several GUI based buttons on the left would provide the driver with control of the presented data. The description below is based on a demonstration version and used previously stored information. It does not operate in real time but uses the data to demonstrate the general capabilities of the proposed display

4.3.1 Initialization

The program first reads the pre-specified road database file, and allocates memory for all the road data points in the form of a single linked list. The road database is a text file with 130 lines, and five fields. It contains the pre-surveyed GPS coordinates of all the survey-nail locations that line

the Mn/ROAD test facility. The first field is the number (or tag) of the point. This number is the survey-nail number on the Mn/ROAD test track. The next two fields contain the GPS coordinates of the point in State-Plane coordinates; first X, then Y. The last two fields contain the lat-long (latitude-longitude) coordinates of the same point; first latitude, then longitude. Below is a clipping from the road database that was used here:

```
158 2697133.529755 1154564.302040 45.26677238 -93.71855618
159 2697212.979935 1154503.577084 45.26660509 -93.71824843
160 2697292.427986 1154442.856071 45.26643781 -93.71794069
161 2697371.879082 1154382.131723 45.26627052 -93.71763294
162 2697451.328062 1154321.407672 45.26610323 -93.71732520
163 2697530.777487 1154260.687570 45.26593595 -93.71701746
164 2697610.224809 1154199.964117 45.26576866 -93.71670973
165 2697689.675163 1154139.240978 45.26560137 -93.71640199
157 2697054.082621 1154625.023662 45.26693966 -93.71886392
```

Figure 4.2 illustrates how the road data points are used to generate the road as a set of three polylines of discrete, connected segments. The road database contains the state-plane format GPS coordinates of the road centerline. These are directly plotted, and connected while drawing the road centerline. A road width parameter (W) is used to compute the left and right road (or lane, as applicable) boundaries. Figure 4.2 shows the road geometry computation around a curve, which is done based on the road centerline, the road width parameter, and the road orientation at the particular road data point at which the computation is performed.

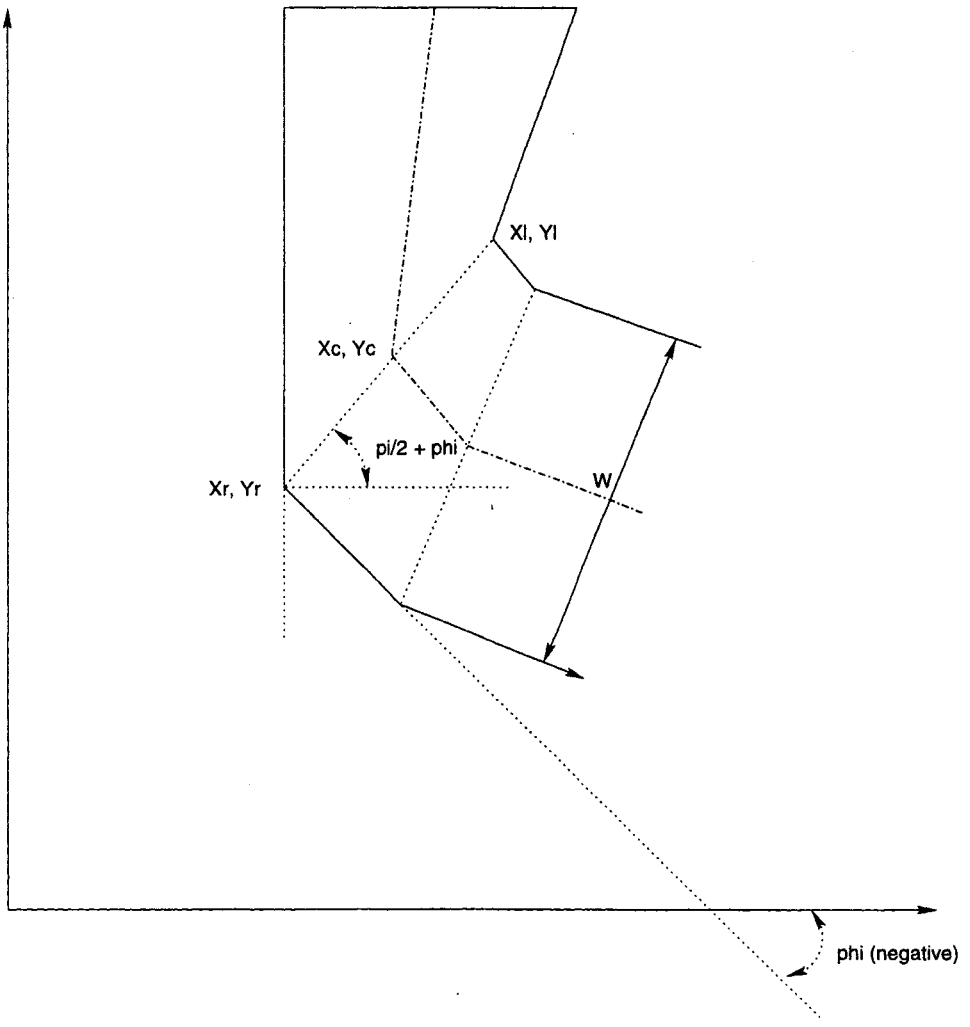

Figure 4.2: Road geometry

The X,Y coordinate system shown represents the GPS state-plane coordinate system. The X axis is along the geographic East direction, while the Y axis is along the geographic North direction. The yaw (or orientation angle) of the road, (or vehicle) is computed as the angle between the direction of motion (or direction of the vector connecting the two road data points along the road centerline), and the positive Y axis (geographic North direction) of the coordinate system.

After the road points have been read into memory, the system proceeds to determine the current location of the vehicle. This can be done in two ways. In the simulation mode, the system is initialized at the first point of the road database. In the real tracking mode, the system will be initialized to the first position update received from the vehicle's sensing system.

4.3.2 Start Tracking

Tracking is the mechanism by which the DAD system updates the graphics on the display screen to represent the "current" vehicle state. The information that comprises the state of the vehicle includes: position (GPS, State-Plane), orientation (degrees from North), and radar range (meters). The position is the X, Y vector obtained from the GPS system. The orientation is obtained from the gyro system, and the radar range is the distance of the object from the vehicle, detected and measured by the radar sensor.

The "current" state is computed by the DAD system in the simulation mode by advancing the vehicle position to the next point in the road database. In the real tracking mode, the state information is continuously available through a network socket programmed into the DAD and interfaced with the vehicle's data acquisition system. The DAD is totally flexible to any type of network communication, as long as the socket driver programs can be successfully written using the 'C' language.

4.3.3 Locate Vehicle on the Road

After the "current" state information is available to the DAD, it proceeds to locate the vehicle on the road. The location function successively scans through the road data points and finds the closest road data point to the current position of the vehicle. This is a simple distance function that computes the Cartesian distance between the current position and the road data point in the scan.

The next part of this subprogram fills the preview buffer based on the vehicle's location on the road, as determined above. The preview buffer is an array of a pre-decided number of road points. The size of the preview buffer determines the amount of road preview that will be displayed from the current position.

4.4 Compute Geometric Transformations

Please refer to Figure 4.1 for graphical illustrations related to this section. Once the part of the road to be displayed is identified (preview buffer), it has to be processed using the correct instantaneous geometric transformation matrices to render the view in the correct perspective as would be see by the driver of the vehicle.

There are five coordinate systems as illustrated in Figure 4.3, and four transformation matrices to transform vectors from one system to the other. The "Global Coordinate System" is aligned with the GPS State-Plane coordinate system, so all positions and orientations specified in the state vector of the vehicle are in the global system. The "Driver Coordinate System" has its origin at the head of the driver, and is oriented such that the Z-axis is parallel to the road and in the direction of motion. The X and Y axes of this coordinate system are arranged in the same format as that of a typical image processing system, with the X axis going left to right, and the Y-axis going top to bottom, as seen by the driver. The "Windshield Coordinate System" is similarly oriented as the driver coordinate system, except that its origin is offset from that of the driver coordinate system in the X, Y, and Z directions. This offset accounts for the relative placement of the driver's head from the top left corner of the vehicle's windshield, which is where the windshield coordinate system is attached.

Note that it would have been possible to directly transform from the global coordinate system to the windshield coordinate system. However, the driver coordinate system has been defined to add the flexibility of tracking the driver's head position inside of the vehicle and using that information for adjusting the driver's view. The parameters that define the transformation from the global coordinate system to the driver coordinate system, are, the instantaneous position and orientation of the vehicle (and hence the driver).

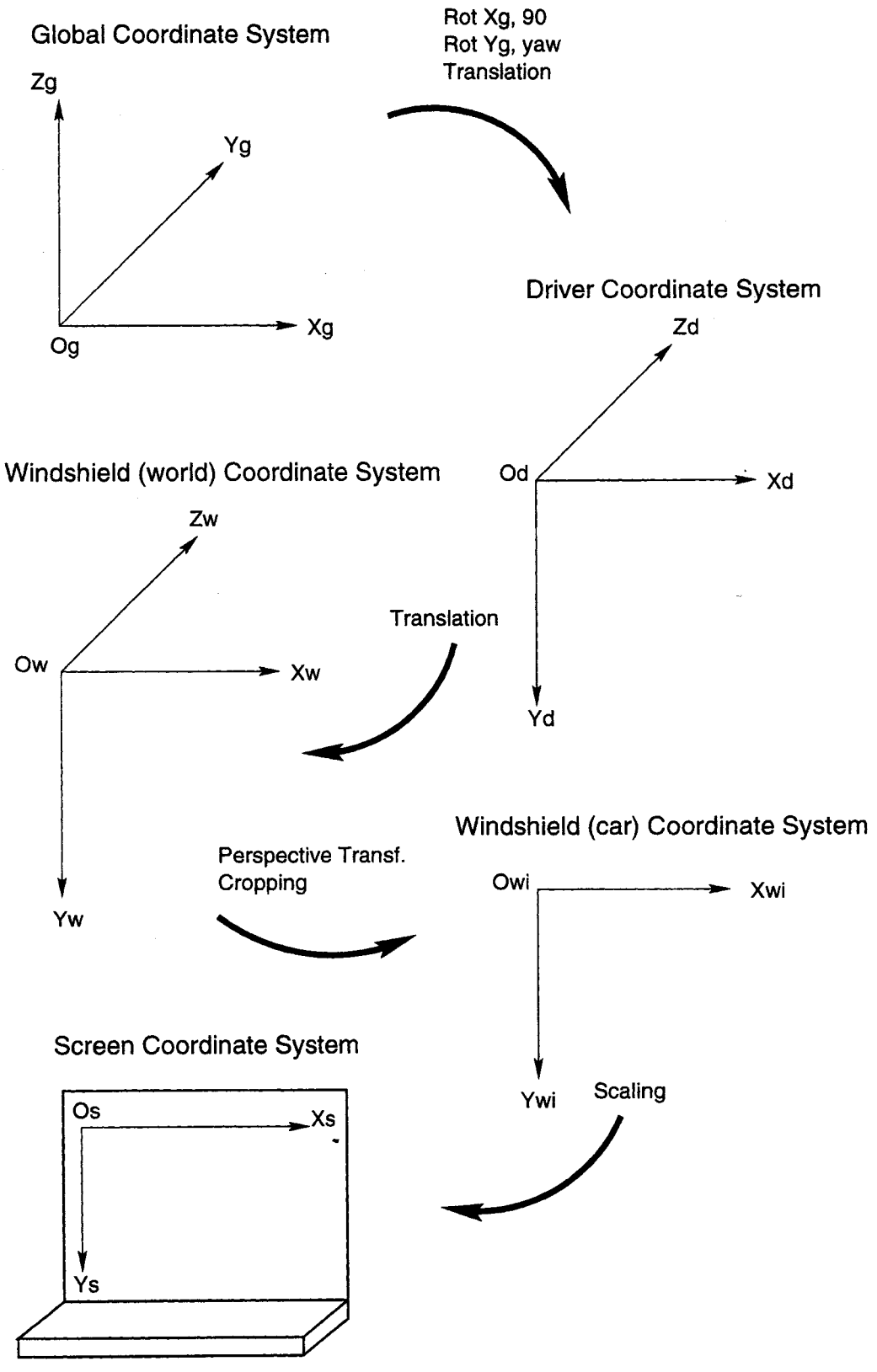

Figure 4.3: Geometric Transformations

There is one more intermediate coordinate system, before the view becomes final in the "Screen Coordinate System". This intermediate system is a 2-Dimensional, reduced version of the windshield (world) coordinate system. It is called the "Windshield (car) Coordinate System". The transformation function from the windshield (world) to the windshield (car) coordinate systems is a perspective transformation (3-D to 2-D camera type transformation) followed by a cropping operation, used to reduce the size of the image. From this point on, we have to deal with only X, Y (image) coordinates.

The windshield coordinate system is based on the logical analog of having the windshield as some form of a screen upon which an image containing all the necessary visual information about the road is projected. The image would then have the same coordinate system as has been assigned to the windshield, i.e. the origin being at the top left corner, the Y axis pointing vertically down, and the X axis pointing horizontally to the right.

The final system is the "Screen Coordinate System", which is similarly oriented and positioned as the "Windshield (car) Coordinate System", and the transformation between the two is a scaling function that appropriately scales the image to be displayed on the electronic viewing screen (of the computer, or any other viewing device such as a Heads-Up-Display).

4.5 Results

The prototype DAD is presented in Figure 4.4. It is important to note that the actual display is in color while this document is printed in black and white. Also, this display is a prototype and is intended to demonstrate the feasibility of the working technology as well as to investigate what software/hardware is capable of handling this type of application. Developing the correct viewing angle/display perspective was not part of the objective of this project. This is being done as part of a different project entitled "Improving Visibility - Heads Up Displays based on Location Sensing" presently underway.

The main window of the DAD consists of five major parts. The buttons will provide us the ability to switch the display into various modes (simulation, real-time, etc.). The buttons have not been programmed in this prototype and are located for illustrative purposes only.

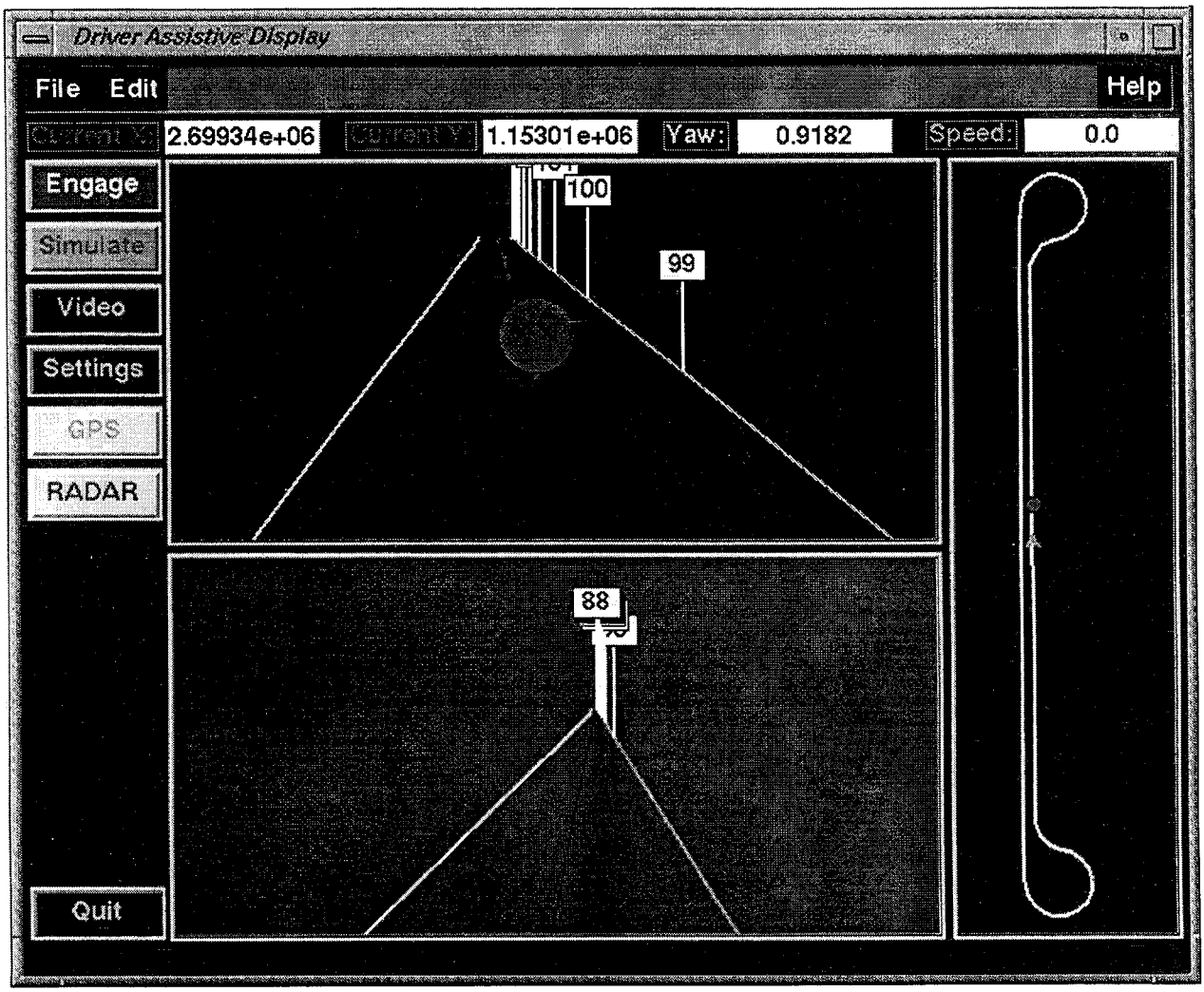

Figure 4.4: The DAD display

The top of the display shows data collected from on-board sensors. This display is currently being driven from data that has been collected and stored on the hard drive, but a switch over to real time presentation of sensor data is possible. The first two columns of data are the X and Y

state plane coordinates (ft) collected from a GPS receiver. The third column is the yaw angle (in radians measured from north) provided by the gyro. The last column of displayed data is the speed of the host vehicle.

The remaining three windows of the DAD are drawings of the instantaneous road scene from three different perspectives. The top center window with the large circle (red in the color display) is the front view from the driver's perspective. The red circle is a target vehicle which will be discuss further in the following paragraphs. Notice the road signs with numbers on them. We use these to calibrate and debug the prototype display.

The window just below the front view is the rear view, as seen from the driver's head location (driver's coordinate system). This is a 'mirrored' view of the back of the host vehicle. Notice that the road signs are not inverted in the rear view as one would expect. It is as if the back of the sign was painted with the backwards number. Again, the road signs are useful as a visual debugging tool and displaying the numbers in a readable format is used for simplicity.

The final window is a bird's eye view of the road scene. The whole Mn/ROAD low volume test track is shown and the host vehicle is represented by a triangle (green) while the target vehicle is represented by a circle (red). Notice that the target is directly in front of the host vehicle which matches what is presented in the front view.

In the next three figures (Figure 4.5 - Figure 4.7) we show what happens when the radar is mounted in the front center of the target vehicle and a target is detected at three different ranges. The radar in this display is simulated, but can be switched to accept a real time data stream sent by real radar hardware. Notice that the target, drawn as a red circle, grows in area as it decreases in range from the host. This provides an intuitive visual cue to the driver as to how far away a detected target is located. This needs to be calibrated based on normal viewing conditions from the vehicle.

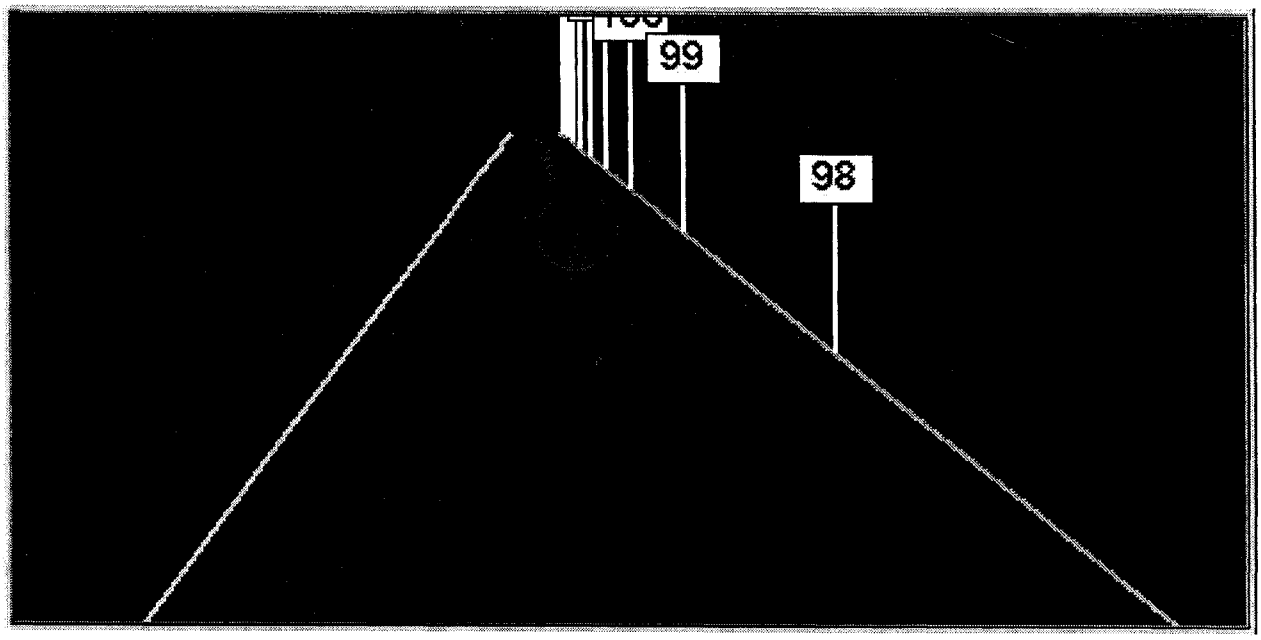

Figure 4.5: The front view with target at a long range

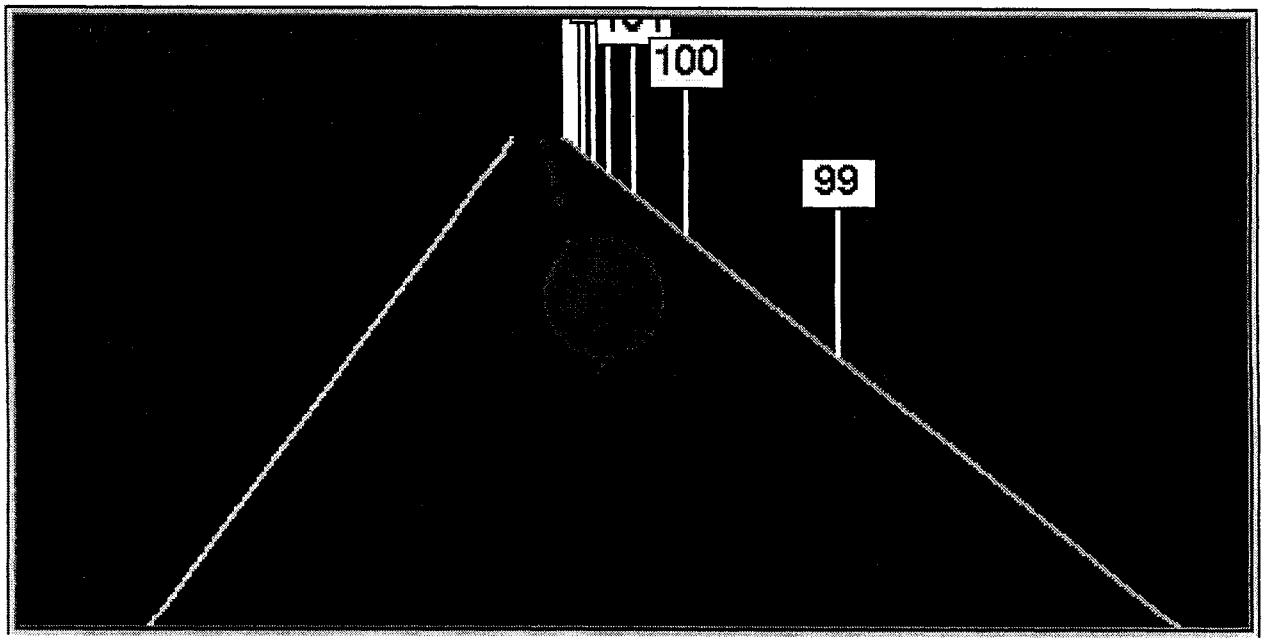

Figure 4.6: The front view with target at medium range

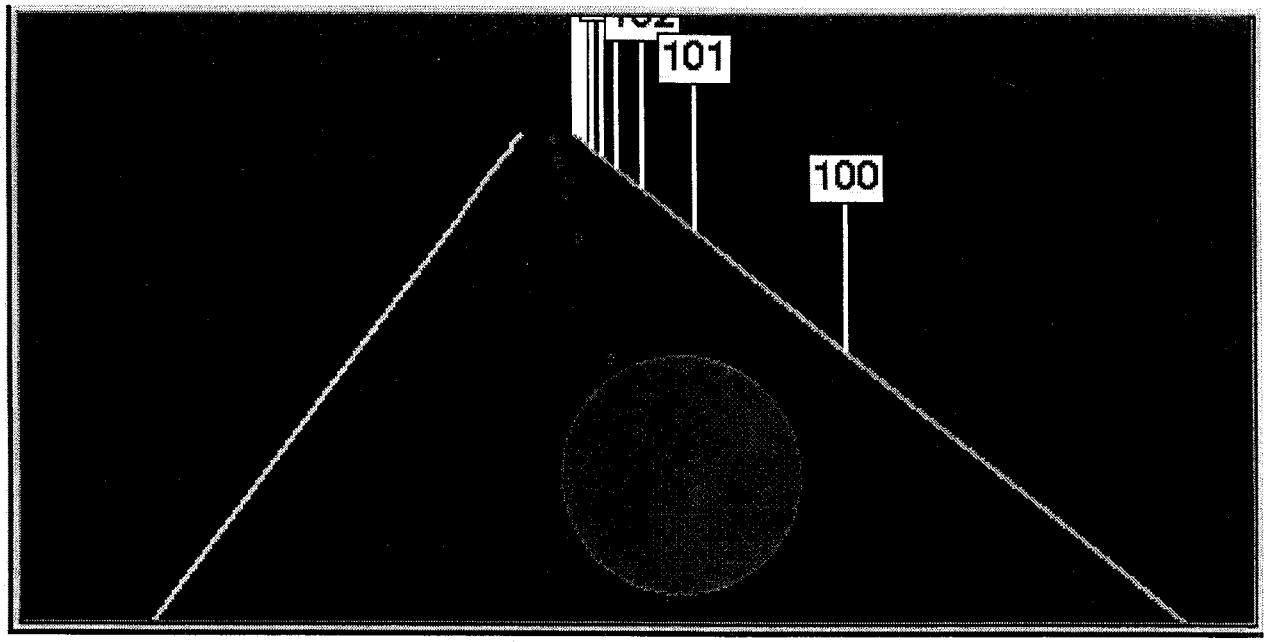

Figure 4.7: The front view with target at close range

The DAD was designed to work with the EVT-200 radar which the previous chapters have documented in detail. One characteristic about this sensor that is important to the operation of the display is that it does not provide information on where within the radar beam's cone angle field of view the target is located. This ambiguity forces us to make the assumption that the target is directly in the center of the radar's line of sight. This assumption is not very good at long ranges, but improves as the range decreases. In fact, using a typical lane width of 12 ft, an azimuth cone angle of four degrees, and the maximum specified range of 350 ft, the radar beam covers the width of a highway lane at a range of about 172 ft. This is why the previous figures showed the target in the center of the lane when the radar was mounted on the front center of the target vehicle.

We moved the simulated radar to the far right front of the host (orientation is straight ahead, yaw and pitch angles are zero) to show what happens when it detects a target. As with the previous mounting location, we assume that the target is in the direct center of the radar's line of sight. This is shown in Figure 4.8.

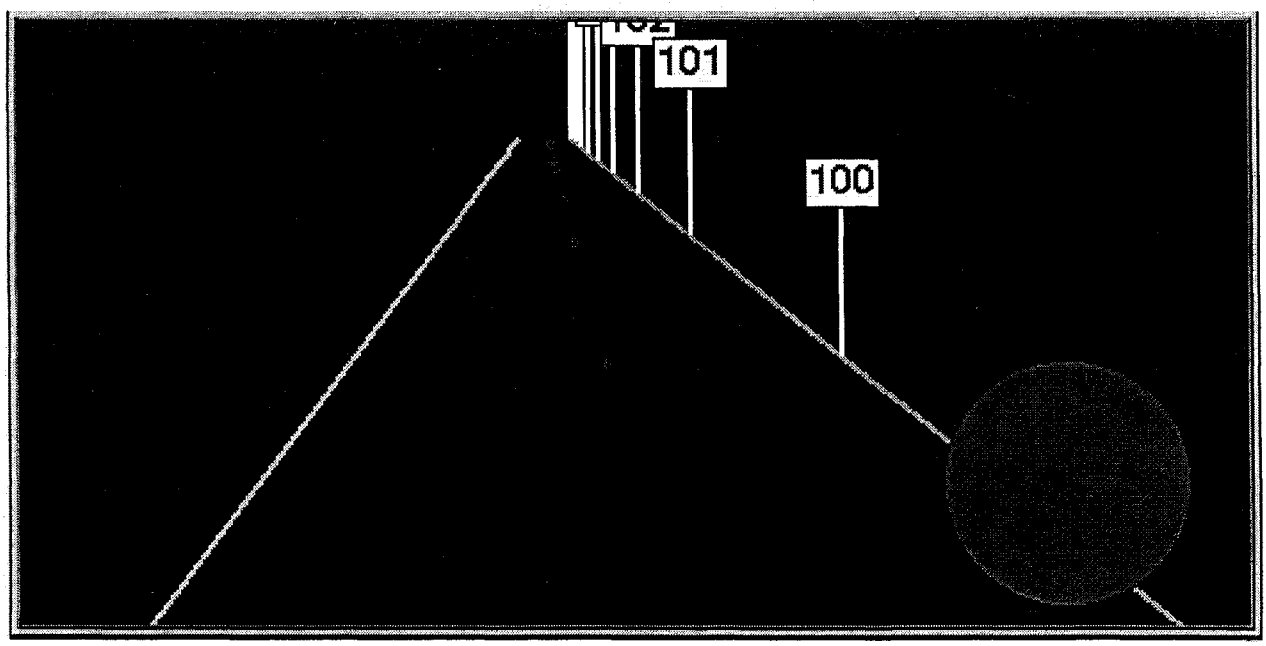

Figure 4.8: The radar mounted on the right front of the host

The radar may be mounted in the back of a host vehicle to detect moving targets approaching from its rear. To demonstrate this scenario, we moved the simulated radar to the back rear of the host. As can be seen (Figure 4.9), the DAD successfully displayed the target vehicle on the right side of the road in the rear view window (the background shade for the rear view mirror is intentionally set to a different level than the forward looking display).

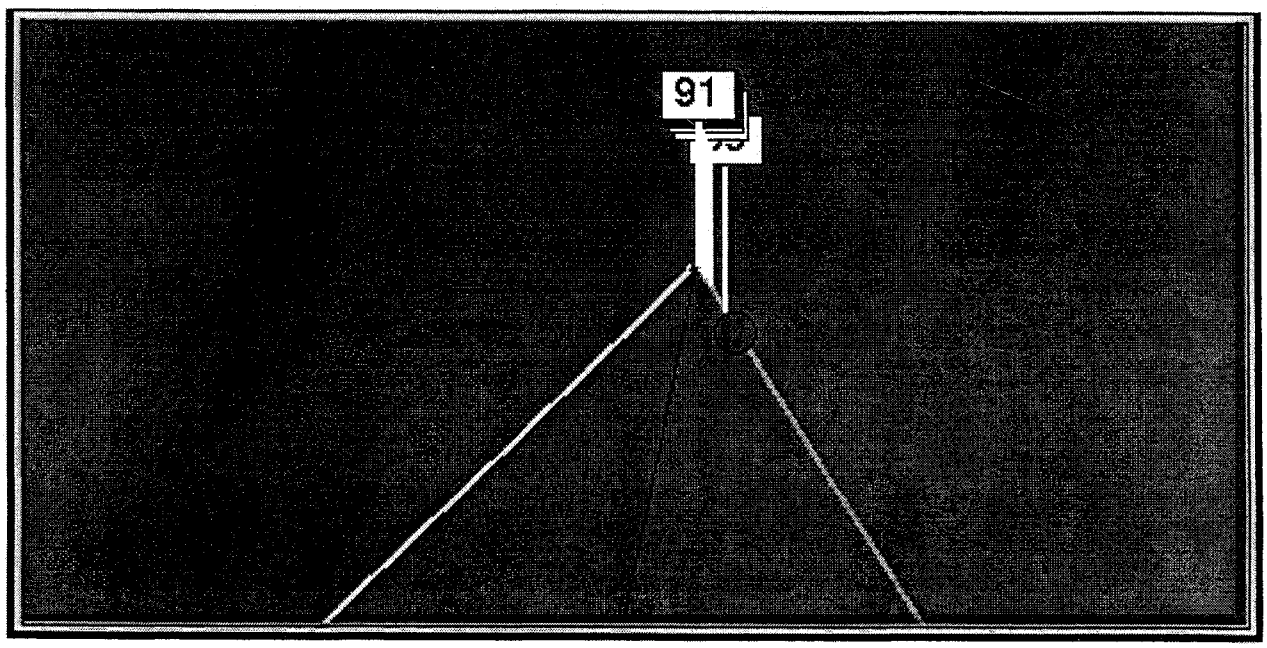

Figure 4.9: Rear view with radar mounted on back right of host

Chapter 5

5. Conclusions and Recommendations

In this chapter, we summarize the results of this phase of the radar evaluation. Particular attention is paid to the effect these results have on potential snow plow applications. We then offer opinions and suggestions on what issues need to be addressed before actual implementation of radar on snow plows can become a reality.

5.1 Results of Radar Experiments

The EVT-200 is able to consistently detect a target vehicle under a variety of circumstances. In particular, the radar is relatively insensitive to orientation deviations that are caused by uncertainty in mounting. Furthermore, the ability to detect vehicles in the far edges of its field of view makes this sensor very robust. It also seems to perform well under light and moderate snow conditions, although due to limited snow events in the winter of 1997/98 we were unable to collect much data. We present the particulars of the experimental results in the following two sub-sections.

5.1.1 Fair Weather Results

In order to assess the robustness of this sensor, we designed a set of experiments to simulate different driving scenarios and manipulated the orientation and location of the radar. The isolation of parameters allowed us to better understand how the radar is affected by each individual parameter. This information can then be used to determine the optimal mounting orientation and location aboard a snow plow.

The radar detects and measures the range and the time derivative of range to vehicles within its field of view using the Doppler effect. Hence, it was logical to test the sensor for a variety of relative velocities between the host and target. The results were as one would expect, namely, that the radar is able to detect vehicles at longer ranges and with more accuracy and robustness at higher relative speeds. This result is favorable due to the inherent danger of a fast moving vehicle

approaching a slower/stopped vehicle. Snow plows have a particular problem with running into an abandoned vehicle which may be buried in the snow. Collisions of this type are particularly dangerous because the high speed differential between the two vehicles can produces collisions leading to severe injuries or fatalities. The radar performs best during this type of scenario.

The opposite is true with low relative velocities between vehicles. It was discovered that at low relative speed, the radar was less effective. During the five mph experiment, the range signal was noisy at long distances but improved at closer ranges. The range rate signal became unpredictable at very slow speeds. This behavior may not be as critical because collisions at low relative speed are likely to produce less material damage and injuries to the occupants of the vehicles. It would however be useful to evaluate radar units capable of better performance at low relative velocities, if these radar still exhibit good performance at higher relative velocities.

The desired location and orientation of the radar mount should allow the radar to point towards the region where detection is most desired. What is not as obvious is how practical mounting inaccuracies and uncertainties affect the sensor's ability to consistently detect vehicles in the region of interest. To that end, we carefully adjusted and measured the yaw and pitch angle at which the radar was pointing. We conclude that the radar performs well even with moderate deviations in the mounting orientation. Yaw deviations of two degrees produced little deterioration of the radar signal. A two degree yaw deviation is noticeable to the eye, hence; we believe practical mounting tolerances less than two degrees are achievable.

The pitch results were as expected. An upward pitch causes the radar beam to miss the target at longer ranges. Even with a very noticeable upward pitch of six degrees, the radar still detected the target vehicle at over 200 ft. It should be noted that the Mn/ROAD low volume test track has no overhead obstructions (i.e. overpasses and road signs). Upward pitch orientations on typical highways would almost certainly cause the radar to detect overpasses and road signs that are common on most roadways. Therefore, an upward pitch is not desired and should not be considered for orientation implementation decisions.

A downward pitch caused the same behavior as an upward pitch. Large downward pitches caused the target vehicle to be detected at lower ranges. Furthermore, very large range readings sporadically occurred with large downward pitch angles. These large range values were rare and can be simply filtered out.

The large blade in front of a snow plow may require an unavoidable downward orientation because the radar must be placed at a high elevation in order to 'see' over the blade. We were unable to test this situation directly, but preliminary experiments showed that the radar did not detect the road because the radar signal was forward scattered. The fact that the radar detected the target vehicle at lower ranges with larger negative pitch angles stemmed from the fact that the target was not within the sensor's field of view (cone). More testing may need to be done if the radar must be mounted at a high elevation on the snow plow, but the results of the negative pitch experiments suggest that if the target is in the radar's field of view, the radar will detect the target and not the road surface.

It may not be possible to point the radar directly at the detection area of interest due to the large blade located in the front of the snow plow. We performed an experiment in which the radar was moved from the center to the extreme right (lateral) side of the target vehicle. The results show that the radar was able to detect a target vehicle located in the same lane in both (FC and FR) mounting positions. The range signal was less consistent when mounted on the far right side, but the effect of lateral offsets is small.

The radar was also mounted in the rear of the target vehicle to determine whether it detects an object with a positive relative speed (traveling away from it). It did so. Since a vehicle moving away from the target poses little threat compared to one traveling towards it, we did not pursue this scenario further. It was investigated in the interest of thoroughness.

The blade scraping along the surface of the road creates an intense vibratory environment. To explore whether the radar's performance is affected by vibration, we performed an experiment in which the host vehicles engine was turned off (no vibration). The experiment was repeated with

the truck engine running to induce normal engine vibrations upon the EVT-200. The static experiment showed that the radar detected a stationary target vehicle when the engine was on (vibration) but not when the engine was off (no vibration). The vibration caused the sensor to detect a target when no relative velocity between the host and target existed. We then drove the target vehicle toward the stationary host. With the engine off, the radar (mounted on the host) readily detected the target vehicle from over 500 ft all the way until it stopped just a few feet in front of the host. The vibration experiment produced a different result. The radar produced range readings that 'wandered' around 100 ft until the target was within this range. Only then did the radar switch to tracking the target. The range rate reading during this experiment provided further evidence that the radar was locked onto the vibration because the range rate to target was constant at 1 ft/s until the target approached within 100 ft. The range rate reading then switched to the closing speed of the target vehicle.

We discussed these results with Eaton VORAD. They stated that they have noticed this type of behavior and have fixed it by replacing a faulty capacitor. They claim that newer units do not have this behavior. Returning the radar unit to Eaton VORAD for a new unit did not correct this behavior. In fact, the new antenna was more noisy than the original. For that reason, we exchanged the new antennae for the original one that we had used for all our experiments. Future testing must be conducted to validate that vibrations no longer affect the performance of the EVT-200.

5.1.2 Simulation Results

The geometric computer simulation validated some of the conclusions obtained from the fair weather experiments and provided further insight into the EVT-200's performance. The simulation showed that the expected range values decrease linearly with time when the host is traveling at a constant speed. The fact that the low speed experimental range plots showed large variation (high frequency noise component) while the high speed experimental data was more linear further validates our conclusion that the sensor performs better at a higher speed differential.

A quantification of sensor accuracy is difficult to obtain because we do not know exactly where on the target vehicle a radar reflection occurs. However, the simulation provides a 'reasonable' expectation of the range value measured from a vertical plane aligned along the front bumper. The uncertainty is less than the vehicle longitudinal length. This bounded uncertainty cannot be blamed for the fact that the radar's range became increasingly divergent from the simulated data as the range increases. We conclude that the range measurements becomes more accurate at closer ranges.

This conclusion doesn't affect the application of this sensor on snow plows because at farther ranges a reduced accuracy is more tolerable. The snow plow driver has more time to react at long preview distances. Furthermore, collision avoidance algorithms are much less sensitive when the target vehicle is far away. Any inaccuracies in the range measurement have a small effect on the driving trajectory because the corrective signal is small. Moreover, we found that the radar understated the range at long distances during same lane experiments which produces a conservative measurement.

The accuracy of the radar signal improves at high relative speed differentials. This effect was noticed during the speed experiments and was validated with the comparison between the experimental and simulated ranges at different speeds.

5.1.3 Snowfall Results

The EVT-200 was able to detect a target vehicle through moderate and light snow under the maximum specified range of 350 ft. Over 350 ft, the radar unit had difficulty detecting the target. Due to the unusually warm winter of 1998, we were unable to test the radar in a severe snow storm.

We also observed that the unit may be sensitive to temperature. It did not perform as well in cold temperatures as it did in warm temperatures. The data taken in cold weather was noisy and had

large 'jumps' in range while the data collected in the summer and fall had less noise and a smooth range profile. To determine whether the unit was malfunctioning, we repeated some of the experiments in the summer of 1998, after the snowfall experiments. The data was very similar to the one collected in the summer/fall of 1997. Since no other parameter was altered except the time of year (temperature) of the experiments, it is likely that radar is sensitive to temperature.

5.1.4 Optech Sentinel 100 Results

Our experimentation with this sensor was limited due to technical difficulties. The laser range finder and the weatherproof enclosure each malfunctioned just before and during the snowfall experiments, respectfully. The data we did collect was encouraging. The sensor was able to detect the target vehicle at 170 ft and 'smoothly' tracked it for the duration of the experiment. The maximum range of this sensor is stated to be 820 ft. This maximum range is for a reflective surface that is normal to the beam of light. A car is contoured and may reflect much of the laser energy away from the sensor if the beam strikes a non-normal surface. More experiments in which the height and pitch of the sensor are varied is needed to further assess the suitability of the Optech Sentinal 100 for automotive applications.

5.2 Issues that Need to be Addressed

We were limited in the amount of driving scenarios in which we could evaluate the radar due to time constraints and the configuration of the Mn/ROAD test track. Other issues presented by normal highway environments should be considered. In this subsection, we discuss some of these issues as well as issues presented by the mounting constraints of a snow plow. We then present some possible solutions as well as recommend future experiments.

5.2.1 Noise From Reflectors other than Vehicles

The Mn/ROAD test track is unlike ordinary highways in that it has no road signs, overheads or guardrails. These obstacles may provide good reflective surfaces that cause the radar to detect them. Since the EVT-200 is a one-dimensional sensor, it is impossible to discern where the actual

reflection took place within the field of view (i.e. no azimuth to the obstacle is determined within the radar's field of view or cone angle). Experiments on real highways should be performed to determine whether this is indeed a problem.

The experiments performed during this past year took place on the straight portion of the Mn/ROAD test track. Highways have curved sections that often contain guardrails that provide a possible source of reflection. Since the radar detects objects directly in front of the direction of travel of the host vehicle, its path will be oriented tangentially to the vehicle's path during the navigation of curves. During such conditions, the radar will be covering areas not directly in its path causing it to detect objects that are probably not a threat to the driver. Filtering algorithms have been developed that incorporate steering angle to limit the maximum range during such maneuvers. However, this can severely reduce the radar performance during curve negotiation.

Another variable that needs to be investigated is the effect of the large pitch caused by a steep hill. Imagine a vehicle, equipped with forward looking radar, descending a steep hill. Under such circumstances, the radar may be oriented such that it directly points towards a section of pavement. The radar may then receive reflections off the road, i.e. a false alarm.

5.2.2 Mounting on a Snow Plow

Mounting a radar unit on a snow plow presents interesting challenges inherent in the location of a large movable blade directly in front (and on the side for snow plows that have wings) of the vehicle (Figure 5.1). The blade is in a position that blocks the field of view of a radar mounted in the most ideal position: where the license plate resides. Thus, it may be necessary to mount the radar at a height where the radar can 'look' over the blade in both of its positions (up and down). This will most certainly introduce a large negative pitch angle so that the radar will have a field of view coincident with the desired target detection area. The height of the blade is often the same as that of a typical passenger vehicle. Our results indicated that the radar signal is forward scattered away (i.e. it does not register a return) for a pitch up to six degrees downward. It should be noted that the radar was mounted at a height of 25.5 inches above the pavement.

Higher elevations and more extreme pitch angles cause the angle between the radar's line of sight and the pavement to become large, which may cause backward scattering of the electro-magnetic wave. This scenario needs to be investigated further.

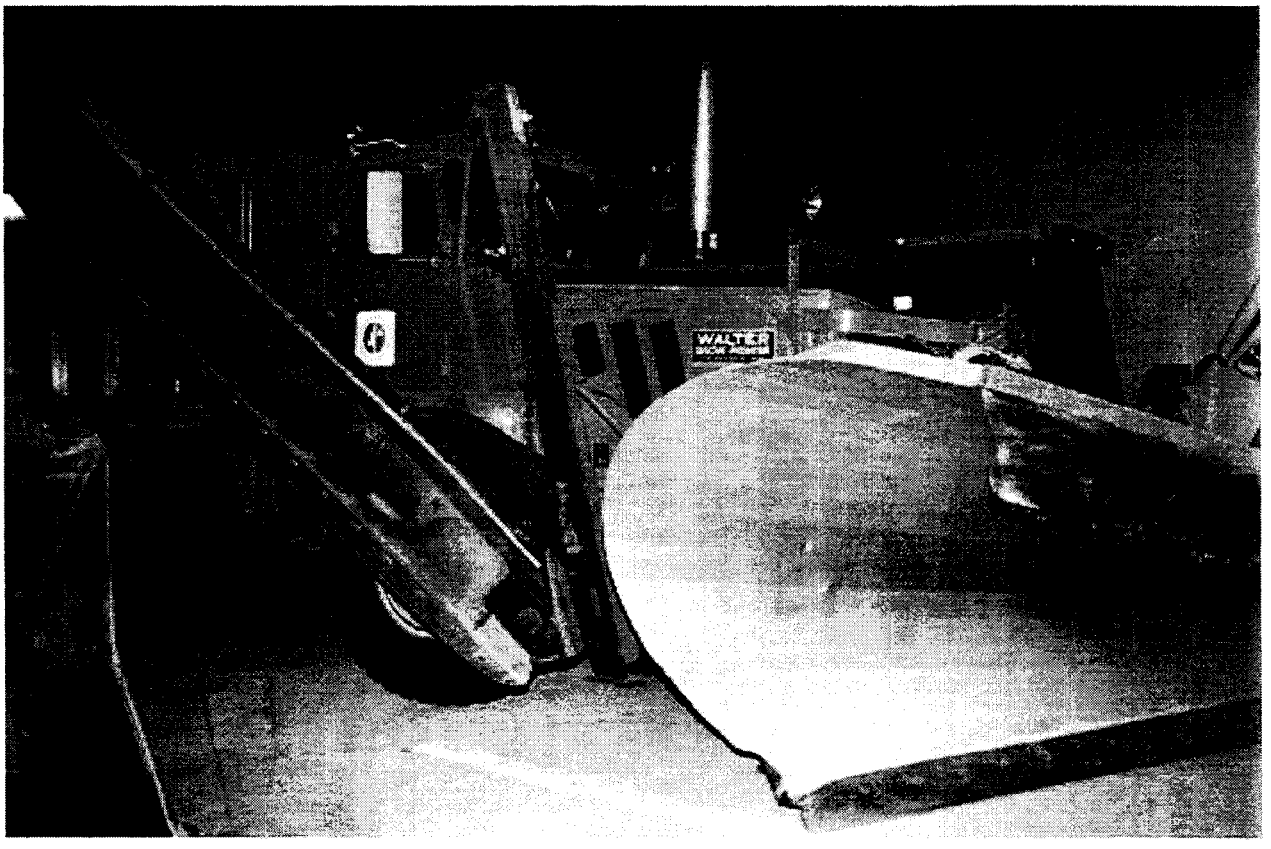

Figure 5.1: Snow plow with hoisted wing

Locating the radar at large vertical distances from the road introduce a new problem. The distance at which target vehicles can be detected is greatly reduced due to the large pitch angle. Pointing the radar downward causes the signal to eventually reflect off the pavement and introduces an unwanted limit to the maximum range of detection. Of coarse, this can be eliminated by reducing the pitch angle but that will create a blind spot in coverage. Vehicles in this region are undetectable. This is certainly an undesirable situation.

We discovered during the vibration experiments that the EVT-200 is sensitive to vibrations caused by the engine. Snow plows have an additional vibratory component caused by the contact

between the blade and the pavement. Eaton VORAD has claimed to have solved the vibration sensitivity problem for the EVT-200, though experiments should be performed to confirm this. Also, it should be determined if the harsher vibratory conditions of a snow plow cause any performance degradation.

5.3 Recommendations

5.3.1 Radar

Recent developments in radar technology have introduced an azimuth angle to the radar's measurement capability. The added dimension presented by the azimuth angle information means that we can now obtain information about where the reflecting target is located. This added information provides many possibilities for filtering out unwanted targets. Road signs and guard rails can be readily filtered. Furthermore, target vehicles in adjacent lanes can be discerned from targets in the same lane as the host. This is very important for displaying information to the driver of the snow plow.

Curved roads present less of problem because filtering can be dynamically linked with steering angle to ignore objects on the side of the road. Little loss of preview distance occurs because azimuth filtering does not reduce the maximum usable range of the sensor. Recent sensors have also increased the azimuth field of view to cover more of the road scene. Under such circumstances, only a very tight radius would reduce the maximum usable detection range.

Eaton VORAD is introducing a new radar unit (the EVT-300 due out in the summer, 1998) which has an azimuth or heading angle associated with the obstacle detection. We suggest acquisition and testing of this sensor so that we will be able to employ all of the benefits that a two dimensional sensor provides.

Mounting issues caused by the unique snow plow geometry need to be tested. We recommend that the next step include mounting the newer radar unit on an actual snow plow. Experiments can be performed to determine the best mounting location and orientation. It may also be

necessary to have more than one radar unit in order to provide coverage across all the regions of interest. Further analysis would be needed in order to determine where the most critical areas are located around a snow plow.

5.3.2 Driver Assistive Display

The prototype display of the radar detected obstacles demonstrated that it was possible to integrate obstacle position on a moving display of the road. A parallel study is presently evaluating a heads up display integrated with a high accuracy GPS based vehicle tracking system. The sensitivity of the system to the driver's eye location and gaze is being evaluated. Once completed, it will be possible to directly integrate obstacle locations (as determined by radar or through other means) within this same field of view, similar in concept to the prototype developed in this study.

References

1. R. Stobart, M. Upton. Techniques for Distance Measurement Between Vehicles. *International Symposium on Automotive Technology and Automation*, Stuttgart, Germany, 1995, pages 417 - 424.

2. Wassim G. Najm. A Review of IVHS Crash Avoidance Technologies. *Collision Avoidance Systems Issues and Opportunities Proceedings*, Reston, Virginia, 1994, pages 103 - 121.

3. H. R. Everett, D. E. DeMuth, E. H. Stitz. Survey of Collision Avoidance and Ranging Sensors for Mobile Robots. Technical Report 1194, Naval command, control and ocean surveillance center RDT&E division, December 1992.

4. Holger H. Meinel. Automotive Applications of Millimeterwaves. *Proceedings of the Mediterranean Electrotechnical Conference*, Bari, Italy, 1996, pages 87 - 94.

5. Craig Shankwitz and Max Donath. MIMIC Sensor Technology for Highway Vehicle Applications: Potential and Challenges for the Future. Technical Report #MN/TC-95/10, Mn/DOT Office of Research Administration, March 1995.

6. Akira Goi. Current Status for Development of Vehicular Radar System Using Millimeter Wave in Japan. *Proceedings of the Second World Congress of ITS*, Yokohama, Japan, 1995, pages 1046 - 1050.

7. Yukiko Hanada and Ryuji Kohno. Performance Analysis and Optimization of Vehicular Spread Spectrum Radar Using Multi-beam Antenna. *Proceedings from the IEEE Conference on Intelligent Transportation Systems*, Boston, Massachusetts, 1997.

8. Stone, A.G. Automotive Radar at 80-90 GHz. *1992 IEEE MTT-S Digest*, 1992, pages 613-616.

9. Lars H. Eriksson, Bengt-Olof Ås. A High Performance Automotive Radar for Automatic AICC. *The Record of the IEEE 1995 International Radar Conference*, Alexandria, Virginia, 1995, pages 380-385.

10. Hermann Rohling, Ernst Lissel. 77 GHz Radar Sensor for Car Application. *The Record of the IEEE 1995 International Radar Conference*, Alexandria, Virginia, 1995, pages 373 - 379.

11. Y. Aoyagi et al. 76 GHz Spread Spectrum Radar for Autonomous Intelligent Cruise Control. *Proceedings from the IEEE Conference on Intelligent Transportation Systems*, Boston, Massachusetts, 1997.

12. Yukinori Yamada, Setsuo Tokoro, and Yasuhiro Fujita. Development of a 60 GHz Radar for Rear-end Collision Avoidance. *Proceedings of the Intelligent Vehicles 1994 Symposium*, Paris, France, 1994, pages 207-212.

13. Paul Ganci, Steven Potts, and Frank Okurowski. A Forward Looking Automotive Radar Sensor. *Proceedings of the Intelligent Vehicles '95 Symposium*, Detroit, USA, 1995, pages 321-325.

14. David Richardson. An FMCW Radar Sensor for Collision Avoidance. *Proceedings from the IEEE Conference on Intelligent Transportation Systems*, Boston, Massachusetts, 1997.

15. John C. Reed. Size Zone Automotive Radar. *Proceedings of the 1997 IEEE National Radar Conference*, Syracuse, New York, 1997, pages 186-190.

16. Jerry D. Woll. Monopulse Doppler Radar for Vehicle Applications. *Proceedings of the Intelligent Vehicles '95 Symposium*, Detroit, USA, 1995, pages 42-47.

17. Leica AG, Product Information and Specifications, Heerbrugg, Switzerland, 1994.

18. P. S. Fancher, R. D. Ervin, Z. Bareket, G. E. Johnson, M. Trefalt, J. Tiedecke, and W. Hagleitner, "Intelligent Cruise Control: Performance Studies Based Upon an Operating Prototype." *IVHS America Annual Meeting,* Atlanta, Georgia, 1994.

19. Ron Sargent. Miniaturized, multi-beam, solid-state scanning laser radar in automobile collision avoidance sensor systems. *Applied laser radar technology II*, Bellingham, Washington, USA, 1995, pages 82-92.

20. Jerry D. Woll. VORAD Collision Warning Radar. *Proceedings of the IEEE International Radar Conference*, Alexandria, Virginia, USA, 1995, pages 369-372.

21. Shubhayu Chakraborty and Daniel G. Smedley. Adaptive Cruise Control for Heavy Duty Vehicles. *Proceedings of the 1995 annual meeting of ITS America*, Washington, D.C., USA, 1995, pages 145-150.

22. D. Farkas, J. Young, B. Baertlein, and Ü. Özgüner. Forward-looking Radar Navigation System for 1997 AHS Demonstration. *Proceedings from the IEEE Conference on Intelligent Transportation Systems*, Boston, Massachusetts, 1997.

23. S. Bajikar, A. Gorjestani, P Simpkins, and M. Donath. Evaluation of In-Vehicle GPS-Based Lane Position Sensing for Preventing Road Departure. *Proceedings from the IEEE Conference on Intelligent Transportation Systems*, Boston, Massachusetts, 1997.

24. Installation Guide, Eaton VORAD, 1995.

25. P. Zoratti, R. Gilbert, R. Majewski, and J. Ference. Millimeter wave scattering characteristics and radar cross section measurements of common roadway objects. *Proceedings / SPIE – the International Society for Optical Engineering*, pages 169 - 179, Philadelphia, Pennsylvania, October, 1995.

26. Eric Foster-Johnson. *Graphical Applications with Tcl & Tk*,. M&T Books, New York, 1997.

27. Present Weather Detector PWD11 User's Guide, Vaisala. January 1997.

28. T. Haavasoja, P. Nylander, M. Sairanen, L. Strom, P. Survo, and P. Utela. A Present Weather Detector for Highways. Vaisala, Oy, Finland.

29. Ronald D. Tabler. Using visual range data for highway ... *Optical Engineering*, Vol. 23 No. 1, Jan/Feb 1984.

30. R. A. Schmidt. Measuring visibility in blowing snow. *Proceedings of the 2nd International Symposium on Snow Removal and Ice Control Research*, Hanover, N. H., May, 1978. Pages 200-207.

Appendix A

Vaisala PWD-11 Weather Sensor Evaluation

A.1 Vaisala PWD-11 Weather Sensor Evaluation

Accurate characterization of weather conditions is important for correctly documenting the relationship between the performance of the radar and weather conditions. The Vaisala Present Weather Detector PWD11 is used to document the weather conditions during the radar experiments. Before the PWD11 can be used, it was necessary to ensure that the detector was calibrated and measuring the actual weather conditions accurately. The visibility measurements of the PWD11 are compared to that of another Vaisala weather detector, namely the AWOS FD12P. This appendix will discuss the comparison results of the visibility data of the two detectors and the precipitation data of the PWD11 versus the Universal Recording Rain Gage (URRG). This section will also discuss the possible explanations for the discrepancies in the visibility data measured by the PWD11 and the FD12P detectors.

A.1.1 Principle of operation of the PWD11

The PWD11, Present Weather Detector (Figure A.1) is a microprocessor controlled sensor that combines optical forward scatter measurement, temperature sensing and capacitive precipitation measurement to measure Meteorological Optical Range (MOR), weather type, intensity and amount of both liquid and solid precipitation. The sensor has a stated visibility measurement accuracy of +/- 20%.

Visibility (MOR) is determined by measuring the intensity of near infra-red light scattered at an angle of 45^0. The received signals are first classified by frequency to get a signal distribution. Using a propriety algorithm, a part of the distribution is selected for signal average calculation. The difference between the signal average and offset average in Hertz is calculated and used as a parameter to a calibrated transfer function. The transfer function converts the frequency into visibility (MOR). The exact form of the transfer function is defined using an accurate transmissometer (Vaisala MITRAS) as a reference [27].

The rain detector sub-sensor of the PWD11outputs a signal proportional to the amount of water on the sensor plate. The presence of water changes the capacitance of the plate which in turn changes the output frequency of the oscillator which is measured by the onboard microprocessor. Intensity of scatter signals measured by the optical sensor is proportional to the volume of the precipitation droplets. In rain the volume measured by the optical sensor and the rain detector are the same. But in snow the optical sensor estimates a volume about 10 times larger than that of the rain detector and this difference is used to distinguished between snow and rain.

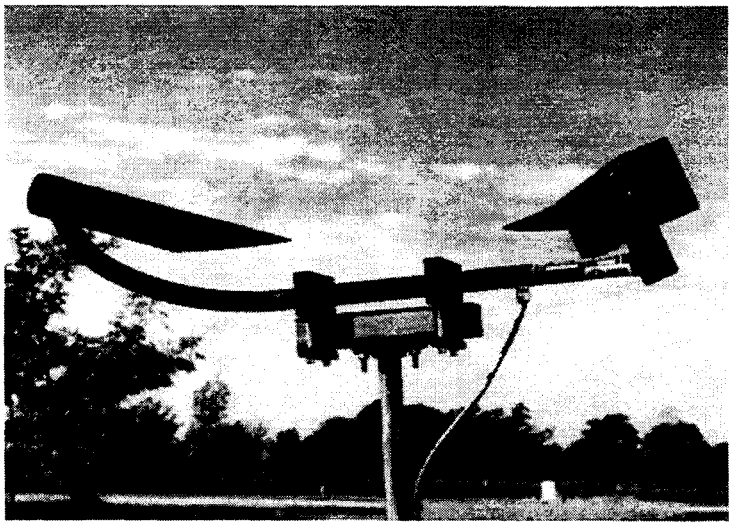

Figure A.1: Vaisala PWD-11

A.1.2 The experiments

The experiments were conducted at three different locations. The first two experiments compared the visibility data between the PWD11 and two different FD12P sensors located at the Cambridge Municipal and Anoka county airports. The third experiment compared precipitation between the PWD11 and a Universal Recording Rain Gage (URRG) and took place at the Chanhassen National Weather Station. Both FD12P detectors were calibrated by the airport technical staff on a regular basis. Similarly the PWD11 was calibrated before being used in the experiments.

The experimental layout at these airports is illustrated in Figure A.2 and Figure A.3. One of the objectives of the experiment layout is to setup the PWD11 as close as possible to the FD12P while not interfering with each other. For both the experiments at the Cambridge and Anoka airports, the distance between the PWD11 and FD12P detectors is relatively large due to requirement that we stay close to an AC outlet (to power the PWD11 and other equipment) and limited access to the FD12P area, located adjacent to the airport tarmac.

For each experiment, the PWD11 collected data in parallel with the FD12P over a week long period. Since the FD12P is in use by the airports, it collects data at all times. At the beginning of each experiment, the time corresponding to the first data sample collected by the PWD11 and its data sampling rate were recorded for synchronizing weather recordings during post experiment data analysis. Furthermore, only data that covered a precipitation event was analyzed. Due to technical reasons, the precipitation data at Cambridge and Anoka airports was not obtained from the FD12P but from a tipping-bucket. The tipping-buckets were located within a few feet of the FD12P (more discussion on tipping-bucket sensors will follow). The FD12P sensors thus only provided visibility data.

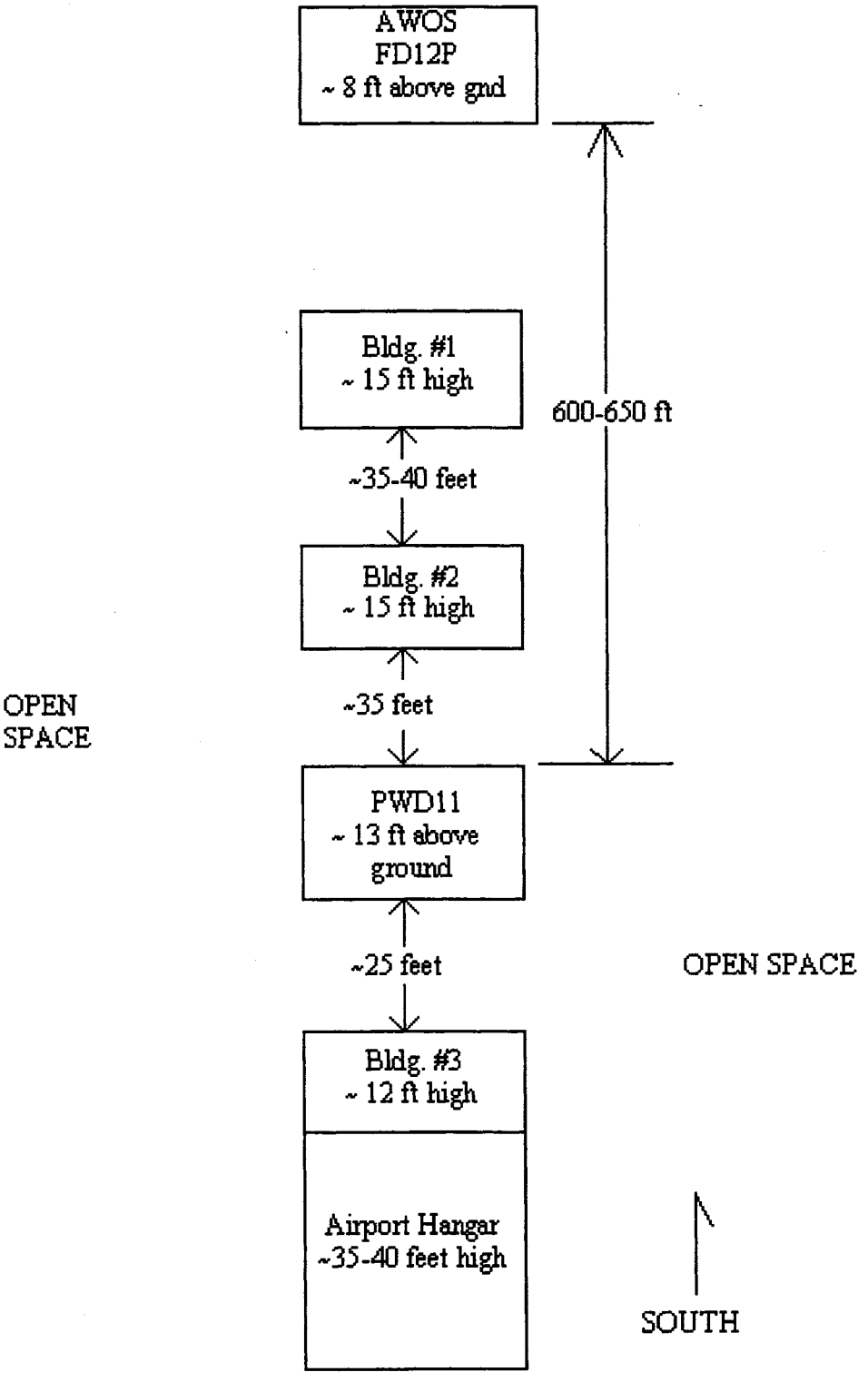

Figure A.2: Experiment layout at the Cambridge airport (not to scale)

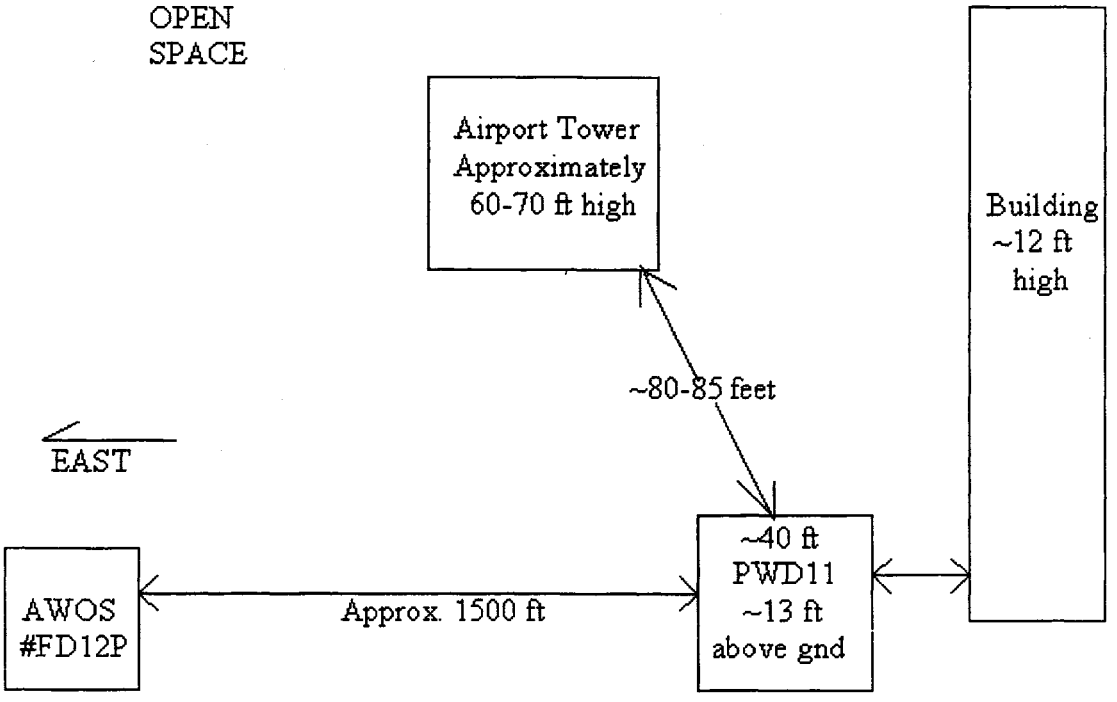

Figure A.3: Experiment layout at the Anoka airport (not to scale)

A.1.3 The data

Analysis shows that the visibility data measured by the PWD11 and the FD12P were significantly different for both experiments, especially at the Cambridge airport. The visibility measurements by the PWD11 and FD12P at the Cambridge and Anoka airports are shown in Figure A.4 and Figure A.5. The difference in visibility data at both airports is greater than 40% of the maximum acceptable tolerance quoted in the Vaisala operation manual [27]. It is worthy to note that the visibility data for the two detectors at the Anoka airport have similar trends but with a constant offset between them. Furthermore, the visibility data from the Anoka airport experiment has a lower offset than the data from the Cambridge airport experiment.

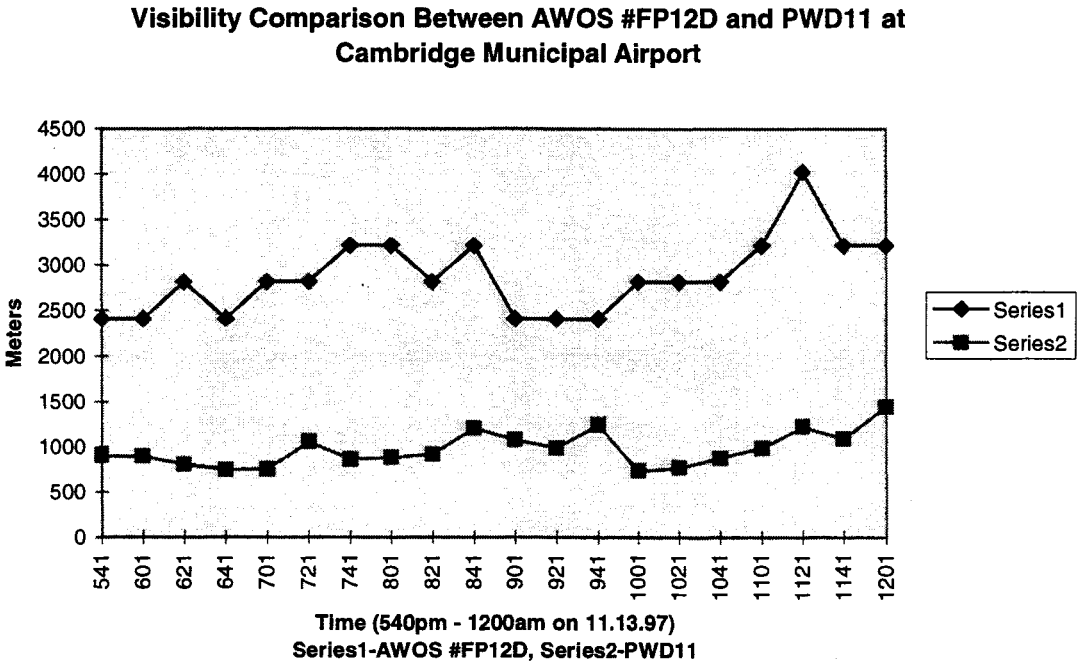

Figure A.4: Visibility comparison at the Cambridge Municipal Airport

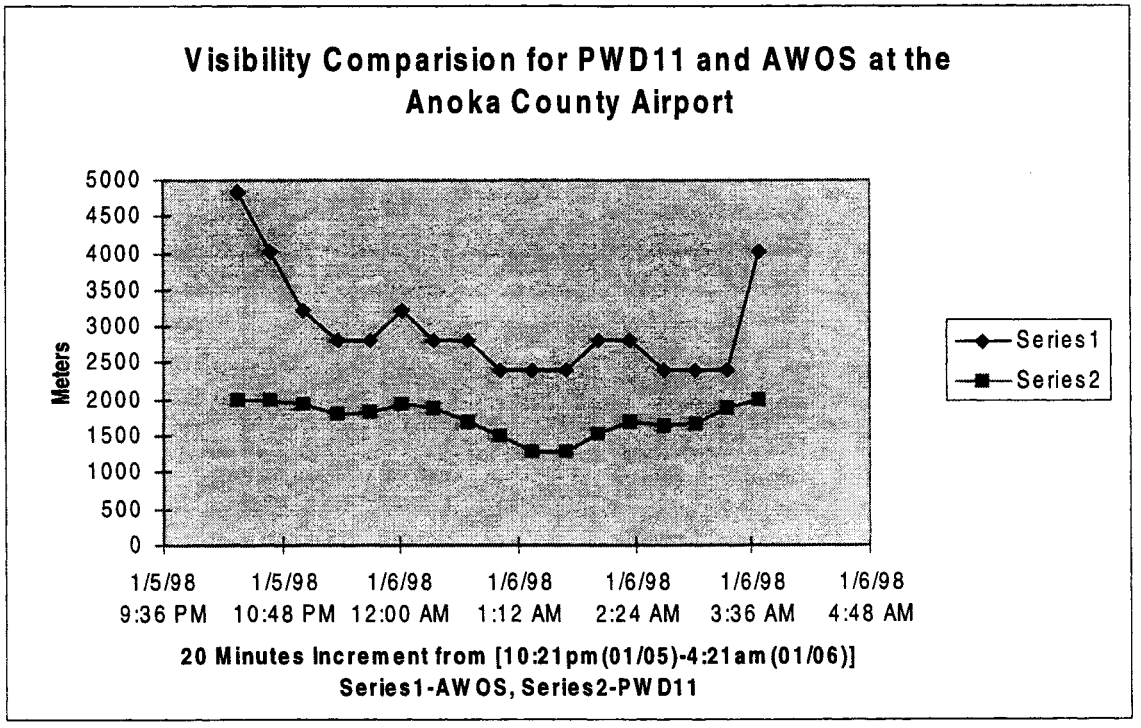

Figure A.5: Visibility comparison at the Anoka County Airport

The PWD11 produces weather codes which describe the type of weather conditions that were present at the time of measurement. A comparison of the weather code with the FD12P weather sensor at the Cambridge airport is shown in Figure A.6. The two sensors had good agreement on the present weather conditions.

The tipping bucket proved to be an inadequate sensor for comparing the cumulative precipitation with the PWD11 as demonstrated in Figure A.7. The tipping-bucket was designed to measure heavy precipitation events and did not measure any precipitation during the experiment.

The Universal Recording Rain Gauge URRG located in Chanhassen had the resolution necessary to measure the water accumulation during an experiment with the PWD11. Results in Figure A.8 show that the two sensors were not at all close in measuring the cumulative precipitation.

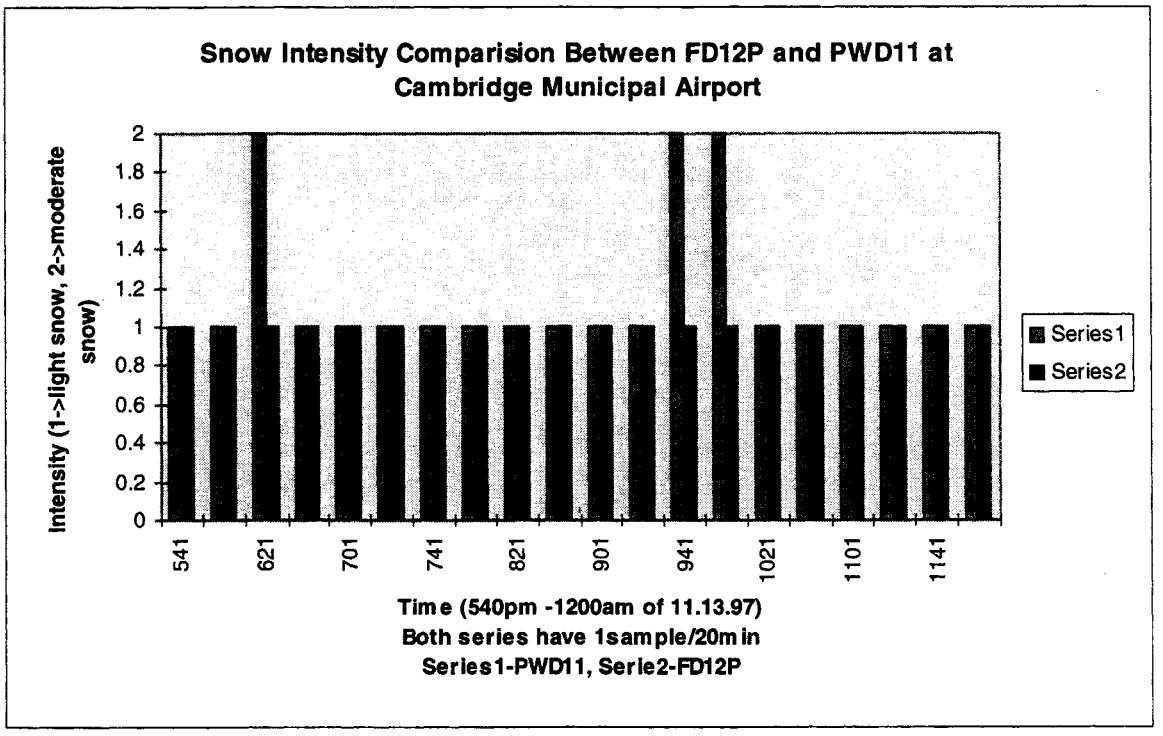

Figure A.6: Weather code comparison at the Cambridge Municipal Airport

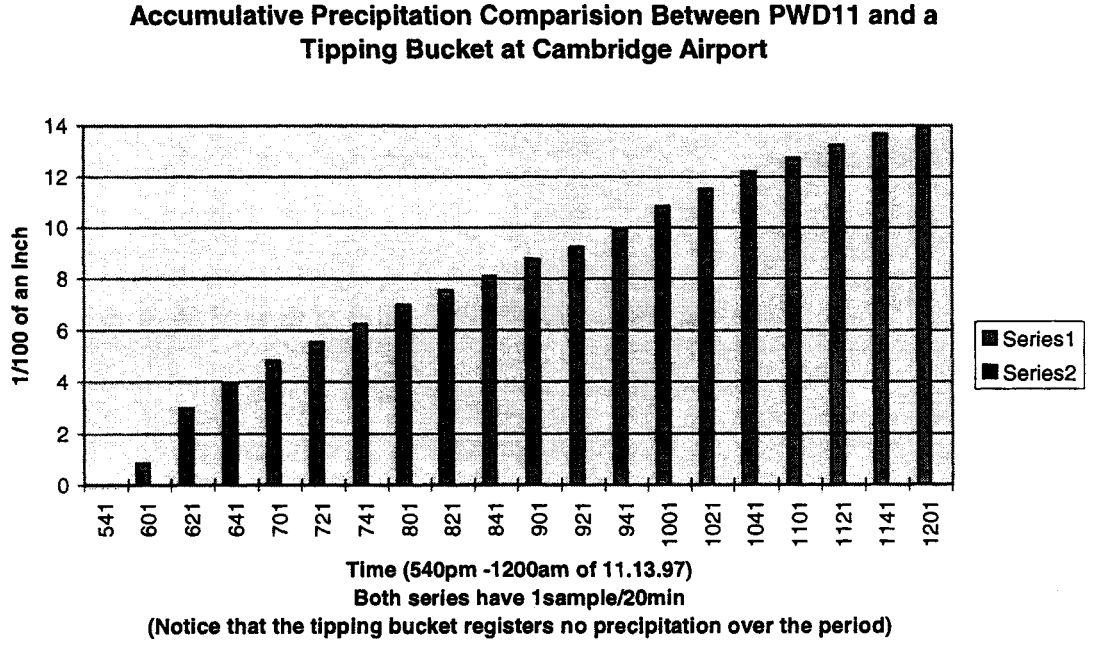

Figure A.7: Cumulative precipitation at the Cambridge Municipal Airport

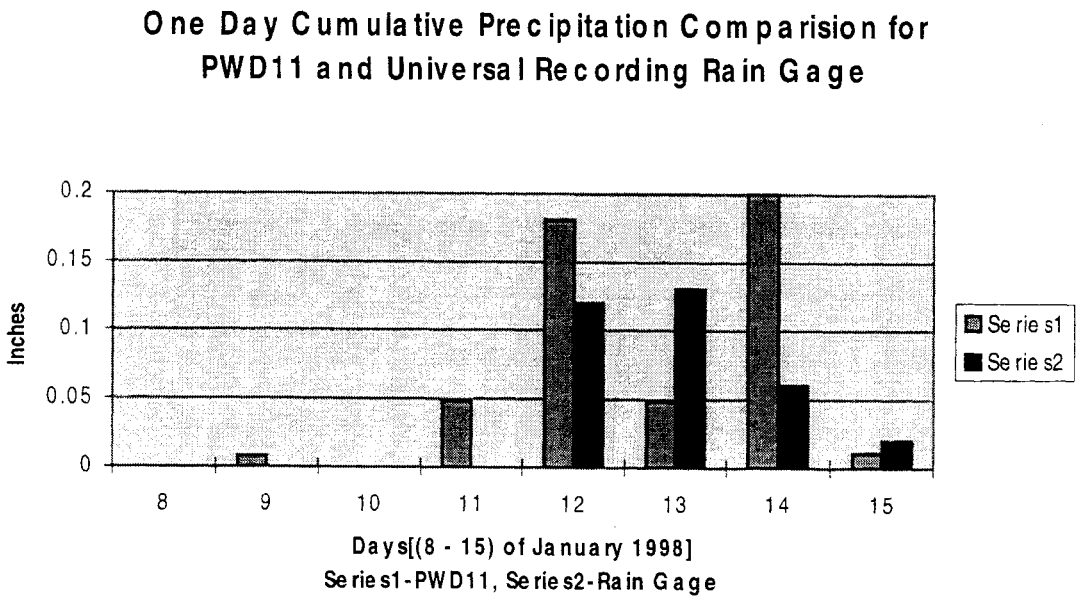

Figure A.8: Cumulative precipitation at the Chanhassen weather service

A.1.4 Analysis

The reasons behind the large difference in visibility data between the two detectors is unclear, though a few experimental and sensor design issues may have affected the results. First, it is possible that the one or both of the detectors are not correctly calibrated or are malfunctioning. Contradicting this possibility, the airport technical staff confirmed that both FD12P detectors that were being used in the experiment were calibrated on regular basis according to the manufacturer's recommendation and were functioning properly. The PWD11 not only was calibrated in the factory, but again by us, using the user's guide and the calibration kit before any experiment was carried out. Furthermore, the PWD11 has a self diagnostic program which produces messages when system malfunctions occur. For these reasons, it would be unlikely that calibration or malfunction caused the visibility discrepancies.

The data produced by the PWD11 such as visibility, precipitation accumulation and weather descriptions were consistent with the observed weather conditions. For example, as precipitation

occurred, visibility started to decrease. The question of integrity for both instruments is difficult to assess by just looking at the data produced by the instrument alone.

One pertinent fact that should be mentioned is that the two sensors were designed for two different purposes. The FD12P was designed for use at airports with maximum visible range measured up to 10 miles (16,090 m). These produce visibility resolution of ¼ of a mile (400 m). It's resolution is 1:40. The PWD11 was designed for monitoring road weather conditions and as such has a much smaller range, 1¼ mile (2000 m) and a visibility resolution of 1 meter [28]. It's resolution is 1:2000. Thus the resolution of the PWD11 is considerably finer even though its visibility range is more limited. The differences in the two detectors' design and specification may have had a bearing on why the visibility data measured by the two detectors at Anoka airport has a very similar trend but a considerable constant offset between them. The difference in their basic design and function may have contributed to the discrepancies between their visibility data. However, this factor alone can not have accounted for the large difference in visible range measured by the two detectors. Another factor which adds to some uncertainty in the FD12P data is that the visibility data was rounded by the airport staff to fit the airport usage standard. This may have affected the accuracy of our comparison between the two detectors, but again cannot explain the large difference.

Factors in the experimental design may also have played a role in contributing to the visibility discrepancies. Tabler [29] shows that the visual range has a strong relationship with wind speed as described by the equation $V = AU^{-B}$, where V is the visual range in meter, A is a coefficient in the range of $1X10^{8}$ m s^{-5} to $2X10^{8}$ m s^{-5} depending on the snow availability and B has a value around five. Wind speed can greatly vary over moderate distances especially if there is a large object such as building or tree in the area. The distance between the two detectors at Cambridge airport was relatively large and there were buildings located between them. This can greatly affect the visual range seen by the two detectors. Beside wind speed, visibility also depends on the particle diameter, particle frequency and the number of particles passing through a unit area per second normal to the wind direction. Both particle diameter and frequency is an exponential

function of height and wind speed. The PWD11 collected data at a height approximately twice as that of the FD12P.

According to Schmidt [30], the particle concentration is independent of wind direction. Hence the orientation of the sensor is not important in calculating the visible range. The fact that the two detectors measure visibility at different heights and were widely separated with large structures between them can very well account for the large difference in the visible range measurements.

Beside the disagreement in visibility range measured by the detectors, precipitation measurement between the PWD11, the tipping bucket and the URRG also showed discrepancies. The URRG and tipping buckets are mechanical devices. Both devices were designed for measuring large quantity precipitation events as compared to the PWD11 which was designed for road weather monitoring and has a resolution for measuring mild precipitation events. Both mechanical precipitation sensors use the measured water in a bucket to measure the precipitation amount. The URRG uses the weight of precipitation in the bucket to draw a corresponding precipitation graph as a function of time. For the period of time we performed the experiments, the PWD11 registered precipitation while the tipping bucket showed no precipitation accumulation. This was obvious in Figure A.7. The AWOS personnel confirm that the accuracy of the tipping bucket is less than that of the PWD11 and should not be used to compare to that of the PWD11. At one point, the precipitation graph produced by the URRG showed a vertical jump equivalent to about a tenth of an inch in zero time. This is a cause for suspicion. Since the electronic means for detecting water intensity of the PWD11 has a much greater resolution than the mechanical URRG, the results of the precipitation experiment aren't conclusive. A comparable sensor should be used in the future for comparison.

A.1.5 Conclusion

The results of the Vaisala sensor evaluation were mixed. We felt that the results from the above experiments were not sufficient to discount the readings provided by the PWD11 sensor. The

visibility results were not conclusive and the precipitation results were ambiguous considering that the PWD11 had a much higher precision that the instruments with which we made the comparison. The weather code however, agreed well with the sensors at both airports. We solicited input from Vaisala as to the discrepancies in the results between the PWD11 and the AWOS FP12D. There was no response.

Given the situation we decided to use the Vaisala present weather detector in the radar experiments because the weather code itself was able to fairly well describe the weather conditions during the experiment. Furthermore, the offset in the visibility readings did not affect the relative visibility readings. We will certainly know which experiment exhibited the least visibility. Finally, we were dealing with a strict deadline and a finite window of possible snow storm weather. We did not have the time or resources to perform the needed experiments to produce more definitive conclusions and still perform the radar experiments.